



ANNUAL REVIEWS **Further**

Click here for quick links to Annual Reviews content online, including:

- Other articles in this volume
- Top cited articles
- Top downloaded articles
- Our comprehensive search

Galaxy Disks

P.C. van der Kruit¹ and K.C. Freeman²

¹Kapteyn Astronomical Institute, University of Groningen, 9700 AV Groningen, The Netherlands; email: vdckruit@astro.rug.nl

²Research School of Astronomy and Astrophysics, Australian National University, Mount Stromlo Observatory, ACT 2611, Australia; email: kcf@mso.anu.edu.au

Annu. Rev. Astron. Astrophys. 2011. 49:301–71

The *Annual Review of Astronomy and Astrophysics* is online at astro.annualreviews.org

This article's doi:

10.1146/annurev-astro-083109-153241

Copyright © 2011 by Annual Reviews.
All rights reserved

0066-4146/11/0922-0301\$20.00

Keywords

disks in galaxies: abundance gradients, chemical evolution, disk stability, formation, luminosity distributions, mass distributions, S0 galaxies, scaling laws, thick disks, surveys, warps and truncations

Abstract

The disks of disk galaxies contain a substantial fraction of their baryonic matter and angular momentum, and much of the evolutionary activity in these galaxies, such as the formation of stars, spiral arms, bars and rings, and the various forms of secular evolution, takes place in their disks. The formation and evolution of galactic disks are therefore particularly important for understanding how galaxies form and evolve and the cause of the variety in which they appear to us. Ongoing large surveys, made possible by new instrumentation at wavelengths from the UV (*Galaxy Evolution Explorer*), via optical (*Hubble Space Telescope* and large groundbased telescopes) and IR (*Spitzer Space Telescope*), to the radio are providing much new information about disk galaxies over a wide range of redshift. Although progress has been made, the dynamics and structure of stellar disks, including their truncations, are still not well understood. We do now have plausible estimates of disk mass-to-light ratios, and estimates of Toomre's Q parameter show that they are just locally stable. Disks are mostly very flat and sometimes very thin, and they have a range in surface brightness from canonical disks with a central surface brightness of about $21.5\ B\text{-mag arcsec}^{-2}$ down to very low surface brightnesses. It appears that galaxy disks are not maximal, except possibly in the largest systems. Their HI layers display warps whenever HI can be detected beyond the stellar disk, with low-level star formation going on out to large radii. Stellar disks display abundance gradients that flatten at larger radii and sometimes even reverse. The existence of a well-defined baryonic (stellar + HI) Tully-Fisher relation hints at an approximately uniform baryonic to dark matter ratio. Thick disks are common in disk galaxies, and their existence appears unrelated to the presence of a bulge component; they are old, but their formation is not yet understood. Disk formation was already advanced at redshifts of ~ 2 , but at that epoch disks were not yet quiescent and in full rotational equilibrium. Downsizing (the gradual reduction with time in the mass of the most actively star-forming galaxies) is now well-established. The formation and history of star formation in S0s are still not fully understood.

1. INTRODUCTION AND OVERVIEW

1.1. Historical Background

Disks are the most prominent parts of late-type spiral galaxies. The disk of our own Milky Way Galaxy stretches as a magnificent band of light from horizon to horizon, particularly from a dark site at southern latitudes, as in the Astronomy Picture of the Day for January 27, 2009 (Pacholka 2009). Its appearance with the Galactic Center high in the sky is reminiscent of the beautiful edge-on spiral NGC 891 (Hawaiian Starlight 1999), which can be regarded as a close twin to our Galaxy (van der Kruit 1984). What might in hindsight be called the first study of the distribution of stars in a galaxy disk is William Herschel's famous cross-cut of the sidereal system based on his star gauges (*On the Construction of the Heavens*, Herschel 1785), from which he concluded that the distribution of stars in space is in the form of a flattened system with the Sun near its center. His counts, on which he based this section of the system, were performed along a great circle on the sky almost perpendicular to the Galactic equator, crossing it at longitudes 45° and 225° and missing the poles by 5° . Comparison to modern star counts shows that Herschel counted stars consistently down to magnitude $V \sim 15$ (van der Kruit 1986).

The next major step in the study of the distribution of stars in the Milky Way was that of Jacobus Kapteyn (Kapteyn & van Rhijn 1920, Kapteyn 1922). In spite of his deduction that interstellar extinction must have the effect of reddening of starlight with increasing distance, Kapteyn (1909a,b, 1914) was unable to establish the existence of interstellar absorption in a convincing way and was led to ignore it. As a result, he ended up with a model for what we now know to be the Galactic disk that erroneously had the Sun located near its center. The proceedings, *The Legacy of J.C. Kapteyn* (van der Kruit & van Berkel 2000), have a number of interesting studies of Kapteyn and astronomy in his time.

Even before galaxies were established to be island universes, spiral structure was discovered in 1845 by William Parsons, the Third Earl of Rosse. His famous drawing of M51 appears in many textbooks, popular literature, and books on the history of astronomy. The importance of the disk and the development of spiral structure were the basis for the classification scheme that John Reynolds and Edwin Hubble developed; the background and early development of galaxy classification were described by Sandage (2005). Eventually the concept of stellar populations, first proposed by Baade (1944), led to the famous Vatican Symposium of 1957 (O'Connell 1958), where a consistent picture was defined to interpret the presence of disk and halo populations in the context of the structure and formation of galaxies.

Not long after that, the collapse picture of Eggen, Lynden-Bell & Sandage (1962) provided a working picture for the formation and evolution of the Galaxy and, by implication, of galaxies in general (Sandage, Freeman & Stokes 1970). It was modified by Searle & Zinn (1978) to include extended evolution, whereby the outer globular clusters originated and underwent chemical evolution in separate fragments that fell into the Galaxy after the collapse of the central halo had been completed. The basic discrete two-component structure of the edge-on galaxy NGC 7814 led van der Kruit & Searle (1982b) to deduce that there are two discrete epochs of star formation, one before and the other after virialization of the spheroid and the formation of the disk.

Two related important developments in understanding the properties of galaxies and their formation were the discovery of dark matter halos, and the appreciation of the role of hierarchical assembly of galaxies. The concepts of hierarchical assembly were already around in the early 1970s and became widely accepted at a landmark symposium on the *Evolution of Galaxies and Stellar Populations* at Yale University in 1977 (Tinsley & Larson 1977). The discovery of dark matter halos (see below) led to the two-stage galaxy formation model of White & Rees (1978), in

which hierarchical clustering of the dark matter took place under the influence of gravity, followed by collapse and cooling of the gas in the resulting potential wells. The *Hubble Space Telescope* (HST) made possible the high-resolution imaging of galaxies at high redshift and showed directly that merging and hierarchical assembly are significant in the formation of massive galaxies.

The significance of internal secular evolution for the evolution of disks has become clear in recent years. The presence of oval distortions, bars, and spiral structure can have a profound effect on the changing structure of disks, as has been extensively reviewed by Kormendy & Kennicutt (2004) and Kormendy (2007).

The rotation of galaxies was discovered early in the twentieth century. For a historical introduction, see van der Kruit & Allen (1978), Gilmore, King & van der Kruit (1990, chapter 10), and Sofue & Rubin (2001), documenting the first derivation of rotation velocities as a function of radius using optical absorption lines (Pease 1914), emission lines (Babcock 1939), and H I (van de Hulst, Raimond & van Woerden 1957; Argyle 1965), all in the Andromeda Nebula M31. The subject developed into the extensive mapping of the velocity fields of disk galaxies in the optical and H I, which eventually led to the discovery of flat rotation curves and the existence of dark matter (see, e.g., reviews by van der Kruit & Allen 1978, Faber & Gallagher 1979, Roberts 2008).

Quantitative surface photometry of disk galaxies to study their structure and luminosity distributions began with the work of Reynolds (1913) for the bulge of M31 (for a review, see Gilmore, King & van der Kruit 1990, chapter 5). Photometry of the much fainter disks came later and revealed the exponential nature of the radial surface brightness distributions. This was first described in a Harvard thesis, using observations of M33 (Patterson 1940): the data appear as figure 10 in the review by de Vaucouleurs (1959a). He had undertaken in the late fifties a systematic survey of the light distributions in nearby spirals, particularly in M31 and M33 (de Vaucouleurs 1958, 1959b), and established the universal exponential disk description of the radial light distribution in galactic disks. At about the same time, Holmberg (1958) completed a survey of the diameters of 300 galaxies from microphotometer tracings of photographic plates in two colors. This heroic effort was the culmination of work started much earlier (Holmberg 1937).

The exponential nature of the radial surface brightness distributions of disks was discussed in detail by Freeman (1970), who noted that many of the larger spirals had a remarkably small range in the extrapolated central (face-on) surface brightness around $21.65 B\text{-mag arcsec}^{-2}$. This result still holds for classical spiral galaxies. The exponential surface brightness distribution of starlight in disks was complemented by the observations of the vertical light distribution in edge-on spirals. The distribution could be approximated very well by an isothermal sheet (Camm 1950, but for practical purposes an exponential can be used as well) with a scaleheight that—surprisingly—is to an excellent approximation independent of galactocentric radius (van der Kruit & Searle 1981a,b, 1982a).

Freeman (1970) also noted that for a self-gravitating exponential disk the expected rotation curve peaks at 2.2 scalelengths and then declines. A decline at 2.2 scalelengths was, however, not observed in the rotation data for NGC 300 and M33 at the time. This 1970 paper appears to be the first indication from rotation curve analysis that the rotation curve is not determined by the mass distribution in the disk alone, but requires a contribution to the amplitude of the rotation curve from an extended distribution of invisible matter. Subsequent observations of rotation curves eventually led to the concept of dark halos in individual galaxies (e.g., Faber & Gallagher 1979, Roberts 2008).

An important concept in the analysis of rotation curves is that of maximum disk, introduced by Carignan & Freeman (1985) and van Albada et al. (1985). In this concept, because the M/L ratio of the disk is unknown, the contribution of the disk mass to the rotation curve is taken to be as large as permitted by the observed rotation curve. In principle, an independent measurement of the

disk mass distribution can be obtained from hydrostatic considerations, comparing the thickness and velocity dispersion of the stars, as was pioneered for the Galaxy by Kapteyn (1922) and Oort (1932), or the HI gas (van der Kruit 1981). Sanders & McGaugh (2002) have reviewed modified Newtonian dynamics as an alternative to dark matter.

Within disks, the star-formation history was studied first in our Galaxy in the Solar Neighborhood. The stellar initial mass function (IMF; the statistical distribution of stellar masses during star formation) was derived first by Salpeter (1959). Schmidt (1959) defined the Schmidt law for the rate of star formation as a function of the density of the ISM, in which the rate of star formation is proportional to the square of the local gas density [see reviews by Kroupa (2002a) and Kennicutt (1998) for subsequent refinements]. Studies of the chemical evolution in the local disk identified the G-dwarf problem in the simple model of chemical evolution (Schmidt 1963). In this simple model, the chemical evolution is followed in a galactic disk starting as pure gas with zero metallicity and without subsequent inflow or outflow; then the result is a much higher fraction of low-metallicity, long-lived stars as G-dwarfs than is observed in the Solar Neighborhood. This can be rectified by extensions of the model (see, e.g., the review by Tinsley 1980). The basic models for chemical evolution were able to represent the radial gradients in metal abundance in the gas of disk galaxies (Searle 1973) in terms of the extent to which star formation and chemical enrichment have proceeded (e.g., Garnett & Shields 1987, for M81). The mean metal abundance of stars that formed over the lifetime of a disk approaches that of the abundance of the gas at the time of disk formation plus an effective yield (the net production of heavy elements, modified by effects of zero-metal inflow or enriched gas outflow). In this “simple model with bells and whistles” (Mould 1984), it follows that, though gas consumption is still proceeding, the abundance gradients in the stars will be, in principle, shallower than that in the gas.

Reviews of stellar populations include those by King (1971), Sandage (1986), Bahcall (1986), Freeman (1987), and Gilmore, Wyse & Kuijken (1989). An IAU Symposium in 1994 on the subject of stellar populations (van der Kruit & Gilmore 1995) includes a historical session. For a recent review on the structure and evolution of the Galaxy, see Freeman & Bland-Hawthorn (2002).

The integral properties of galaxies and the systematics of their distribution have been used as tools toward understanding galaxy formation and the origin of the variety among them. Chief among these relationships are those between the morphological type and properties of their stellar and gas content, such as HI content and integrated color (Roberts & Hayes 1994). These latter properties were convincingly interpreted as a measure of the process of depletion of the interstellar gas in star formation and the rate of current star formation relative to that averaged over a galaxy’s lifetime (Searle & Sargent 1972; Searle, Sargent & Bagnuolo 1973; Larson & Tinsley 1978), which then correlate with galaxy type. The Tully-Fisher relation (Tully & Fisher 1977) provides a tight correlation of rotation velocity and integrated luminosity, although it still is not clear why it is so tight when the rotation velocity is determined not only by the mass in the stars that provide the luminosity but also by the dark matter halo.

We should mention here the discovery of low surface brightness (LSB) galaxies, which was anticipated by the work of Disney (1976). Disney & Phillipps (1983) showed that the observed range in central surface brightness of galaxy disks (and also of elliptical galaxies) is severely restricted by the necessity for them to stand out against the background sky; the exponential nature of disks naturally restricted samples to a small range in central surface brightness comparable to the value first noted by Freeman (1970). This selection effect had been described earlier in qualitative and more general terms by Arp (1965). Many LSB galaxies are known today, although it appears that the bright limit of the surface brightnesses seen by Freeman (1970) is not an effect of observational selection (Allen & Shu 1979, Bosma & Freeman 1993).

1.2. Setting the Scene

This brief description of the historical development of our subject already indicates that a comprehensive treatment of all aspects of galaxy disks is beyond the scope of a single Annual Reviews chapter. Topics that we do not review in detail include radio continuum studies and magnetic fields (van der Kruit & Allen 1976, Condon 1992, Beck 2008), AGNs and black holes in the centers of galaxies (Kormendy & Richstone 1995, Ferrarini & Ford 2005, Pastorini et al. 2007), spiral structure (Toomre 1977), bars (Sellwood 2011b), and secular evolution (Kormendy & Kennicutt 2004). Also we do not review issues related to physical or chemical processes in the ISM. We refer the reader to the proceedings of some recent symposia that concentrate on disks in galaxies, including *The Dynamics, Structure and History of Galaxies* (Da Costa & Jerjen 2002), *Island Universes: Structure and Evolution of Disk Galaxies* (de Jong 2007), *Formation and Evolution of Galaxy Disks* (Funes & Corsini 2008), *Unveiling the Mass: Extracting and Interpreting Galaxy Masses* (Courteau & de Jong 2009),¹ and *Galaxies and Their Masks* (Block, Freeman & Puerari 2010).

Despite the correlations between overall properties, there are galaxies with very similar properties but very different morphologies. M33 and the Large Magellanic Cloud (LMC) provide an example. Both galaxies have very similar central surface brightnesses (~ 21.2 B-mag arcsec⁻²), scalelengths (~ 1.6 kpc), integrated magnitudes (~ -18.5 in B), (B–V) colors (~ 0.51), Infrared Astronomical Satellite (IRAS) luminosities ($\sim 1.0 \times 10^8 L_\odot$), HI masses ($\sim 9.5 \times 10^8 M_\odot$), and rotation velocities (~ 90 – 100 km s⁻¹) (see Gilmore, King & van der Kruit 1990, chapter 10). The point is that these two systems differ significantly only in morphological classification and nothing else. The detailed structure of a galaxy, its morphology, and spiral structure may be determined by external properties such as environment or may even be transient, so that during the lifetime of the systems there might have been periods when M33 looked very much like the LMC and vice versa.²

In the final section, we discuss the origin of S0 galaxies. Originally introduced by Hubble as a transition class between elliptical and spirals, they were believed to be systems that had quickly used all of their remaining gas. Alternative theories were suggested, involving the stripping of gas from existing spirals by collisions (Spitzer & Baade 1951) or intergalactic gas (Gunn & Gott 1972).

2. SURVEYS

Surveys provide the basis of much of the observational studies of disk galaxies. In the past, major surveys were very time consuming. For example, the *Hubble Atlas of Galaxies* (Sandage 1961), which provided the basic source list for much of the past work on nearby galaxies, was the culmination of decades of photography of galaxies by Hubble, Sandage, and others in order to survey the variety of morphologies among galaxies. For many years, the Humason, Mayall & Sandage (1956) survey was a main source of galaxy redshifts and magnitudes; it was the result of 20 years of observations at Mount Wilson, Palomar, and Lick, and was only surpassed decades after its publication. The advent of dedicated, automated survey telescopes, multiobject spectrographs, and high-resolution imaging and spectroscopic space facilities has transformed our ability to make surveys of galaxies. In this section, we give a brief overview of surveys, currently or recently undertaken, that are relevant to studies of disks in galaxies as discussed in later sections of this review.

¹For this symposium on the occasion of Vera Rubin's 80th birthday, there will be no printed proceedings—electronic versions of presentations or posters are available through the conference website.

²Sidney van den Bergh pointed out that M33 has a central star cluster and the LMC does not. Such clusters are likely to remain visible at all times, even if their star formation is intermittent (see Section 3.9). They are common in spirals but not in irregular galaxies, which makes it less likely that an individual galaxy could sometimes be a spiral and sometimes an irregular. We thank Sidney van den Bergh for this remark.

Kinematic surveys aimed at the dynamics of (stellar) disks (see Section 3) using integral field spectrographs include DiskMass (Bershady et al. 2010a) (146 nearly face-on galaxies for which H α velocity fields have already been measured, and a subset of 46 galaxies with stellar velocities and velocity dispersions) and PINGS (*PPAK IFS Nearby Galaxies Survey*; <http://www.ast.cam.ac.uk/research/pings/html/>) (Rosales-Ortega et al. 2010), which will provide two-dimensional spectroscopy in 17 nearby galaxies. For these surveys, the data are supplemented by extensive observations at other wavelengths.

Surveys specifically designed to gather detailed information on the properties of disks in galaxies usually involve samples of nearby galaxies that are not statistically complete but are designed to cover the range of morphological types. HI surveys of individual galaxies are often complemented by optical or near-IR surface photometry to aid the analysis of their rotation curves (see Section 4). A first such survey of spiral galaxies, combining imaging (three-color photographic surface photometry) at optical wavelengths and mapping of distributions and kinematics of HI, was made by Wevers, van der Kruit & Allen (1986). This Palomar-Westerbork Survey of Northern Spiral Galaxies included only 16 galaxies, but required 64 observing periods of 12 hours with the Westerbork Synthesis Radio Telescope (WSRT) and 42 dark nights at the Palomar 48-inch Schmidt. This was extended substantially in the WHISP survey (Westerbork observations of neutral Hydrogen in Irregular and SPiral galaxies; <http://www.astro.rug.nl/~whisp>) (van der Hulst 2002, Noordermeer et al. 2005) of a sample of a few hundred galaxies. THINGS (The HI Nearby Galaxy Survey; <http://www.mpia.de/THINGS/>) (Walter et al. 2008) is the most detailed recent uniform set of high-resolution and high-sensitivity data on 34 nearby disk galaxies available at this time; data were taken with the Very Large Array (VLA). A special section, devoted to THINGS, appeared in the December 2008 issue of the *Astronomical Journal*. Another major survey of nearby galaxies is SINGS (*Spitzer Infrared Nearby Galaxies Survey*; <http://sings.stsci.edu>) (Kennicutt et al. 2003). This is a comprehensive imaging and spectroscopic study of 75 nearby galaxies in the IR.

Other surveys provide large samples of galaxy data of various kinds in different wavelength regions. Images of galaxies in two UV bands from the *Galaxy Evolution Explorer* (GALEX) (Martin et al. 2008) survey are particularly useful for estimating the recent star-formation history of galaxies. In the optical B-band, the Millennium Galaxy Catalogue (see <http://www.eso.org/~jliske/mgc>) comes from a 37.5 deg² medium-deep imaging survey of galaxies in the range $13 < B < 24$, connecting the local and distant Universe. The 6dF and 2dF Galaxy Redshift Surveys (<http://www.aao.gov.au/local/www/6df> and <http://msowwww.anu.edu.au/2dFGRS>) and the SDSS (Sloan Digital Sky Survey; <http://www.sdss.org>) (York et al. 2000) provide vast samples of optical galaxy redshifts and spectroscopic properties related to their star-formation history (see Section 5). The 2MASS (Two Micron All Sky Survey; <http://www.ipac.caltech.edu/2mass>) (Skrutskie et al. 2006) gives integrated near-IR photometry for a very large sample of galaxies and also relatively shallow near-IR images for the brighter galaxies. High-resolution deep imaging in the near- and mid-IR over a wide redshift range is provided by the *Spitzer Space Telescope* mission [see Soifer, Helou & Werner (2008) for a recent summary of extragalactic studies]. Large HI surveys are of interest for studies of the HI mass function in the Universe, and also for scaling laws (see Section 6). For example, the HIPASS (HI Parkes All-Sky Survey; <http://www.atnf.csiro.au/research/multibeam/release>) survey gives integrated HI data for galaxies south of declination +25° out to velocities of 12,700 km s⁻¹.

Two major surveys are using HST to study resolved stellar populations in nearby galaxies. ANGST (ACS Nearby Galaxy Survey Treasury; <http://www.nearbygalaxies.org>) (Dalcanton et al. 2009) establishes a legacy of uniform multicolor photometry of resolved stars for a volume-limited sample of nearby galaxies. GHOSTS (Galaxy Halos, Outer disks, Substructure, Thick

disks and Star clusters; <http://www-int.stsci.edu/~djrs/ghosts>) (de Jong et al. 2007a) is imaging several edge-on galaxies with a range in masses to study their stellar populations. These population studies are important for understanding the star-formation history in galaxies (see Sections 5 and 7). For more nearby population studies, SEGUE (Sloan Extension for Galactic Understanding and Exploration; <http://www.sdss.org/segue/>) and RAVE (RADial Velocity Experiment; <http://www.rave-survey.aip.de/rave/>) focus on kinematic and chemical surveys of very large samples of stars in the Galactic disk and halo.

For studies of disk galaxies at high redshift, the Hubble (Ultra-)Deep Fields (Williams et al. 1996, 2000; Beckwith et al. 2006) and the GOODS (Great Observatories Origin Deep Survey; <http://www.stsci.edu/science/goods>) and COSMOS surveys have been very influential. The GOODS (Dickinson, Giavalisco & the GOODS Team 2003) survey involves two fields centered on the Hubble Deep Field North and the Chandra Deep Field South and combines deep observations from NASA's Great Observatories, *Spitzer*, *Hubble*, and *Chandra*, ESA's *Herschel* and *XMM-Newton*, and from the most powerful ground-based facilities such as Keck, VLT, Gemini, and Subaru. The *Cosmological Evolution Survey* (COSMOS; <http://cosmos.astro.caltech.edu>) covers a two-square-degree equatorial field with a similar range of facilities, aimed at probing the formation and evolution of galaxies with cosmic time (see Section 8).

Astronomy profits enormously from new facilities, and this is equally true for our subject of disk galaxies. For the future, we look forward to new insights from major facilities. In the submillimeter and radio, *Herschel* and the Atacama Large (sub-)Millimeter Array (ALMA) will revolutionize studies of star formation and the ISM in disk galaxies. The Low Frequency Array (LOFAR), its southern Murchison Widefield Array (MWA) counterpart, the Karoo Array Telescope (MeerKAT) and Australian Square Kilometer Array Pathfinder (ASKAP) arrays, and ultimately the Square Kilometer Array (SKA) itself, will have a profound impact on studies of the formation of galaxies and the structure of disk galaxies. Current deep HST surveys (see, for example, <http://candels.ucolick.org>) and surveys to come with the James Webb Space Telescope (JWST), promise to bring new insights into the properties of disk galaxies and their assembly. For studies of the structure and evolution of the Milky Way, the *Global Astrometric Interferometer for Astrophysics* (Gaia) mission will give astrometric data of unparalleled precision. Combined with panoramic surveys like those planned with Pan-Starrs, SkyMapper, and LSST, these data will help us understand the structure and genesis of the different components of our disk galaxy.

3. STELLAR DISKS

In this section we discuss the three-dimensional distribution of stars in disks of galaxies, including warps and truncations, and the kinematics and dynamics of the stellar components. We then turn to the inferred distributions of stellar mass, the disk stability and the total mass distribution in galaxies.

3.1. Luminosity Distributions

We start by describing the luminosity distributions as inferred from surface photometry. First we concentrate on the radial distribution of flat disks and next turn to the three-dimensional one, including a description of the vertical distribution.

3.1.1. Exponential disks. The structure and general properties of stellar disks have previously been reviewed by us (e.g., van der Kruit 2002, Freeman 2007). As mentioned in the introduction,

the radial distribution of surface brightness in the disks of face-on or moderately inclined galaxies can be approximated by an exponential: $I(R) \propto \exp(-R/b)$. Fits to actual surface photometry result in two parameters, the radial scalelength b and the (extrapolated and corrected to face-on) central surface brightness μ_o , both as a function of photometric band. The determination of these parameters can in general be done in a reasonably reliable way from component separations (Kormendy 1977); Schombert & Bothun (1987) and Byun & Freeman (1995) showed from realistic simulations that one-dimensional and two-dimensional bulge-disk separations do return input values for bulge and disk parameters very well. Nevertheless, independent determinations of scalelengths of the same galaxies in the literature give results that differ with a standard deviation of 20% (Knapen & van der Kruit 1991). In his CCD study of exponential disks in a sample of bright UGC galaxies, Courteau (1996) also stresses the pitfalls and cautions that comparison of central surface brightnesses and scalelengths is complicated by the subjective nature of their measurement. We note that older fits adopt the $R^{1/4}$ law $I(R) \propto \exp R^{-1/4}$ for the bulge, whereas most researchers now use the more general Sérsic (1963) profiles $I(R) \propto \exp R^{-1/n}$, with the Sérsic index $n = 1$ for the exponential disk and $n = 4$ for the $R^{1/4}$ law. In the context of two-component decompositions of radial surface brightness distributions, we note that the flat pseudobulge structures discussed by Kormendy & Kennicutt (2004) have values for n of about 2.5.

The original publication on exponential disks by Freeman (1970) used observations in the B -band. In that paper, the distribution of the two parameters was discussed, finding an apparent constancy of μ_o for about 75% of the sample and that disk galaxies have scalelengths with a wide range of values (predominantly small in later-type galaxies). We already noted in Section 1.1 that the apparent constancy of central surface brightness is seriously affected by observational selection (Arp 1965, Disney 1976, Disney & Phillipps 1983), leading to the conclusion that there must be many lower surface brightness galaxies. However, the upper limit is believed to be real (Allen & Shu 1979, Bosma & Freeman 1993, de Jong 1996b).

With the advent of large datasets of surface photometry (such as from the SDSS), it has become possible now to study large samples of galaxies. For example, Gadotti (2009) has collected g , r , and i -band images of a representative sample of nearly 1,000 galaxies from the SDSS and decomposed them into bulges, bars, and disks. Pohlen & Trujillo (2006) and Pohlen et al. (2007) have used SDSS data to determine radial luminosity distributions and look for radial truncations (see Section 3.8). Fathi et al. (2010) determined scalelengths, using an automatic technique, for over 30,000 galaxies in five wavelength bands, together with indices for asymmetry and concentration. Comparison with the overlap with the sample of Gadotti (2009) shows, in general terms, good agreement (see figure 1 of Fathi 2010, which concerns the same sample). Fathi et al. (2010) form subsamples for which reliable morphological types or central velocity dispersions are available. As before, the average scalelength (3.8 ± 2.0 kpc) is independent of morphological type and is very similar in the optical bands (g , r , i , and z). In the u -band, they find a mean scalelength of 5 ± 3 kpc. Galaxies of smaller mass (10^9 to $10^{10} M_\odot$) have smaller scalelengths (1.5 ± 0.7 kpc) than larger mass (10^{11} to $10^{12} M_\odot$) galaxies (5.7 ± 1.9 kpc). The distributions in this study have not been corrected for sample selection.

It is possible to study the bivariate distribution function of the disk parameters. It is most important for such studies that the sample is complete with respect to well-defined selection criteria and that the distribution in the (μ_o, b) plane is corrected for the effect of these selection criteria (following the prescriptions of Disney & Phillipps 1983). This was first done by van der Kruit (1987), later at various optical and near-IR colors by de Jong & van der Kruit (1994) and de Jong (1996a–c), and more recently by Fathi (2010) using the large SDSS (Fathi et al. 2010) sample. The study of the distribution of parameters in this plane reveals important results that bear on the formation models of disks.

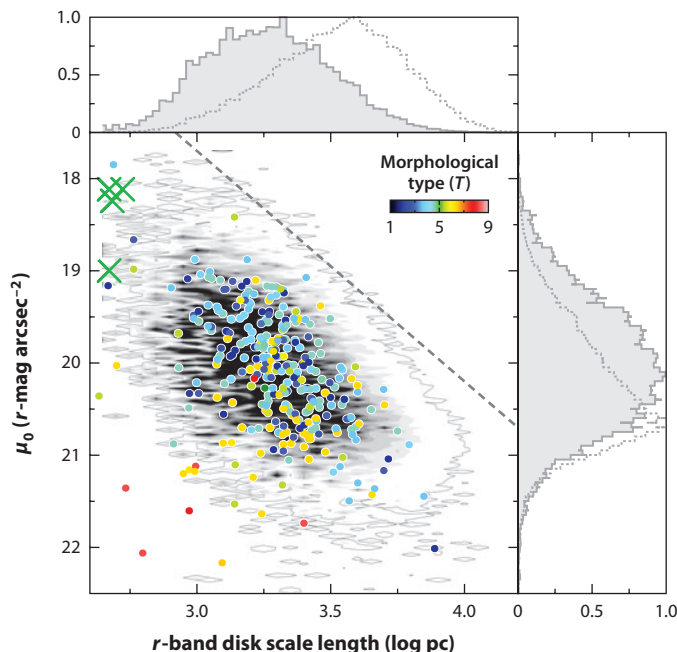


Figure 1

The bivariate distribution function of face-on central surface brightness and scalelength of galaxy disks in a sample of almost 30,000 galaxies taken from SDSS, corrected for selection effects. Superposed are the 282 most reliable data as colored points (coding for revised Hubble type) and a few disk ellipticals as green crosses. The gray diagonal dashed line shows a slope of 2.5 corresponding to a constant disk luminosity. The distributions on the right and top are as observed (*dotted*) and after correcting for sample selection (*solid with gray fill*). (From Fathi 2010).

The distribution in the $(\mu_0, \log b)$ diagram (**Figure 1**) shows a broad band running from bright, large disks to faint, small disks (van der Kruit 1987, de Jong 1996b, Graham & de Blok 2001, Fathi 2010). Graham & de Blok (2001) find that there is a morphological-type dependence in this plane: among LSB galaxies [central surface brightness more than 1 mag fainter than the 21.65 B -mag arcsec $^{-2}$ mean value of Freeman (1970)], the early-type spiral galaxies have large scalelengths (larger than 8–9 kpc), whereas the late-type spirals have smaller scalelengths. Further, de Jong (1996b) finds that the scale parameters of disks and bulges are correlated at all morphological types, but are not correlated themselves with Hubble type. However, LSB galaxies are usually of late Hubble type. He also concludes that the bulge-to-disk ratio is not correlated with Hubble type, nor is the disk central surface brightness. The significant parameter that does correlate with morphological type is the effective surface brightness of the bulge. Color information shows that, within and among galaxies, LSB corresponds to bluer colors (de Jong 1996c). This results from the combined effect of mean stellar age and metallicity and not from dust reddening and implies significant mass-to-light ratio variations. **Figure 2** shows the modern version of figure 5 of Freeman (1970), corrected for volume selection effects. There is still a mean value (but with a large scatter around it) that does not depend on morphological type, except for the later ones.

What properties of galaxies do correlate with b and μ_0 ? Courteau et al. (2007) collected surface photometry of 1,300 galaxies and determined the photometric parameters from either one-dimensional bulge-disk decompositions of the surface brightness profile or by using the so-called marking-the-disk method, where the extent of the exponential disk profile is judged by eye. They

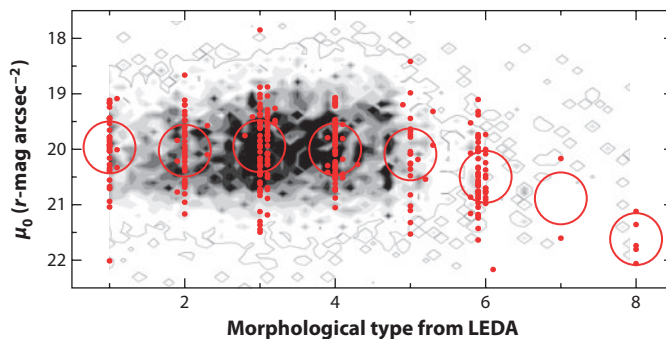


Figure 2

The distribution of face-on central surface brightness for the same sample as in **Figure 1** as a function of Hubble type, corrected for selection and again with the 282 most reliable determinations as red points. The large red open circles show the average surface brightness for each type. (From Fathi 2010).

also find some variation of central surface brightness or scalelength as a function of morphological type, with earlier types having fainter surface brightness and larger scalelengths, but the effects are marginal. In addition, they find well-defined relationships between luminosity, scalelength, and rotation velocity, but the slopes show a definite dependence on morphological type and a small but significant dependence on the wavelength band. The scalelengths in the *I*-band correlate with integrated luminosity and rotation velocity (see Equation 25 and **Figure 18** below). In summary, although *b* has no strong dependence on morphological type, it is clearly larger in the mean for more luminous and more massive galaxies.

There is some argument concerning the scalelength of the disk of our own Galaxy. If $V_{\text{rot}} = 220 \text{ km s}^{-1}$, then the expected scalelength of the Galactic disk would be 4.4 kpc with a one-sigma range between 3.6 and 6.6 kpc (see slide 19 in van der Kruit 2009). These values would be larger if $V_{\text{rot}} = 250 \text{ km s}^{-1}$ (Reid et al. 2009). The often quoted values of 2.5 to 3.0 kpc (Sackett 1997, Freudenreich 1998, Hammer et al. 2007, Reyl   et al. 2009, Yin et al. 2009) put the Galaxy outside the one-sigma range of scalelengths for its rotation speed. A value more like 4.5 kpc (van der Kruit 2008, 2009) (or even the probably too large $5.5 \pm 1.0 \text{ kpc}$ from the Pioneer 10 photometry alone; van der Kruit 1986) would be more typical for our Galaxy. However, Hammer et al. (2007) argue that our Galaxy is exceptional in many aspects: Their adopted low value for the scalelength of the disk is a major contributor to this conclusion.

The origin of the exponential nature of stellar disks is still uncertain. Freeman (1970, 1975) already pointed out that the distribution of angular momentum in a self-gravitating exponential disk resembles that of the uniform, uniformly rotating sphere (Mestel 1963). This is also true for an exponential density distribution with a flat rotation curve (Gunn 1982, van der Kruit 1987). A model in which the disk collapses with detailed conservation of angular momentum (Fall & Efstathiou 1980) would give a natural explanation for the exponential nature of disks and maybe even their truncations (see below). However, bars or other nonaxisymmetric structures may give rise to severe redistribution of angular momentum; nonaxisymmetric instabilities and the secular evolution of disks and their structural parameters may be important (Debattista et al. 2006).

Before leaving the subject of luminosity distributions, we briefly address the issue of LSB disks. Often these have central (face-on) surface brightnesses that are 2 magnitudes or more fainter than the canonical $21.65 \text{ } B\text{-mag arcsec}^{-2}$ of Freeman (1970). Traditionally, these are thought to be galaxies with low (gas) surface densities, in which the star formation proceeded slowly. Analysis of available data (HI rotation curves, colors, and stellar velocity dispersions) led de Blok & McGaugh

(1997) to argue that LSB galaxies are not described well by models with maximum disks (see Section 3.2.4). LSB galaxies appear to be slowly evolving, low-density, dark matter-dominated systems. The star formation in LSB disks can now be studied with GALEX by directly mapping their near-UV flux. Wyder et al. (2009) combined such data with existing HI observations and optical images from the SDSS for 19 systems. Comparison with far-IR data from *Spitzer* shows that there is very little extinction in the UV, consistent with the fact that LSB galaxies appear to have little dust and molecular gas (see, e.g., de Blok & van der Hulst 1998a,b). The star-formation rate in LSB galaxies lies below the extrapolated rate as a function of gas surface density for high surface brightness galaxies, implying a lower mean star-formation efficiency in LSB systems. This may be related to the lower density of molecular gas.

3.1.2. Three-dimensional distributions. We now turn to the three-dimensional distribution. The vertical distribution of luminosity within a galactic disk can be modelled to a first approximation with an isothermal sheet (Camm 1950) with a scaleheight that is independent of galactocentric distance (van der Kruit & Searle 1981a). This is a surprising observational result. We discuss its possible origin in Section 3.2.3. In a more general form, the luminosity density distribution can be written as (van der Kruit 1988)

$$L(R, z) = L(0, 0)e^{-R/b} \operatorname{sech}^{2/n} \left(\frac{nz}{2b_z} \right). \quad (1)$$

This ranges from the isothermal distribution [$n = 1$: $L(z) \propto \operatorname{sech}^2(z/z_0)$ with $z_0 = 2b_z$] to the exponential function [$n = \infty$: $L(z) \propto \exp(-z/b_z)$], as was used by Wainscoat, Hyland & Freeman (1989, 1990) and allows for the more realistic case that the stellar distribution is not completely isothermal in the vertical direction. The uncertainty resulting from what the detailed vertical distribution of stellar mass really is in a disk can be estimated by taking a realistic range in the parameter n , as we have done, for example, in Equation 7 below. **Figure 3** shows the fits of this

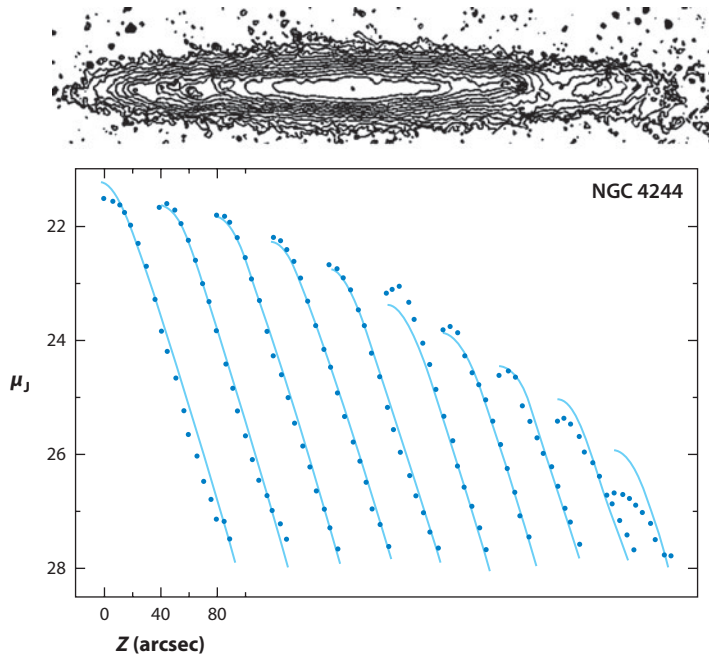


Figure 3

The surface brightness distribution in the edge-on, pure disk galaxy NGC 4244. At the top, the isophotes in blue light at 0.5 mag arcsec⁻² intervals. At the bottom, vertical z -profiles at a range of distances from the center after averaging over the four equivalent quadrants. The lighter blue curves are those for an isothermal sheet with $n = 1$ in Equation 1. (After van der Kruit & Searle 1981a).

distribution projected in edge-on orientation to the surface brightness distribution in the pure-disk, edge-on galaxy NGC 4244, for the case of the isothermal sheet ($n = 1$). The outer profile does not fit, because the truncation (see Section 3.8) has not been taken into account. From actual fits in I and K' , de Grijs, Peletier & van der Kruit (1997) found

$$\frac{2}{n} = 0.54 \pm 0.20 \quad (2)$$

for a sample of 24 edge-on galaxies. A detailed study by de Grijs & Peletier (1997) has shown that the constancy of the vertical scaleheight b_z is accurate in disks of late-type spirals, but in early-type galaxies b_z may increase outward by as much as 50% per scalelength b .

The distribution of the scale parameters is most easily studied in edge-on galaxies. Following the work by van der Kruit & Searle (1981a,b, 1982a), an extensive sample of edge-on galaxies was studied by de Grijs (1998) and reanalyzed by Kregel, van der Kruit & de Grijs (2002). Both scalelength b and scaleheight b_z correlate well with the rotation velocity of the galaxy: for example, for the scaleheight

$$b_z = (0.45 \pm 0.05) (V_{\text{rot}}/100 \text{ km s}^{-1}) - (0.14 \pm 0.07) \text{ kpc}, \quad (3)$$

with a scatter of 0.21 kpc. This relation is important as it can be used to make a statistical estimate of the thickness of disks in galaxies that are not seen edge-on. The correlation between b and V_{rot} is comparable to that found by Courteau et al. (2007). The flattest galaxies (largest ratio of b and b_z) appear to be those with late Hubble-type, small rotation velocity, and faint (face-on) surface brightness. Among galaxies with large HI content, a large range of flattening is observed, becoming smaller with lower HI mass. The flattest disks occur among galaxies with about $10^{10} M_{\odot}$ in HI. We return to this subject in Section 3.6 when we discuss super-thin galaxies.

3.2. Stellar Kinematics, Stability, and Mass

The stellar kinematics together with the distribution of the stars can be used to study the dynamics of disks, estimate the mass distribution, and address issues like the local and global stability of stellar disks.

3.2.1. Vertical dynamics. We first turn to the dynamics of stellar disks in the vertical (z) direction. At the basis of the analysis of the vertical dynamics of a stellar disk, we have the Poisson equation for the case of axial symmetry,

$$\frac{\partial K_R}{\partial R} + \frac{K_R}{R} + \frac{\partial K_z}{\partial z} = -4\pi G\rho(R, z), \quad (4)$$

where K_R and K_z are the gravitational force components. At small z , the first two terms on the left are equal to $2(A - B)(A + B)$ (e.g., Oort 1965, Freeman 1975), and this is zero for a flat rotation curve.³ So we have

$$\frac{dK_z}{dz} = -4\pi G\rho(z). \quad (5)$$

This is the plane-parallel case, and flat rotation curves do make this an excellent approximation at low z (van der Kruit & Freeman 1986). The Jeans equation then becomes

$$\frac{d}{dz} [\rho(z)\sigma_z^2(z)] = \rho(z)K_z. \quad (6)$$

³The Oort constants are $A = 1/2\{V_{\text{rot}}/R - (dV_{\text{rot}}/dR)\}$ and $B = -1/2\{V_{\text{rot}}/R + (dV_{\text{rot}}/dR)\}$, so $A + B = -(dV_{\text{rot}}/dR)$.

Combining these gives (e.g., van der Kruit 1988)

$$\sigma_z(R) = \sqrt{c \pi G \Sigma(R) h_z}, \quad (7)$$

where the velocity dispersion σ_z is now the velocity dispersion integrated over all z (corresponding to the second moment of the distribution observed when the disk is seen face-on), and the constant c varies between 3/2 for an exponential [$n = \infty$ in Equation 1] to 2 for an isothermal distribution ($n = 1$). Equation 7 is the equation for hydrostatic equilibrium that relates the vertical distribution of the stars and their mean vertical velocity dispersion to the distribution of mass; this principle was used already by Kapteyn (1922) and Oort (1932) to derive the mass density in the Solar Neighborhood. If the mass-to-light ratio M/L is constant with radius, the exponential radial distribution and the constant scaleheight imply, through hydrostatic equilibrium, that the vertical velocity dispersion $\sigma_z(R)$ of the old stars in the disk should be proportional to the square root of the surface density Σ or as an exponential with galactocentric radius, but with an e-folding of twice the scalelength.

The mass-to-light ratio M/L is a crucial measure of the contribution of the disk to the rotation curve and the relative importance of disk mass and dark matter halo in a galaxy. An often used hypothesis is that of the maximum disk (see also Section 4.2), in which the disk contribution to a galaxy's rotation curve is maximized in the sense that the amplitude of the disk-alone rotation curve is made as large as the observations allow. Using hydrostatic equilibrium, we may estimate M/L and obtain information on whether or not the disk is maximal or submaximal. This can, in principle, be done from Equation 7 by measuring the velocity dispersion in a face-on galaxy and using a statistical estimate of the scaleheight.

In 1984, van der Kruit & Freeman (1984) made the first successful measurements of stellar velocity dispersion in the face-on spirals NGC 628 and 1566.⁴ This work was followed by more detailed observations by van der Kruit & Freeman (1986) for NGC 5247 (inclination about 20°), where the prediction was verified: The e-folding length of σ_z was 2.4 ± 0.6 photometric scalelengths, the predicted value of 2.0 being well within the uncertainty. Many studies have since shown that σ_z decreases with galactocentric radius (e.g., Bottema 1993; Kregel, van der Kruit & Freeman 2004, 2005; Kregel & van der Kruit 2005, and references therein). Gerssen, Kuijken & Merrifield (1997) found in NGC 488 that the kinematic gradient was comparable to the photometric gradient, which they attributed to the fact that the scalelength should really be measured in K -band to represent the stellar distribution. The same researchers (Gerssen, Kuijken & Merrifield, 2000) found, in NGC 2985, that these scalelengths were indeed as expected from a constant M/L . There is certainly support from stellar dynamics that, in general, there are no substantial gradients in mass-to-light ratios in disks.

Two recent developments are making an impact on this issue. The first is the use of integral field units that enable a more complete sampling of the disks. The DiskMass Project (Verheijen et al. 2007; Westfall et al. 2008; Bershadsky et al. 2010a,b) aims at mapping the stellar vertical velocity dispersion in 46 face-on or moderately inclined spiral galaxies. This will provide a kinematic measurement of the mass surface density of stellar disks. The final results have not yet appeared in the literature, but recent conference presentations show that the kinematics follows the light, i.e., the velocity dispersions drop off according to the rule described above. Also the actual values indicate relatively low mass-to-light ratios and disk masses that are well below those required for maximum disk fits.

⁴At the same time and independently, Kormendy (1984a,b) succeeded in measuring stellar velocity dispersions in the disks of two S0 galaxies with more or less the same aim; we discuss this in Section 9.

Similarly, the use of planetary nebulae (PNe) as test particles in the disks (Herrmann et al. 2008; Herrmann & Ciardullo 2009a,b) of five face-on spirals allows the velocity dispersion of these representative stars of the old disk population to be measured out to much larger radii (see also Section 9). In general, the findings are similar: Except for one system, the M/L is constant out to about three radial scalelengths of the exponential disks. Outside that radius, the velocity dispersion stops declining and becomes flat with radius. Possible explanations proposed for this behavior include an increase in the disk mass-to-light ratio, an increase in the importance of the thick disk, and heating of the thin disk by halo substructure. They also find that the disks of early-type spirals have higher values of M/L and are closer to the maximum disk than later-type spirals.

In summary, the vertical dynamics of stellar disks show that in general the velocity dispersions of the stars fall off with an e-folding length double that of the exponential light distribution, as required for a constant M/L , whereas for the majority of disks the inferred mass-to-light ratios are almost certainly lower than required in the maximum disk hypothesis.

3.2.2. Stellar velocity dispersions in the plane. The stellar velocity dispersions in the plane are more complicated to determine from observations. The radial and tangential components are not independent, but governed by the local Oort constants⁵

$$\frac{\sigma_\theta}{\sigma_R} = \sqrt{\frac{-B}{A-B}}. \quad (8)$$

For a flat rotation curve, $A = -B$ and this ratio is 0.71. In highly inclined or edge-on systems, the dispersions can be measured both from the line profiles and the asymmetric drift equation,

$$V_{\text{rot}}^2 - V_\theta^2 = \sigma_R^2 \left\{ \frac{R}{b} - R \frac{\partial}{\partial R} \ln(\sigma_R) - \left[1 - \frac{B}{B-A} \right] \right\}, \quad (9)$$

where the circular velocity V_{rot} can be measured with sufficient accuracy from the gas (optical emission lines or HI observations), which have velocity dispersions of order 10 km s^{-1} or less and have therefore very little asymmetric drift.

The stability of a galactic disk to local axisymmetric disturbances depends on the (stellar) radial velocity dispersion σ_R , the epicyclic frequency κ , and the local mass surface density Σ . Toomre's (1964) criterion is

$$Q = \frac{\sigma_R \kappa}{3.36 G \Sigma}. \quad (10)$$

On small scales, local stability results from a Jeans-type stability, where tendency to collapse under gravity is balanced by the kinetic energy in random motions, but only up to a certain (Jeans) scale. On larger scales, shear as a result of galactic differential rotation provides stability. In the Toomre Q -criterion, this smallest scale is just equal to the (maximum) Jeans scale, so that local stability exists on all scales. According to Toomre (1964), local stability requires $Q > 1$. Numerical simulations suggest that galaxy disks are on the verge of instability (Hohl 1971, Sellwood & Carlberg 1984, Athanassoula & Sellwood 1986, Mihos, McGaugh & de Blok 1997, Bottema 2003), having stellar velocity dispersions that are slightly larger than Toomre's critical velocity dispersion. The simulations suggest $Q = 1.5$ – 2.5 .

The first attempt to measure these in-plane velocity dispersion components was by van der Kruit & Freeman (1986) for the highly inclined galaxy NGC 7184. They fitted their data using two

⁵For small deviations from circular motions around the galactic center, the stellar orbit may be described by a small epicycle superposed on the circular motion around the galactic center. The frequency in the epicycle is $\kappa = 2\sqrt{-B(A-B)}$ and its axis ratio $\sqrt{-B/(A-B)}$ (Oort 1965). The ratio between the two velocity dispersions derives from the shape of the epicycle.

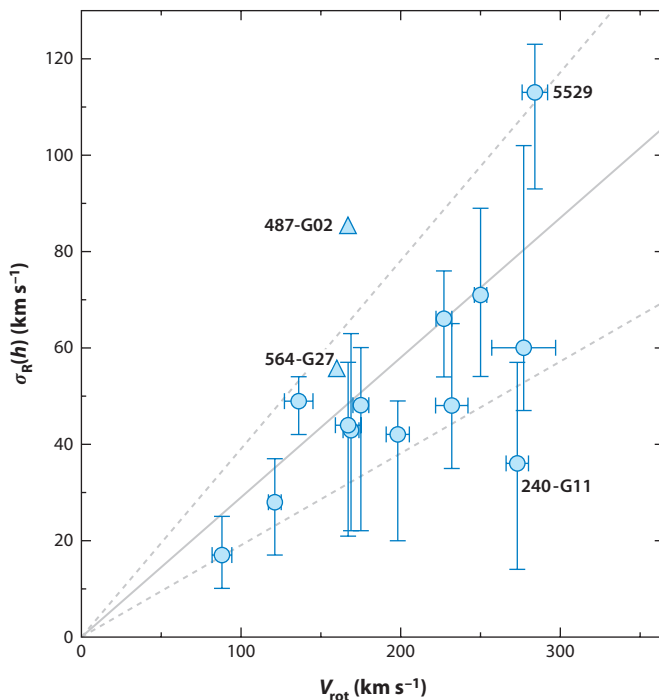


Figure 4

Stellar disk velocity dispersion, measured at one scalelength in edge-on galaxies versus the maximum rotational velocity. The gray solid and dashed lines indicate the relation and scatter $\sigma_R(h) = (0.29 \pm 0.10)V_{\text{rot}}$. (From Kregel, van der Kruit & Freeman 2005).

different assumptions for the radial dependence of the radial velocity dispersion: one that the axis ratio of the velocity ellipsoid (between the vertical and radial dispersion) is the same everywhere, and the other that the Toomre Q is constant with radius. Both assumptions worked well; over the observed range of one or two scalelengths from the center, the two assumptions correspond to similar variations (see Gilmore, King & van der Kruit 1990, p. 196).

More extensive observations by Bottema (1993) on a sample of 12 galaxies (including the Milky Way Galaxy from Lewis & Freeman 1989) resulted in the discovery of a relation between a fiducial value of the velocity dispersion (either the vertical one measured at or extrapolated to the center or the radial velocity dispersion at one scalelength) and the integrated luminosity or the rotation velocity. Luminosity and rotational velocity are equivalent through the Tully-Fisher relation. This has been confirmed by Kregel & van der Kruit (2005) and Kregel, van der Kruit & Freeman (2005) (see **Figure 4**). The relation⁶ is

$$\sigma_z(0) = \sigma_R(h) = (0.29 \pm 0.10)V_{\text{rot}}. \quad (11)$$

It extends to very small dwarf galaxies, e.g., UGC 4325 with a velocity dispersion of 19 km s⁻¹ still falls on the relation (Swaters 1999, chapter 7). The scatter in this relation is not random but appears related to other properties. Galaxies with lower velocity dispersions have higher flattening, lower central surface brightness, or dynamical mass ($4bV_{\text{rot}}^2/G$) to disk luminosity ratio.

The linear σ – V_{rot} relation follows from straightforward arguments, presented in Gilmore, King & van der Kruit (1990, chapter 10) (see also Bottema 1993, van der Kruit & de Grijs 1999). We evaluate properties at one radial scalelength ($R = 1b$) without using subscripts to indicate this.

⁶The formal fit to the sample in Kregel, van der Kruit, & Freeman (2005) is $\sigma_R(h) = (-2 \pm 10) + (0.33 \pm 0.05)V_{\text{rot}}$; the equation above gives the relation adopted from all available studies.

Using the definition for Toomre Q for a flat rotation curve, so that $\kappa = \sqrt{2}V_{\text{rot}}/R$, and eliminating b using a Tully-Fisher relation $L_{\text{disk}} \propto \mu_o b^2 \propto V_{\text{rot}}^4$ results in

$$\sigma_R \propto Q \frac{\mu_o (M/L)_{\text{disk}} b}{V_{\text{rot}}} \propto Q \left(\frac{M}{L} \right)_{\text{disk}} \mu_o^{1/2} V_{\text{rot}}. \quad (12)$$

This shows that, when Q and M/L are constant among galaxies, the Bottema relation follows, with indeed the proviso that galaxy disks with lower (face-on) central surface brightness μ_o at a given value of V_{rot} have lower stellar velocity dispersions than given by the mean $\sigma - V_{\text{rot}}$ relation.

3.2.3. Origin of the constant scaleheight. The origin of the constant scaleheight of stellar disks—or of the fall-off of stellar vertical velocity dispersion so as to precisely compensate for the decline in surface density—is not obvious. If the evolution of the stellar velocity dispersions (the heating of the disk) is similar at all radii and if it evolves to a radial velocity dispersion such that the disk is just stable everywhere, we may expect σ_z/σ_R (the axis ratio of the velocity ellipsoid) and Toomre Q to be independent of galactocentric radius. This would, however, imply that $\sigma_z \propto (R/b) \exp(-R/b)$. Although this is not all that much different from the exponential decline $\exp(-R/2b)$ that follows from Equation 7 between say one and three scalelengths,⁷ it is significantly different at larger radii. In fact, the simple assumption would result in $b_z \propto (R/b)^2 \exp(-R/b)$, which is far from constant over the range $R = 0$ to $R = 5b$.

There are three general classes of models for the origin of the velocity dispersions of stars in galactic disks. The first, going back to Spitzer & Schwarzschild (1951), is scattering by irregularities in the gravitational field, later identified with the effects of giant molecular clouds (GMCs). The second class of models can be traced back to the work of Barbanis & Woltjer (1967), who suggested transient spiral waves as the scattering agent; this model has been extended by Carlberg & Sellwood (1985). More recently, the possibility of infall of satellite galaxies has been recognized as a third option (e.g., Velázquez & White 1999).

Almost all of the observational information about the evolution of velocity dispersion with age in galactic disks comes from the Solar Neighborhood, and we must stress that this information remains quite insecure. Although much of the earlier work invokes the results of Wielen (1977), which indicates a steady increase of stellar velocity dispersion with age, some of the more recent observational studies indicate that the velocity dispersion increases with age for only 2 to 3 Gyr and then saturates, remaining constant for disk stars of older age (see, e.g., Edvardsson et al. 1993, 1994; Freeman 1991; Soubiran et al. 2008). The observational situation regarding disk heating is far from certain, and this in turn must reflect on the various theories of disk heating.

In the Solar Neighborhood, the ratio of the radial and vertical velocity dispersion of the stars σ_z/σ_R is usually taken as roughly 0.5 to 0.6 (Wielen 1977, Gomez et al. 1990, Dehnen & Binney 1998, Mignard 2000), although values on the order of 0.7 are also found in the literature (Woolley et al. 1977; Meusinger, Reimann & Stecklum 1991). The value of this ratio can be used to test predictions for the secular evolution in disks and perhaps distinguish between the general classes of models. Lacey (1984) and Villumsen (1985) have concluded that the Spitzer-Schwarzschild mechanism is not in agreement with observations; the predicted time dependence of the velocity dispersion of a group of stars as a function of age disagrees with the observed age-velocity dispersion relation (see also Wielen 1977), though it would not be possible for the axis ratio of the velocity ellipsoid σ_z/σ_R to be less than about 0.7 (but see Ida, Kokuba & Makino 1993).

⁷The reason why the two analyses of the measurements of velocity dispersion in van der Kruit & Freeman (1986) and in Bottema et al. (see references in Bottema 1993) both gave good fits.

Jenkins & Binney (1990) argued that it is likely that the dynamical evolution in the directions in the plane and that perpendicular to it could have proceeded with both mechanisms contributing, but in different manners. Scattering by GMCs would then be responsible for the vertical velocity dispersion, whereas scattering from spiral irregularities would produce the velocity dispersions in the plane. The latter would be the prime source of the secular evolution; the scattering by molecular clouds is a mechanism by which some of the energy in random motions in the plane is converted into vertical random motions, hence determining the thickness of galactic disks. The effects of a possible slow, but significant accretion of gas onto the disks over their lifetimes have been studied by Jenkins (1992), who pointed out strong effects on the time dependence of the vertical velocity dispersions, in particular giving rise to enhanced velocities for the old stars. However, Hänninen & Flynn (2000, 2002) conclude that observations such as the radial dependence of stellar velocity dispersions in the Milky Way Galaxy by Lewis & Freeman (1989) can be reproduced if scattering occurs by a combination of massive halo objects (black holes) and GMCs. Dehnen & Binney (1998) conclude that spiral structure is probably a major contributor to disk heating. More recently, Minchev & Quillen (2006) suggested from 2D simulations that multiple patterns of spiral structure could cause strong variations of stellar velocity dispersions with galactocentric radius, which has not been observed. Our conclusion is that there still is much uncertainty about the process of heating of the (thin) disk. Some of this uncertainty is due to uncertainty in the observational relation between stellar ages and velocity dispersions, because stellar ages are so difficult to measure.

Theoretical arguments suggest that a constant axis ratio of the velocity ellipsoid is a fair approximation in the inner parts of galaxy disks (Cuddeford & Amendt 1992; Famaey, van Caelenberg & DeJonghe 2002). An observational argument for the approximate constancy of the velocity anisotropy is provided by the ages and kinematics of 182 F and G dwarf stars in the Solar Neighborhood (Edvardsson et al. 1993). This indicates that the anisotropy was set after an early heating phase and, although the Galaxy has probably changed much over its lifetime, has remained constant throughout the life of the old disk (Freeman 1991).

So, where does this leave us with respect to the origin of the constant scaleheight? As long as there is no detailed understanding of the evolution of the velocity dispersions as a function of galactocentric radius, we cannot even begin to address this in a meaningful way. A constant stability parameter Q and a constant axis ratio of the velocity ellipsoid σ_z/σ_R do give an approximate constant thickness over the inner few scalelengths, but this fails at larger radii.

3.2.4. Mass distributions from stellar dynamics. The stellar velocity dispersions can still be used to derive information on the disk mass distribution. For a self-gravitating disk that is exponential in both the radial and vertical direction, the vertical velocity dispersion goes as (cf. van der Kruit 1988)

$$\sigma_z(R, z) = \sqrt{\pi G b_z (2 - e^{-z/b_z}) (M/L) \mu_0} e^{-R/2b}. \quad (13)$$

Assuming a constant (but unknown) axis ratio of the velocity ellipsoid σ_z/σ_R , the radial velocity dispersion becomes

$$\sigma_R(R, z) = \sqrt{\pi G b_z (2 - e^{-z/b_z}) (M/L) \mu_0} \left(\frac{\sigma_z}{\sigma_R} \right)^{-1} e^{-R/2b}. \quad (14)$$

The distribution of the products $\sqrt{M/L_I} (\sigma_z/\sigma_R)^{-1}$, deduced from this equation in the Kregel, van der Kruit & Freeman (2005) sample, is shown in **Figure 5**. This sample of edge-on galaxies has a range of Hubble types from Sb to Scd, absolute I -magnitudes between -23.5 and -18.5 , and a range in rotation velocities from 89 to 274 km s $^{-1}$. Thirteen of the fifteen disks have $1.8 \lesssim \sqrt{M/L_I} (\sigma_z/\sigma_R)^{-1} \lesssim 3.3$. The values of the outliers may have been overestimated (see Kregel,

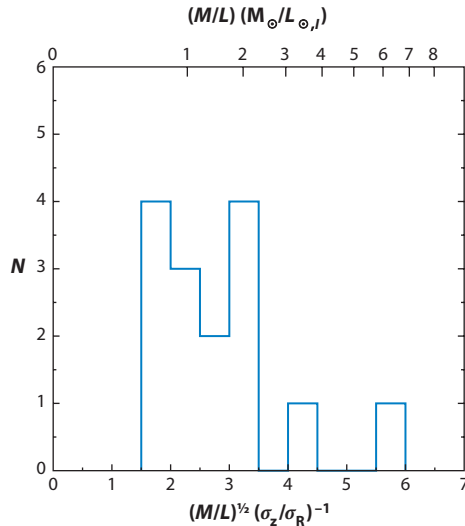


Figure 5

Histogram of the product $\sqrt{M/L_I}(\sigma_z/\sigma_R)^{-1}$ from stellar kinematics in edge-on galaxies. Except for two outliers, the distribution of $\sqrt{M/L_I}(\sigma_z/\sigma_R)^{-1}$ is rather narrow. The outliers are ESO 487-G02 and 564-G27; data for these galaxies are less complete than for the other ones. Along the top we show the values of M/L_I implied by $\sigma_z/\sigma_R = 0.6$. (From Kregel, van der Kruit & Freeman 2005).

van der Kruit & Freeman 2005). Excluding these, the average is $\langle \sqrt{M/L_I}(\sigma_z/\sigma_R)^{-1} \rangle = 2.5 \pm 0.2$ with a 1σ scatter of 0.6. The near constancy of the product can be used with mass-to-light ratios based on stellar population synthesis models to estimate the axis ratio of the velocity ellipsoid. Conversely, the upper scale of **Figure 5** indicates that a typical M/L in the I -band of a galactic stellar disk is of order unity and, for the majority of systems, lies between 0.5 and 2.

It is possible to relate the axis ratio of the velocity ellipsoid to the flattening of the stellar disk, i.e., the ratio of the radial exponential scalelength and the vertical exponential scaleheight (van der Kruit & de Grijs 1999). In the radial direction, the velocity dispersion at one scalelength can be written using the definition of Toomre Q as $\sigma_{R,h} \propto Q \Sigma(b) b / V_{\text{rot}}$, where a flat rotation curve has been assumed. At this radius of one scalelength, the hydrostatic equation gives $\sigma_z \propto \sqrt{\Sigma(b) b_z}$. Eliminating $\Sigma(b)$ between these two equations then gives

$$\left(\frac{\sigma_z}{\sigma_R} \right)_h^2 \propto \frac{1}{Q} \frac{b_z}{b}. \quad (15)$$

If Q is constant within individual disks, then the disk flattening depends directly on the axis ratio of the velocity ellipsoid.

Equation 12 shows that when Q and M/L are constant among galaxies, galaxy disks with lower (face-on) central surface brightness μ_o have lower stellar velocity dispersions. Combining Equation 12 with the hydrostatic equilibrium of Equation 7 and using Equation 11 gives (Kregel, van der Kruit & Freeman 2005, van der Kruit & de Grijs 1999)

$$\frac{b}{b_z} \propto Q \left(\frac{\sigma_R}{\sigma_z} \right) \sigma_z^{-1} V_{\text{rot}} \propto Q \left(\frac{\sigma_R}{\sigma_z} \right). \quad (16)$$

The observed constancy of $\sqrt{M/L}(\sigma_z/\sigma_R)^{-1}$ implies that the flattening of the disk b/b_z is proportional to $Q\sqrt{M/L}$.

For a self-gravitating exponential disk, the expected rotation curve peaks at 2.2 scalelengths. The ratio of this peak of the rotation velocity of the disk to the maximum rotation velocity of the galaxy ($V_{\text{disk}}/V_{\text{rot}}$) is

$$\frac{V_{\text{disk}}}{V_{\text{rot}}} = \frac{0.880 (\pi G \Sigma_0 b)^{1/2}}{V_{\text{rot}}}. \quad (17)$$

Using Equations 7 and 11, this can be rewritten as

$$\frac{V_{\text{disk}}}{V_{\text{rot}}} = (0.21 \pm 0.08) \sqrt{\frac{b}{b_z}}. \quad (18)$$

So, we can estimate the disk contribution to the rotation curve from a statistical value for the flattening (see also Bottema 1993, 1997; van der Kruit 2002). For the sample of Kregel, van der Kruit & de Grijs (2002), this then results in $V_{\text{disk}}/V_{\text{rot}} = 0.57 \pm 0.22$ (rms scatter). In the dynamical analysis of Kregel, van der Kruit & Freeman (2005), the ratio $V_{\text{disk}}/V_{\text{rot}}$ is known up to a factor σ_z/σ_R and distance-independent. The derived disk contribution to the observed maximum for the same sample rotation is, on average, $V_{\text{disk}}/V_{\text{rot}} = 0.53 \pm 0.04$, with a 1σ scatter of 0.15. Both estimates agree well.

In the maximum disk hypothesis, $V_{\text{disk}}/V_{\text{rot}}$ will be a bit lower than unity to allow a bulge contribution and let dark matter halos have a low-density core. A working definition that has been adopted generally is $V_{\text{disk}}/V_{\text{rot}} = 0.85 \pm 0.10$ (Sackett 1997). Thus, at least for this sample, the average spiral has a submaximal disk. Note that Equation 17 strictly applies to a razor-thin disk. For a disk with a flattening of $b/b_z \simeq 10$, the radial gravitational force is weaker, leading to decrease of about 5% in $V_{\text{disk}}/V_{\text{rot}}$ (van der Kruit & Searle 1982a). Taking the gravity of the gas layer and dark matter halo into account would yield a 10% effect, also in this direction. So, these effects work in the direction of making the disks more submaximal.

The values obtained from stellar dynamics are illustrated in **Figures 6** and **7**. The measurement of stellar velocity dispersions can be used to derive the disk surface density at some point (e.g., one scalelength) up to a factor $(\sigma_z/\sigma_R)^2$, but can be estimated also from the velocity dispersion for an assumed value of Q . Comparing the two then gives an estimate of the axis ratio of the velocity ellipsoid. In **Figure 7a**, Q is assumed to be 2.0 and **Figure 7b** the velocity anisotropy is assumed to be 0.6 and then a value for Q results. Most galaxies are not maximum disk. The ones that may be maximum disk have a high surface density according to **Figure 5**. From the panels, we also note that disks that are maximal appear to have more anisotropic velocity distributions or are less stable according to Toomre Q . We return to the maximum disk hypothesis below (Section 4.2).

3.3. Age Gradients and Photometric M/L Ratios

Colors contain information on the history of star formation, as can be studied in the context of integrated colors of galaxies, pioneered by Searle, Sargent & Bagnuolo (1973) and Larson & Tinsley (1978) and described in much detail by Tinsley (1980), and also as a function of radius in a galaxy disk. Observing and interpreting color gradients in galactic disks is not straightforward. Obviously one needs accurate photometry for unambiguous interpretation in terms of stellar synthesis and star-formation histories. However, the effects of age⁸ and metallicity are difficult to separate. Dust absorption is also a major factor, often making degenerate the effects of stellar age and metallicity on the one hand and extinction and reddening by dust on the other.

⁸It should be noted that in discussions of these subjects the property “stellar age” is usually the mean age of all stars derived as a luminosity-weighted average, further weighted by the star-formation rate over the lifetime of the disk, and should not be confused with the age of the oldest stars.

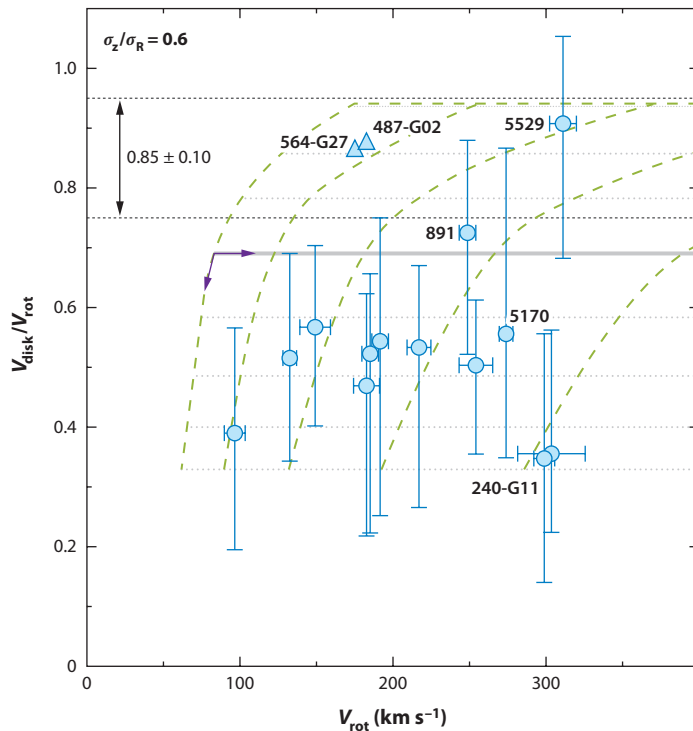


Figure 6

The contribution of the disk to the amplitude of the rotation curve $V_{\text{disk}}/V_{\text{rot}}$ for a sample of 15 edge-on galaxies as a function of the rotation velocity itself. The dotted lines at the top and arrow show the limits and interval of 0.85 ± 0.10 from Sackett (1997) for maximum disk fits. The axis ratio of the velocity ellipsoid is assumed to be 0.6. The dotted gray lines correspond to the collapse models of Dalcanton, Spergel & Summers (1997); the dashed green lines connect models of the same total mass [$\log_{10}(M_{\text{tot}}) = 10 - 13$ in steps of 0.5], and dotted lines connect models with the same spin parameter λ [see Equation (22)]. The purple arrows indicate the direction of increasing M_{tot} and λ . The two galaxies without error bars are the same ones as the outliers in **Figure 5**. (From Kregel, van der Kruit & Freeman 2005).

Figure 7 of Larson & Tinsley (1978) is instructive. It shows a sequence of population synthesis models in the two-color ($U-B$) versus ($B-V$) diagram, with ages of 10^{10} years and star-formation histories ranging from initial burst to constant with time. The effects of age, metallicity, and absorption, and even changes in the IMF, shift the models in very similar directions!

Wevers, van der Kruit & Allen (1986) were the first to undertake a systematic survey of the luminosity, color, and HI distributions in a well-defined set of spiral galaxies. The surface photometry was based on photographic plates and, although the data did show color gradients, Wevers (1984) was not sufficiently confident to conclude that these were significant. In hindsight, this was not justified: A detailed comparison by Begeman (1987) with later CCD photometry by Kent (1987) for three systems showed deviations of at most 0.2 mag in the radial profiles down to 26 r -mag arcsec $^{-2}$. Although common wisdom holds that old photographic surface photometry is not reliable, at least some of it certainly is.

A comprehensive study of the broadband optical and near-IR colors in a sample of 86 disk galaxies was performed by de Jong & van der Kruit (1994) and de Jong (1996a–c). These studies established the existence of color gradients both within and among galaxy disks, with fainter surface brightness systematically corresponding to bluer colors. It was also found that the degeneracies

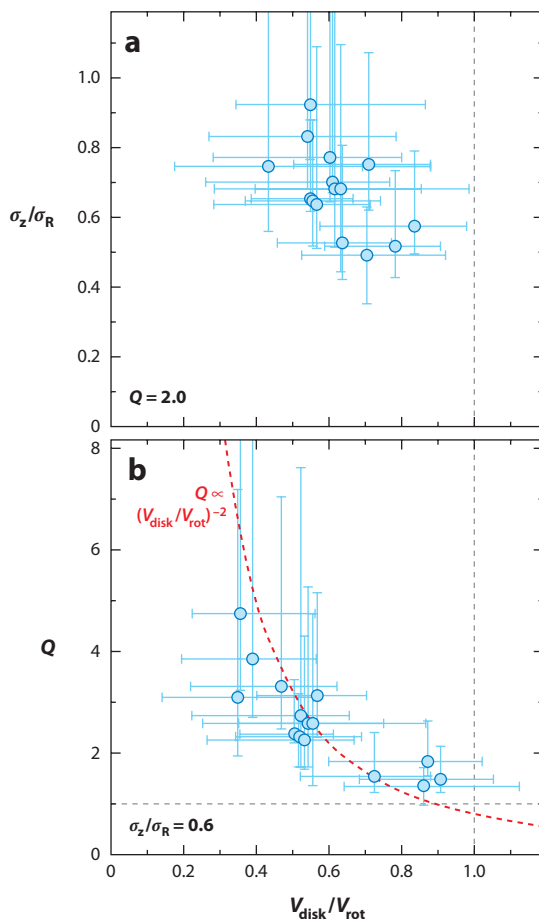


Figure 7

Stellar dynamics parameters for edge-on galaxies. (a) The axis ratio of the velocity ellipsoid as a function of $V_{\text{disk}}/V_{\text{rot}}$ for $Q = 2.0$. (b) $V_{\text{disk}}/V_{\text{rot}}$ as a function of Q for an assumed axis ratio of the velocity ellipsoid of 0.6. (From Kregel, van der Kruit & Freeman 2005).

between dust absorption, stellar age, and metallicity can be broken to a large extent by use of a set of photometric bands from the blue (B -band) to the near-IR (K), and it was concluded from 3D radiative transfer models that dust extinction cannot be the major cause of the observed gradients. The color gradients must be the result of significant differences in star-formation history, whereby the outer regions are younger and of lower metallicity than the central parts. The lack of suitable stellar population models made it impossible to quantify the trends, although the extreme variations predicted by the models of Larson (1976) seemed outside the range of possibilities offered by the observed color gradients.

Peletier & de Grijs (1998) used $(I-K)$ colors in edge-on galaxies away from the central planes to derive a dust-free, near-IR, color-magnitude relation for spiral galaxies. The slope of this relation is steeper for spirals than for elliptical galaxies. This is most likely not a result of vertical abundance gradients, but of average age with height. The surprising thing is that the scatter in this relation is small, possibly even only due to observational uncertainty. Average stellar age must be an important contributor to variations in broadband colors.

Bell & de Jong (2000) made an important step forward by using maximum-likelihood methods to match observed colors with stellar population synthesis models, using simple star-formation histories. These showed that spiral galaxies almost all have significant gradients in the sense that the inner regions are older and more metal rich than the outer regions. The amplitude of these

gradients is larger in high surface brightness galaxies than in low surface brightness ones, and the progress of star formation (as evidenced by decreasing age and increasing metallicity) depends primarily on the surface brightness (most clearly in the K -band) or surface density. The local surface density seems to shape the star-formation history in a disk more strongly than the overall mass of the galaxy.

These models can also be used to derive values and gradients of the mass-to-light ratio M/L in and among disks. This was done by Bell & de Jong (2001) under the assumption of a universal IMF. They conclude that their relative trends in M/L with color are robust to uncertainties in the stellar populations and galaxy evolution models. They also find that limits on the M/L ratios derived from maximum disk fits to rotation curves [for galaxies in the Ursa Major cluster by Verheijen (2001), Verheijen & Sancisi (2001)] match their M/L ratios well, providing support for the universality of the IMF and the notion that at least some high surface brightness galaxies are close to maximum disk. The variations in M/L span a factor between 3 and 7 in the optical and about 2 in the near-IR.

The IMF provides the normalization of the M/L through the numbers of low-mass stars, but the slope of the relation between color and M/L is largely independent of what models are used or what IMF is adopted (de Jong & Bell 2009). The Salpeter IMF gives too massive a normalization (Bell & de Jong 2001), which can be remedied by using a “diet” Salpeter IMF (i.e., deficient in low-mass stars such that it has only 70% of the mass for the same color; Bell & de Jong 2001), or adopting an IMF that is itself more deficient in low-mass stars (Kennicutt 1983, Kroupa 2001, Chabrier 2003). Kroupa (2002a) has rather convincingly argued that the IMF is universal to the extent that its variations are smaller than would follow from the expected varying conditions on the basis of elementary considerations. Bastian, Covey & Meyer (2010, see abstract) have recently concluded that “there is no clear evidence that the IMF varies strongly and systematically as a function of initial conditions after the first few generations of stars.”

Default models, produced by adopting a declining star-formation rate, the population synthesis models of Bruzual & Charlot (2003), and the IMFs listed above, give consistent estimates of M/L (de Jong & Bell 2009). In fact, the M/L_I values implied in **Figure 5** on the top axis (derived for an axis ratio of the velocity ellipsoid of 0.6) are 0.2 dex lower than from Bell & de Jong (2001) but, as de Jong & Bell (2009) point out, the axis ratio of the velocity ellipsoid scales with the square of M/L . The conclusion is that the determination of mass-to-light ratios from broadband colors is reliable and robust in a relative sense, but that there are still some uncertainties in the normalization resulting from imprecise knowledge of the faint part of the IMF.

3.4. Global Stability, Bars, and Spiral Structure

Local stability of stellar disks has already been discussed in relation to local stellar velocity dispersions, Toomre’s Q , and the secular evolution (heating) of disks. We say a few words here about global stability, bars in galaxies, and spiral structure. Much of these subjects has been covered recently in the reviews, such as that on dynamics of galactic disks by Sellwood (2011a) and for the case of bars in relation to pseudobulges by Kormendy & Kennicutt (2004).

Global stability of disks has been a subject ever since numerical simulations became possible, starting about 1970 (e.g., Miller et al. 1970, Hohl 1971). Criteria for stability were formulated empirically by Ostriker & Peebles (1973) and Efstathiou et al. (1982). In the latter criterion, the halo stabilizes the disk; the criterion is in terms of observables,

$$Y = V_{\text{rot}} \left(\frac{b}{GM_{\text{disk}}} \right)^{1/2} \gtrsim 1.1, \quad (19)$$

where the disk is assumed to be exponential with scalelength b and total mass M_{disk} . Because the rotation velocity V_{rot} is related to the total mass, it is a criterion that relates to the relative mass in disk and halo. It can be rewritten to say that within the radial distance from the center corresponding to the edge of the disk, the dark matter halo contains up to 60–70% of the total mass (van der Kruit & Freeman 1986). Such galaxies are in fact submaximal. Sellwood (2011a) concludes that these criteria are only necessary for disks that have no dense centers, because central concentrations of mass in disks themselves could also provide global stability. It was shown already some decades ago (Kalnajs 1987) that halos are not very efficient in stabilizing disks as compared to bulges.

We do not discuss the formation of bars in galaxies, as this subject has been covered in detail by Kormendy & Kennicutt (2004), in relation to pseudobulges, and by Sellwood (2011a). We do want to stress the fundamental point that the incidence of bars is much larger than traditionally thought; a typical fraction that figured in previous decades—although admittedly for strongly barred galaxies as in Sandage (1961)—was of the order of a quarter to a third. Current estimates are much higher; Sheth et al. (2008) found in the COSMOS field that, in the local Universe, about 65% of luminous spiral galaxies are barred. This fraction is a strong function of redshift, dropping to 20% at a redshift of 0.8. The *Spitzer Survey of Stellar Structure in Galaxies* S⁴G (Sheth et al. 2010) aims, among other goals, at studying this in the near-IR. As an example, we show in **Figure 8a** a blue and near-IR image of the large spiral M83. Although it appears mildly barred in the optical, it is clear that in the K -band the bar is very prominent and extended.

Throughout the previous century, much attention has been paid to the matter of the formation and maintenance of spiral structure. It was extensively reviewed by Toomre (1977, 1981). Spiral structure in itself is unquestionably an important issue (see the quotation of Richard Feynman in the introduction in Toomre's review), as it is so obvious in galaxy disks and appears to play a determining role in the evolution of disks through the regulation of star formation and, therefore, the dynamical, photometric, and chemical evolution. We do not discuss theories of spiral structure itself, as progress in this area has recently been somewhat slow. We refer the reader to the contributions of Kormendy & Norman (1979), Sellwood & Carlberg (1984), Elmegreen,

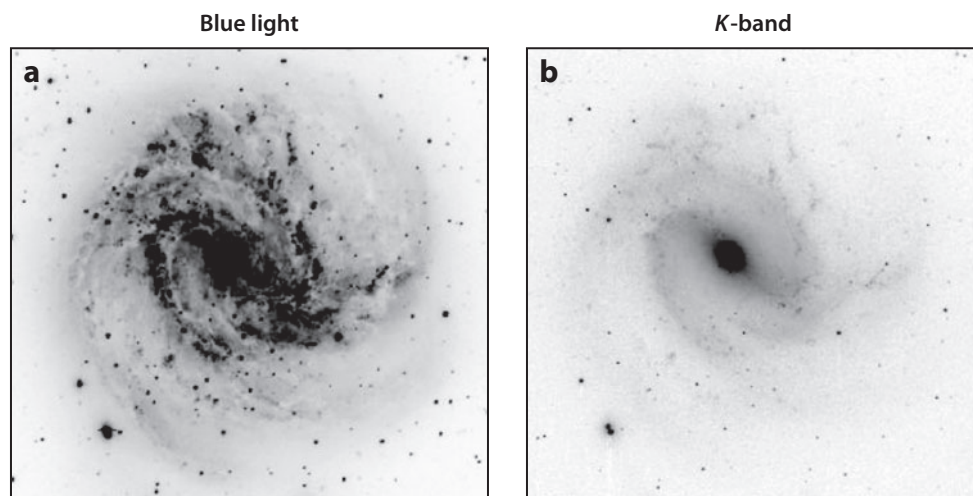


Figure 8

M83 (*a*) in blue light and (*b*) in the K -band. The bar is much more obvious in the near-IR. (Unpublished images by O.-K. Park and K.C. Freeman).

Elmegreen & Leitner (2003), and Sellwood (2008, 2011a,b). Spiral structure is often related to gravitational interaction between galaxies; for interactions and subsequent merging, see the work of Toomre & Toomre (1972), Schweizer (1986), and Barnes (1988).

3.5. The Flatness of Disks

The inner disks of galaxies are often remarkably flat. For the stellar disks, this can be studied in edge-on systems by determining the centroid in the direction perpendicular to the major axis at various galactocentric distances (e.g., Sanchez-Saavedra, Battaner & Florido 1990; Florido et al. 1991; de Grijs 1997, chapter 5). These studies were aimed at looking for warps in the outer parts of the stellar disks (see below), but it is obvious from the distributions that in the inner parts the systematic deviations are very small.

The evidence for the flatness of stellar disks is more compelling when we look at the flatness of the layers of the ISM. First, look at the dustlanes. In **Figure 9**, we collect some images of edge-on disk galaxies. In the top row are two super-thin galaxies (which we discuss further in Section 3.6); the disks are straight lines to within a few percent. The same holds for the dustlanes in NGC 4565 (*second row, left*; allow for the curvature due to its imperfectly edge-on nature) and NGC 891 (*second row, right*). Again the dustlanes indicate flat layers to a few percent. In the third row, the peculiar structure of NGC 5866 (*left*) has no measurable deviation from a straight line, whereas for the Sombrero Nebula (*right*) the outline of the dustlane fits very accurately to an ellipse. In the bottom row, NGC 7814 (*fourth row, right*) is straight again to within a few percent, but NGC 5866 (*third row, left*) is an example of a galaxy with a large warp in the dust layer.

The HI kinematics provide probably the strongest indications for flatness. In three almost completely face-on spirals (NGC 3938, 628, and 1058), van der Kruit & Shostak (1982, 1984)

Edge-on disks and dustlanes

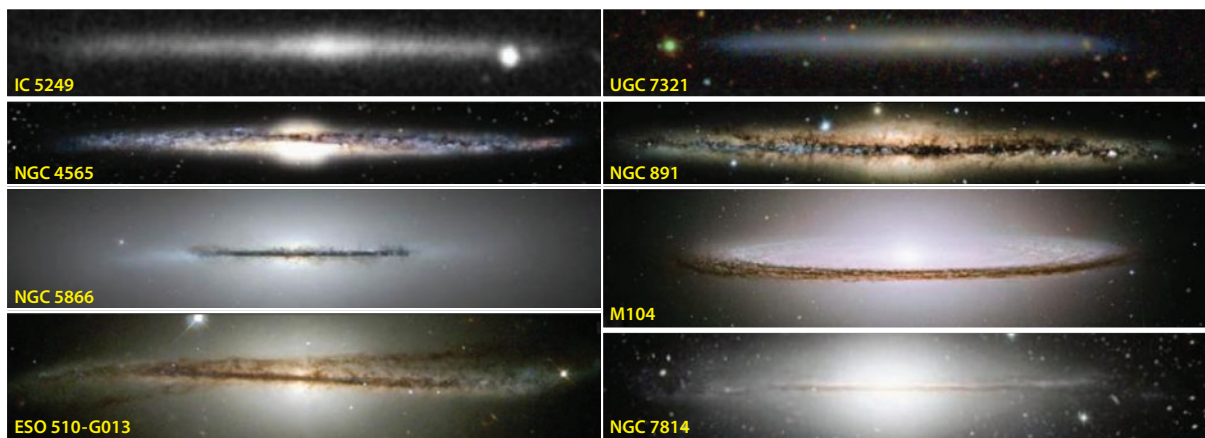


Figure 9

Selected images of edge-on disks and dustlanes from various public Web-galleries. First row: Super-thin galaxies, IC 5249 (*left*; from the Sloan Digital Sky Survey, van der Kruit et al. 2001) and UGC 7321 (*right*; http://cosmo.nyu.edu/hogg/rc3/UGC_732_1rg_hard.jpg); second row: NGC 4565 (*left*; <http://www.cfht.hawaii.edu/HawaiianStarlight/AIOM/English/2004/Images/Nov-Image2003-CFHT-Coelum-1999.jpg>) and NGC 891 (*right*; <http://www.cfht.hawaii.edu/HawaiianStarlight/Posters/NGC891-CFHT-Cuillandre-Coelum-1999.jpg>); third row: NGC 5866 (*left*; <http://heritage.stsci.edu/2006/24/big.html>) and M104 (*right*; <http://heritage.stsci.edu/2003/28/big.html>); fourth row: ESO 510-G013 (*left*; <http://heritage.stsci.edu/2001/23/big.html>) and NGC 7814 (*right*; <http://www.cfht.hawaii.edu/HawaiianStarlight/English/Poster50x70-NGC7814.html>).

and Shostak & van der Kruit (1984) found that the residual velocity field after subtraction of that of the systematic rotation shows no systematic pattern and had a root-mean-square value of only 3–4 km s⁻¹. So, vertical motions must be restricted to only a few kilometer per second (a few parsecs per million years). Then, even a vertical oscillation with a period equal to the typical time of vertical oscillation of a star in the Solar Neighborhood (10⁷ years) or of the rotation of the Sun around the Galactic Center (10⁸ years) would have an amplitude of only 10 to 100 pc. Again, this is of order a few percent or less of the diameter of a galaxy like our own. The absence of such residual patterns shows that the HI layers and, thus, because they are more massive, the stellar disks must be extraordinarily flat, except maybe in their outer regions. This obviously does not hold for galaxies that are or have recently been in interaction.

Recently, Matthews & Uson (2008a,b) found evidence for a pattern of corrugation in the disk of the edge-on galaxy IC 2233. The excursion of the plane is most pronounced in younger tracer populations, such as HI or young stars. The amplitude is up to 250 pc (compared to a radius of order 10 kpc). The older disk shows much less of an effect. IC 2233 is a relatively small galaxy (rotation velocity about 100 km s⁻¹) and has extensive star formation; it appears that the effect is related to the process of star formation.

3.6. Super-Thin Galaxies

We have indicated above that the flattening of the stellar disk b_z/b is smallest for systems that are of late Hubble type, small rotation velocity, and faint (face-on) surface brightness. It is of interest then to look more closely at systems at this extreme end of the range of flattening; such systems are referred to as superthin. Of course, the ones we can identify are seen edge-on. A prime example is the galaxy UGC 7321, studied extensively by Matthews, Gallagher & van Driel (1999), Matthews (2000), Matthews & Wood (2003), Uson & Matthews (2003), and Banerjee, Matthews & Jog (2010). This is a very LSB galaxy (its face-on *B*-band central surface brightness would be ~ 23.4 mag arcsec⁻²) with a scalelength of about 2 kpc, but a projected vertical scaleheight of only 150 pc. There is evidence for vertical structure: It has a color gradient (bluer near the central plane) and appears to consist of two components. Rotation curve analysis (Banerjee, Matthews & Jog 2010; O'Brien, Freeman & van der Kruit 2010c) indicates that it has a large amount of mass in its dark matter halo compared to the luminous component. Its HI is warped in the outer parts, starting at the edge of the light distribution. Extended HI emission is visible at relative high z (more than 2 kpc out of the plane). Pohlen et al. (2003) argue that the deviation in the light profile in the central regions and the shape of the isophotes point at a presence of a large bar.

Another good example of a superthin galaxy is IC 5249 (Byun 1998, Abe et al. 1999, van der Kruit et al. 2001). This also is an LSB galaxy with presumably a small fraction of the mass in the luminous disk. However, the disk scaleheight is not small (0.65 kpc). It has a very long radial scalelength (17 kpc); its faint surface brightness μ_0 then causes only the parts close to the plane to be easily visible against the background sky, while the long radial scalelength assures this to happen over a large range of R . Therefore, it appears thin on the sky. The flattening b_z/b is 0.09 (versus 0.07 for UGC 7321). The stellar velocity dispersions are similar to those in the Solar Neighborhood; disk heating must have proceeded at a pace comparable to that in the Galaxy.

The flattest galaxies appear not only very flat on the sky, but have indeed very small values of b_z/b . However, these two examples show that the detailed structure may be different. Super-thin galaxies do share the property of late-type, faint, face-on surface brightness and small amounts of luminous disk mass compared to that in the dark matter halo.

Kautsch (2009) has reviewed the observations of flat and super-thin galaxies, especially in view of the fact that these late-type, bulgeless systems present challenges to models of disk galaxy

formation within the hierarchical growth context of Λ CDM. These pure disk systems have LSB blue structures with low angular momenta, which may have formed with a lower frequency of merging events than disk galaxies with bulges and thick disks. In large and giant galaxies, the question of the frequency of the presence of a “classical” bulge has been addressed by Kormendy et al. (2010). They find that giant, pure disk galaxies are far from rare, and their existence presents a major challenge to formation pictures with histories of merging in an hierarchical clustering scenario.

3.7. Warps in Stellar Disks

In their outer parts, stellar disks have deviations from both the plane of the inner parts (warps) as well as deviations from the extrapolated exponential surface brightness distributions (truncations). We discuss these phenomena in turn.

First, we examine warps in the outer parts of stellar disks. Studies referred to above (Sanchez-Saavedra, Battaner & Florido 1990; Florido et al. 1991; de Grijs 1997; Reshetnikov et al. 2002) have indicated that most, if not all, disks display warps in their very outer parts, often up to $0.5 h_z$ or more. Recently, Saha, de Jong & Holwerda (2009) have studied edge-on galaxies observed with *Spitzer* in the $4.5\text{-}\mu$ band.⁹ Out of 24 galaxies, they found evidence for warps in 10. The radius of the onset of the warp indicates that there must also be a moderate amount of flaring, in order to match the response to the indicated mass distribution from the light distribution and rotation curve. The warp onset is asymmetric and the more so in small scalelength systems. The reason for this is not clear, but could point to asymmetries in the dark matter distribution. The warp profiles shown in their figures reinforce the point made above about the flatness of disks; in the inner parts, the deviations from a straight line are exceedingly small (only a percent or less of the radial extent). Theoretical work related to warps and dynamics in stellar disks has recently been reviewed by Sellwood (2011a), in the context of collective global instabilities, bending waves, bars, and spiral structure.

Sometimes optical warps are very pronounced, such as in the so-called Integral Sign galaxy UGC 3697 (Burbidge, Burbidge & Shelton 1967; Ann 2007). There have recently been a number of statistical studies (e.g., Schwarzkopf & Dettmar 2001, Ann & Park 2006) from large samples that contain more and less isolated systems. The conclusions are that strong warps are probably all a result of interactions, whereas at least a fraction may arise from accretion of gaseous material. An important point to note is that even isolated galaxies show signs of accretion. Beautiful examples have recently been presented in much detail, including NGC 5907 (Morrison, Boroson & Harding 1994; Martínez-Delgado et al. 2008), NGC 4736 (Trujillo et al. 2009), and NGC 4013 and NGC 5055 (Martínez-Delgado et al. 2009). In NGC 5055, the brightest part of the faint loops has been registered also in the photographic surface photometry of van der Kruit (1979) in two colors; it appeared definitely red and presumably dominated by older stars. These relatively isolated systems appear to show signs for recent accretion events, which therefore must be common. Of course, much is known now about substructure in the halo of our Galaxy (Helmi 2008) and M31 (Ferguson 2007) and the evidence for continuing accretion that this provides, but that is beyond the scope of this review.

3.8. Truncations

Truncations in stellar disks were first found in edge-on galaxies, where the remarkable feature was noted that the radial extent did not grow with deeper photographic exposures (van der Kruit

⁹This paper contains also a rather complete inventory of publications concerning warps, optical, near-IR, as well as HI.

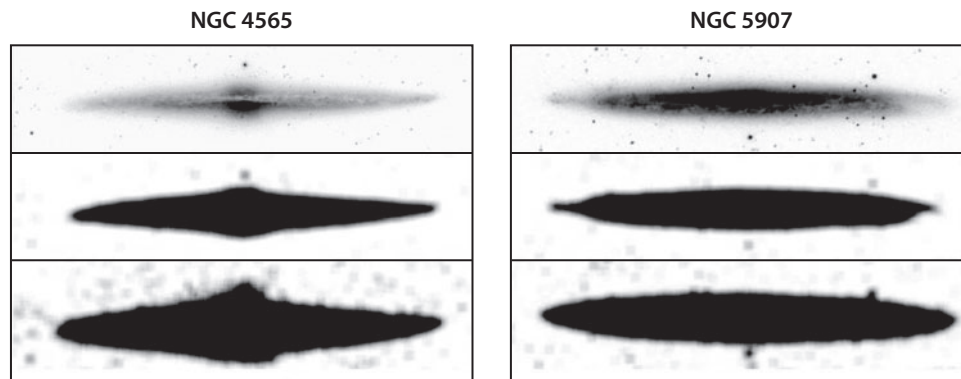


Figure 10

NGC 4565 and NGC 5907 at various light levels. These have been produced from images of the Sloan Digital Sky Survey, which were clipped at three different levels (*top to bottom*), turned into two-bit images, and subsequently smoothed (see van der Kruit 2007, for an explanation of the details). Note that the disks grow significantly along the minor axes but not in radial extent.

1979). Detailed surface photometry (van der Kruit & Searle 1981a,b) confirmed the presence of these truncations in the four brightest, edge-on, disk-dominated galaxies in the northern sky, NGC 891, 4244, 4565, and 5907. For the last two we illustrate this phenomenon of truncation in **Figure 10**. The truncations appear very sharp, although of course not infinitely.¹⁰ Sharp outer profiles are actually obtained after deprojecting near-IR observations of edge-on galaxies (e.g., Florido et al. 2006). Fry et al. (1999), using CCD surface photometry, and de Jong et al. (2007b), using HST star counts, show that the disk of NGC 4244 has a sharp truncation, occurring over only about 1 kpc.

Various models have been proposed for the origin of truncations. In the model by Larson (1976), the truncations are the current extent of the disks while they are growing from the inside out from accretion of external material. This predicts larger age gradients across disks than are observed (de Jong 1996b). Another possibility is that star formation is inhibited when the gas surface (or space?) density falls below a certain threshold for local stability (Fall & Efstathiou 1980, Kennicutt 1989, Schaye 2004). The Goldreich–Lynden-Bell criterion for stability of gas layers gives a poor prediction for the truncation radii (van der Kruit & Searle 1982a). Another problem is that the rotation curves of some galaxies, e.g., NGC 5907 and NGC 4013 (Casertano 1983, Bottema 1996), show features near the truncations that indicate that the mass distributions are also truncated.

Obviously, the truncation corresponds to the maximum in the specific angular momentum distribution of the present disk, which would correspond to that in the protogalaxy (van der Kruit 1987) if the collapse occurs with detailed conservation of specific angular momentum (Fall & Efstathiou 1980). As noted above, if the protogalaxy starts out as a Mestel (1963) sphere with uniform density and angular rotation in the force field of a dark matter halo with a flat rotation curve, a roughly exponential disk results. This disk has then a truncation at about 4.5 scalelengths, so this hypothesis provides at the same time an explanation for the exponential nature of the disk as well as for the occurrence of the truncations. However, it is possible that substantial redistribution of

¹⁰In fact, the statement in van der Kruit & Searle (1981a) reads, “This cut-off is very sharp with an e-folding of less than about 1 kpc,” based on the spacing of the outer isophotes.

angular momentum takes place, so that its distribution now is unrelated to the initial distribution in the material that formed the disks. Bars may play an important role in such redistribution, as suggested by Debattista et al. (2006) and Erwin et al. (2007). In fact, a range of possible agents in addition to bars, such as density waves, heating and stripping of stars by bombardment of dark matter subhalos, has been invoked (de Jong et al. 2007b). Roškar et al. (2008a,b) have studied the origin of truncations or breaks in the radial distributions in stellar disks as related to a rapid drop in star formation and include the effects of radial migration of stars. Observations of stellar populations and their ages in the regions near the truncation (Yoachim, Roškar & Debattista 2010) have been used to provide evidence that migration of stars is a significant phenomenon in the formation and evolution of stellar disks. Finally, there are models (Battener, Florido & Jiménez-Vicente 2002; Florido et al. 2006) in which a magnetic force breaks down as a result of star formation so that stars escape. The evidence for sufficiently strong magnetic fields needs strengthening.

Kregel & van der Kruit (2004b) derive correlations of the ratio of the cut-off radius R_{\max} to the radial scalelength b with b itself and with the face-on central surface brightness $\mu_{0,I}^{\text{fo}}$ (Figure 11). R_{\max}/b does not depend strongly on b , but is somewhat less than the 4.5 predicted from the collapse from a simple Mestel sphere. There is some correlation between R_{\max}/b and $\mu_{0,\text{fo}}$, indicating approximately constant disk surface density at the truncations, as possibly expected in the star-formation threshold model. But this model predicts an anticorrelation between R_{\max}/b and b (Schaye 2004), which is not observed. The maximum angular momentum hypothesis predicts that R_{\max}/b should not depend on b or $\mu_{0,\text{fo}}$ and such a model therefore requires some redistribution of angular momentum in the collapse or somewhat different initial conditions.

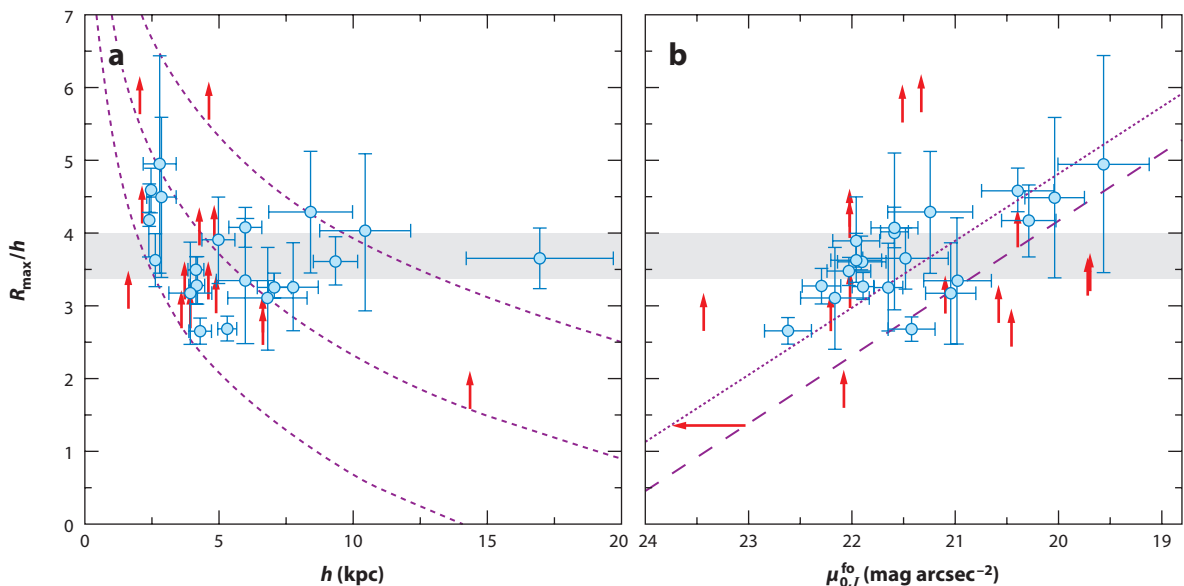


Figure 11

Correlations of R_{\max}/b with scalelength b and face-on central surface brightness $\mu_{0,I}^{\text{fo}}$ for a sample of edge-on galaxies. The gray regions show the prediction from a collapse model as in van der Kruit (1987) and Dalcanton, Spergel & Summers (1997). In panel a, the purple dotted lines show predictions from the star-formation threshold model of Schaye (2004) for three different values of the disk mass; in panel b, the dashed purple line corresponds to the Schaye (2004) prediction, whereas the dotted purple line is the same but arbitrarily shifted by 0.7 mag for an optimum fit. The red arrows are lower limits. (From Kregel & van der Kruit 2004b, and see there for details of the models).

Due to line-of-sight integration, truncations should be more difficult to detect in face-on galaxies than in edge-on ones. The expected surface brightness at 4 scalelengths is about 26 B -mag arcsec⁻², only a few percent of the dark sky.¹¹ In face-on galaxies like NGC 628 (Shostak & van der Kruit 1984, van der Kruit 1988), an isophote map shows that the outer contours have a much smaller spacing than the inner ones. In the usual analysis, one determines an azimuthally averaged radial surface brightness profile. But this will smooth out any truncation if its radius is not exactly constant with azimuthal angle. At this level, spiral disks are indeed often lopsided, as is seen from the $m = 1$ Fourier component of surface brightness maps (Rix & Zaritsky 1995, Zaritsky & Rix 1997), presumably as a result of interactions and merging. The effects are nicely illustrated in the study of NGC 5923 by Pohlen et al. (2002, their figure 9), which has isophotes in polar coordinates. The irregular outline shows that some smoothing occurs contrary to observations in edge-on systems. Unless special care is taken we will always find a (much) less sharp truncation in face-on than in edge-on systems.

Although we do not discuss oval distortions of disks here because they were reviewed by Kormendy & Kennicutt (2004), we emphasize that they are potentially important for studies of truncations and are also of intrinsic interest. Oval distortions in unbarred galaxies can have significant kinematical and dynamical effects.

Pohlen & Trujillo (2006) studied a sample of moderately inclined systems through ellipse-fitting of isophotes in SDSS data. They distinguish three types of profiles: *Type I*, no break; *Type II*, downbending break; and *Type III*, upbending break. Pohlen et al. (2007) have reported that the same profiles occur in edge-on systems; however, of their 11 systems there was only one for each of the types I and III.

Various correlations have been reviewed by van der Kruit (2009). In general, the edge-on and face-on samples agree in the distribution of R_{\max}/b ; however, the fits in moderately inclined systems result in small values of the scalelength. A prime example of a Type III profile in Pohlen & Trujillo (2006) is NGC 3310, which is a well-known case of a merging galaxy (van der Kruit 1976, Kregel & Sancisi 2001). In fact, on close examination of their images at faint levels, many of the Type III systems show signs of outer distortions, presumably due to interactions.

The truncation in the stellar disk in our Galaxy has also been identified using star counts in a number of surveys (Robin, Crézé & Mohan 1992; Ruphy et al. 1996) to occur at a galactocentric radius of 14 to 15 kpc. Typical values for the ratio between the truncation radius and the radial scalelength R_{\max}/b are 3.5 to 4 (see **Figure 11**), so that the Galaxy's scalelength is expected on this basis to be 3.5 to 4 kpc. There is a good correlation between the truncation radius R_{\max} and the rotation velocity (van der Kruit 2008). On average, a galaxy like our own would have an R_{\max} of 15–25 kpc. It is of interest to compare this correlation to the case of NGC 300 (Bland-Hawthorn et al. 2005), which has no truncation even at 10 scalelengths from the center ($R_{\max} > 14.4$ kpc), and therefore is an example of a type I disk in the terminology of Pohlen & Trujillo (2006). Despite showing no sign of truncation down to a very faint surface brightness level, we note that its lower limit to R_{\max} is still consistent with the observed correlation between R_{\max} and V_{rot} in edge-on systems (NGC 300 has a rotational velocity of ~ 105 km s⁻¹, which would give an R_{\max} of 8–15 kpc and an b of 2–4 kpc). NGC 300 could be interpreted as having an unusually small b for its V_{rot} rather than an unusually large R_{\max} for its scalelength. These examples show that at least

¹¹This surface brightness is close to that often associated with the Holmberg diameters (Holmberg 1958), which are often assumed to be diameters at 26.5 B -mag arcsec⁻² and corrected for inclination. For a discussion of the history of Holmberg radii, see the appendix in van der Kruit (2007). Contrary to common belief, they are defined in terms of photographic density (rather than a well-defined surface brightness) in two bands (photographic and photovisual rather than the B -band) and not corrected for inclination.

some of the type III galaxies could arise from the effects of interactions and merging, and type I systems could at least partly be disks with normal truncation radii, but large R_{max}/b and small scalelengths, so that their truncations occur at much lower surface brightness.

3.9. Nuclei of Pure-Disk Galaxies

Late-type pure disk galaxies are commonly nucleated, with central nuclear star clusters (e.g., M33: Kormendy & McClure 1993). For a sample studied by Walcher et al. (2005), the dynamical masses of the nuclear clusters are in the range 8×10^5 to $6 \times 10^7 M_{\odot}$. These star clusters usually lie within a few arcsec of the isophotal centers of the galaxies (e.g., Böker et al. 2002). How are the nuclei able to locate accurately the centers of the apparently shallow central potential wells of their exponential disks? The reason may be that the center of the gravitational field of an exponential disk is actually well-defined: The radial gradient of its potential does not vanish at its center, so the force field defines the center of the disk to within a fraction of the scaleheight of the ISM of the disk, which is of order 100 pc.

Structurally the nuclear star clusters are much like Galactic globular clusters (Böker et al. 2004). Their stellar content is, however, very different. The light of the nuclear star clusters is typically dominated by a relatively young star population (Rossa et al. 2006, Kormendy et al. 2010), but the young population provides only a few percent of the stellar mass. They have an underlying older population with an extended history of episodic star formation (Walcher et al. 2006). This episodic star formation may come from gas funnelled into the center of the galaxy by local torques.

AGNs are rare or absent from these nuclei of pure disk galaxies (Satyapal et al. 2009). For the nucleus of the nearby system M33, with a total nuclear mass of about $2 \times 10^6 M_{\odot}$, Gebhardt et al. (2001) were able to derive an upper limit of $1,500 M_{\odot}$ for a supermassive black hole within the nuclear star cluster.

These nuclear star clusters, with their episodic and extended star-formation history, are interesting in their possible relation to some of the Galactic globular clusters, such as the massive cluster ω Centauri, which also shows evidence of an extended history of episodic star formation (e.g., Bellini et al. 2010) and an inhomogeneous distribution of heavy element abundances. This is unusual in globular clusters. Based on chemical evolution arguments, Searle & Zinn (1978) proposed that the Galactic globular clusters originated in small satellite galaxies that were accreted long ago by the Milky Way. The small galaxies are tidally disrupted but the globular clusters survive. Freeman (1993) and Böker (2008) argued that at least some of the globular clusters may have been the nuclei of such satellite systems.

4. HI DISKS

In this chapter we discuss the distribution and kinematics of the gas in galaxy disks, concentrating on the HI, including that at large radii and warps. We end this section with a brief discussion on dust and dustlanes in disks.

4.1. HI Distributions, Kinematics and Dynamics

The study of the distribution of HI in samples of more than a few disks in galaxies has been possible only since the advent of aperture synthesis measurements of the 21-cm line. Early observations with single disk instruments could be made only for the very nearest systems, notably the Andromeda Nebula (in particular, Roberts & Whitehurst 1975). Observations with the necessary angular resolution started with the Owens Valley Two-Element Interferometer (e.g., Rogstad & Shostak 1971), the Half-Mile Telescope at Cambridge (e.g., Baldwin et al. 1971), and the WSRT

(e.g., Allen, Goss & van Woerden 1973). This early work up to about 1977 has been reviewed in van der Kruit & Allen (1978), although mostly in the context of kinematics.

These studies revealed distributions of the HI in most cases to be much more extended than the stellar disks and often warped away from the plane of the stellar disk beyond the boundaries of the light distribution, both in edge-on (Sancisi 1976) and moderately inclined systems (Rogstad & Shostak 1971; Bosma 1981a,b). The most important finding was that the rotation curves at these radii remained flat (see Section 1.1).

Since then, many observations of disk galaxies have been taken. The first extensive survey, including comparison with optical surface photometry, was done by Wevers, van der Kruit & Allen (1986). More recently, the extensive WHISP survey (Kamphuis, Sijbring & van Albada 1996; van der Hulst, van Albada & Sancisi 2001; García-Ruiz, Sancisi & Kuijken 2002; Swaters et al. 2002; Swaters & Balcells 2002; Noordermeer et al. 2005; Noordermeer et al. 2007) was made. The most advanced survey at this stage is THINGS (de Blok et al. 2008, Walter et al. 2008), which provides very high-resolution HI maps and rotation curves and has been analyzed by comparison with 3.6- μm data from SINGS. The details of the rotation curves correlate with the absolute magnitude of the galaxies, as was first described by Broeils (1992). Luminous galaxies have rotation curves that rise steeply, followed by a decline and an asymptotic approach to the flat outer part of the curve; low-luminosity galaxies show a more gradual increase, never quite reaching the flat part of the curve over the extent of their HI disks. Although in some curves the rotation velocity does decrease at large radii, none of the galaxies shows a decline in their rotation curves that can unambiguously be associated with a cut-off in the mass distribution so that in no case has the rotation curve been traced to the limit of the dark matter distribution (de Blok et al. 2008).

We comment on a number of properties of the surface density distribution of the neutral hydrogen first. The total content, especially relative to the amount of starlight M_{HI}/L (a property that is distance independent), is well-known to correlate with morphological type (e.g., Roberts & Hayes 1994), whereas in later types the more luminous galaxies contain relatively less HI (Verheijen & Sancisi 2001). The HI diameter compared to the optical diameter (at 25 B -mag arcsec $^{-2}$) is about 1.7 with a large scatter, but does not depend on morphological type or luminosity, according to Broeils & Rhee (1997). However, there are very good correlations between HI mass and diameter, $\log M_{\text{HI}}$, and $\log D_{\text{HI}}$, both with slopes of about 2. This implies that the HI surface density averaged over the whole HI disk is constant from galaxy to galaxy, independent of luminosity or type. Also note that there is a relatively well-defined maximum surface density in disks of galaxies observed (at least with resolutions of the current synthesis telescopes), which amounts to about $10 M_{\odot} \text{ pc}^{-2}$ (Wevers, van der Kruit & Allen 1986).

Many systems have asymmetries in their HI morphologies or kinematics. Often this is in the form of lopsidedness in the surface density distributions. This can to some extent already be seen in the asymmetries in integrated profiles; studies have claimed that up to 75% of galaxies are asymmetric or lopsided (Matthews, van Driel & Gallagher 1998; Hayes et al. 1998; Swaters et al. 1999; Noordermeer et al. 2005) at some detectable level. Lopsidedness appears to be independent of whether or not the galaxy is isolated, so interactions or mergings cannot always be invoked as its origin. It is suggested that it either is an intrinsic property of the disks or is induced by asymmetries in the dark matter distribution (Noordermeer, Sparke & Levine 2001).

The extraction of kinematic data from the raw observations of moderately inclined systems has often been discussed. The basics are summarized in van der Kruit & Allen (1978), Bosma (1981a), Wevers, van der Kruit & Allen (1986), and Begeman (1987). The results are a radial distribution of HI surface brightness, a rotation curve, and a radial distribution of velocity dispersion; from these one can, in principle, make maps of residuals compared to these azimuthal averages. The

derivation of the HI velocity dispersions is easiest in face-on spirals, where there is no gradient in the systematic motions across a telescope beam (van der Kruit & Shostak 1982, 1984; Shostak & van der Kruit 1984).

For edge-on systems, the procedure is more complicated as a result of the line-of-sight integration. Various methods have been devised, initially only to derive the rotation curve and the radial distribution of HI surface brightness, later in some cases also the flaring (the increasing thickness as a function of galactocentric radius) of the HI layer (e.g., Sancisi & Allen 1979; van der Kruit 1981; Rubin et al. 1985; Sofue 1986; Mathewson, Ford & Buchhorn 1992; García-Ruiz, Sancisi & Kuijken 2002; Takamiya & Sofue 2002; Uson & Matthews 2003; Kregel & van der Kruit 2004a; Kregel, van der Kruit & de Blok 2004). Recently, Olling (1996a,b) and O'Brien and colleagues (O'Brien et al. 2010; O'Brien, Freeman & van der Kruit 2010a,b) have also fit for the HI velocity dispersion. The paper by O'Brien, Freeman & van der Kruit (2010a) provides a detailed description of the various methods and a discussion on the relative merits and pitfalls.

In general, for larger disk galaxies, the radial distributions show (sometimes in addition to a central depression) a radial surface density that falls off more slowly than that of the starlight, a rotation curve that rises to a maximum and stays at that level, and a velocity dispersion of 7–10 km s⁻¹, often near the higher end of this range in the inner regions and in spiral arms and in the lower range in the outer parts and interarm regions (Shostak & van der Kruit 1984, van der Kruit & Shostak 1984, Sicking 1997).

The velocity dispersion of the HI can be measured only in cases where there is a negligible gradient in the overall radial velocity over the beam of the radio telescope. Early determinations have been made in our Galaxy, e.g., van Woerden (1967) found 7 km s⁻¹ for the Solar Neighborhood, and Emerson (1976) found 12 ± 1 km s⁻¹ from aperture synthesis observations using the Half-Mile Telescope at Cambridge. For larger angular size galaxies, the use of face-on galaxies (as judged from the narrowness of their integrated HI profiles) is required to fulfill this condition. It was done in much detail on three galaxies that are only a few degrees from face-on (NGC 3938, 628, and 1058; van der Kruit & Shostak 1982, 1984; Shostak & van der Kruit 1984). They found that the dispersions over the optical extent of the disks were rather constant, with no significant decline with radius at 7–10 km s⁻¹. Only in NGC 628 was a systematic difference seen between the interarm region (at the lower end of the range quoted) and the spiral arms themselves (the higher end).

The most recent study of galaxies that are not very close to face-on is THINGS by Tamburro et al. (2009), where references to other earlier work can be found. They do find significant declines of velocity dispersion with radius in their sample, but there appears a characteristic value of 10 ± 2 km s⁻¹ at the outer extent of the star-forming part of the disk. Inward of this, the dispersion correlates with indicators of star formation, suggesting that the supernovae associated with this star-formation activity are driving the turbulence, although magnetorotational instabilities may add significantly to the random motions as well. In edge-on galaxies, O'Brien, Freeman & van der Kruit (2010a,b) made detailed analyses to retrieve the radial distributions of HI surface density, rotation velocity, and velocity dispersion, and found that there is significant structure, but not much systematic radial decline. This study involved HI rich, dwarf systems, quite dissimilar from the THINGS sample. Typical dispersions are 6.5 to 7.5 km s⁻¹, increasing with the amplitude of the rotation curve. In the Solar Neighborhood, the velocity dispersion of OB stars is comparable to that in the HI, so stars are born with that same amount of random motion, which then increases as a result of secular evolution. The same will happen in other spirals, but in dwarf galaxies the stellar velocity dispersions are similar to the ones reported in HI. This may suggest that no significant secular evolution of random motions occurs in dwarf systems.

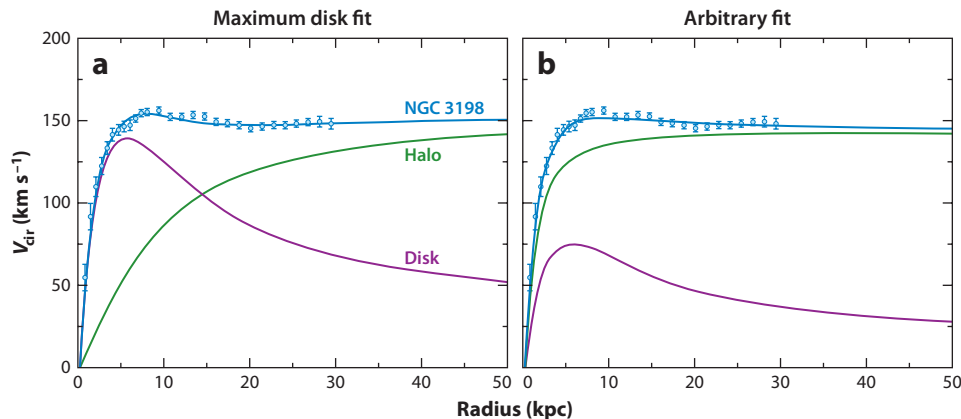


Figure 12

The rotation curve decomposition for NGC 3198. The shape of the curve for the dark matter halo is set by a core radius that determines the initial rise and tends asymptotically to that of a mass density distribution that falls off $\propto R^{-\gamma}$ with γ close to 2. The shape of the disk curve is that of the exponential disk with a scalelength from the light distribution. (a) The maximum disk fit that maximizes the amplitude of the disk rotation curve; and (b) an arbitrary fit with a disk mass 0.3 times that of the maximum disk. (From van Albada et al. 1985).

4.2. Dark Matter Halos

The discovery of dark matter halos has been described very briefly in Section 1.1, where also the concept of the maximum disk hypothesis (see **Figure 12**) was introduced, in which the contribution of the stellar disk to the rotation curve is taken to be as large as possible, consistent with the observations (Carignan & Freeman 1985, van Albada et al. 1985, van Albada & Sancisi 1986). As mentioned above, this contribution has, in practice, an amplitude at its maximum within the range 0.85 ± 0.10 of the observed maximum rotation, following Sackett (1997). The evidence from stellar dynamics (see Section 3.2) is that the majority of galaxies have disk masses significantly below maximum disk, except for some galaxies with the highest surface brightness.

Recent reviews of disk masses in galaxies and implications for decompositions of rotation curves into contributions from dark and baryonic matter have been presented by van der Kruit (2009) and McGaugh (2009) at the Kingston symposium. These reviewers take the view that most galaxy disks are submaximal, except possibly those with the highest surface brightness and surface density. In contrast to these studies involving mostly nonbarred galaxies, we note that Weiner, Sellwood & Williams (2001) and Pérez et al. (2004) find, from detailed fluid dynamical gas flows in some barred galaxies, that their disks are close to maximal. Debattista & Sellwood (2000) argue, from the observed rapid rotation of the bars of barred galaxies, that the stars are dominating the gravitational field in the inner regions of these galaxies.

The thickness of the gas layer in a disk galaxy can be used to measure the surface density of the disk. It has been known for a long time that this layer in our Galaxy is flaring (for a recent discussion, see Kalberla & Kerp 2009). Assume that the vertical density distribution of the exponential stellar disk is locally isothermal ($n = 1$ in Equation 1). If the HI velocity dispersion is $\langle V_z^2 \rangle_{\text{HI}}^{1/2}$ and isotropic, and if the stars dominate the gravitational field, then the HI layer has a full width at half maximum (to $\lesssim 3\%$) of

$$W_{\text{HI}} = 1.7 \langle V_z^2 \rangle_{\text{HI}}^{1/2} \left[\frac{z_0}{\pi G(M/L)\mu_0} \right]^{1.2} e^{R/2b}. \quad (20)$$

So, if the HI velocity dispersion is independent of radius, the HI layer increases exponentially in thickness with an e-folding length of $2\,b$. This was first derived and applied to HI observations of NGC 891 by van der Kruit (1981) to demonstrate that the dark matter indicated by the rotation curve did indeed not reside in the disk but in a more spherical volume. Using the photometry in van der Kruit & Searle (1981b) and the observed HI flaring (Sancisi & Allen 1979) and taking a gaseous velocity dispersion of $10\,\text{km s}^{-1}$ resulted in a rotation curve of the disk alone with a maximum of $\sim 140\,\text{km s}^{-1}$. A smaller value for $\langle V_z^2 \rangle_{\text{HI}}^{1/2}$ would, according to Equation 20, result in a smaller value for the inferred M/L for the same HI thickness and, therefore, to a lower value for the maximum disk-alone rotation. The observed maximum rotation velocity is $225 \pm 10\,\text{km s}^{-1}$, which indicates that NGC 891 is not maximum disk. In a similar analysis, Olling (1996b) inferred for NGC 4244 that the maximum disk-alone rotation velocity is between 40% and 80% of the observed rotational velocity.

Another important property of dark matter halos for understanding galaxy formation is their three-dimensional shape. There are various ways to address this issue, of which the use of the flaring of the HI layer is the most prominent. It was first developed by Olling (1995) and subsequently applied to the nearby edge-on dwarf galaxy NGC 4244 (Olling 1996a,b). He found the dark halo of this galaxy to be highly flattened. Observations of the kinematics in polar ring galaxies provide estimates of the potential gradients in the two orthogonal planes of the galaxies. These galaxies can potentially give useful information about the shapes of their dark halos (Sackett 1999), although it is possible that special halos are needed to host these rare polar ring systems. The resulting halo flattenings derived for polar ring galaxies and also for streams in the halo of the Galaxy (Helmi 2004) range from a few tenths to unity.

A more extensive survey of a sample of eight late-type, HI-rich dwarfs in which the dark halo appears to dominate the gravitational field even in the disk was undertaken by O'Brien et al. (2010). The basic premise of the approach is that the radial gradient of the dark matter halo force $\partial K_R / \partial R$ can be measured from the rotation curve after correction for the contribution of the stellar disk and its ISM, whereas the flaring of the HI layer together with a measurement of the velocity dispersion of the HI provides a measure of the vertical gradient $\partial K_z / \partial z$. The ratio of the two force gradients is related to the flattening of the dark halo (assumed spheroidal), as measured by the axis ratio c/a . The derivation of the necessary properties from the HI observations has been presented by O'Brien, Freeman & van der Kruit (2010a,b). The method relies on two assumptions concerning the HI velocity dispersion, that it is isotropic (because we measure in an edge-on galaxy the line-of-sight dispersion component parallel to the plane and use in the analysis the vertical component) and isothermal with z .

The first galaxy for which this analysis has been completed is UGC 7321 (O'Brien, Freeman & van der Kruit 2010c). The halo density distribution was modelled as a pseudoisothermal spheroid (Sackett et al. 1994) and the disk as a double exponential determined from R -band surface photometry. After allowing for the gravitational field of the gas layer, the hydrostatic equations give the M/L of the disk and a value for the flattening of the dark matter halo. For UGC 7321, the M/L in the disk is very low: The contribution of the stellar disk to the radial force is small and is far below maximum disk in this LSB galaxy [Banerjee, Matthews & Jog (2010) reached the same conclusion]. The best fits of the force gradients $\partial K_z / \partial z$ from the various components are shown in **Figure 13**. The vertical gradient of the total vertical force field derived from the hydrostatics of the flaring gas layer (for stars + gas + halo) is shown in purple as a function of radius. After taking off the known contribution from the gas layer, the light blue curve labeled halo + stars shows the remaining contribution from the halo + stars. This is well modelled for $R > 3\,\text{kpc}$ by the adopted contributions from the stars and the dark halo model (*dashed curve*). Note that the shape of the observed and fitted curves is remarkably similar for $R > 3\,\text{kpc}$. For this best fit, the

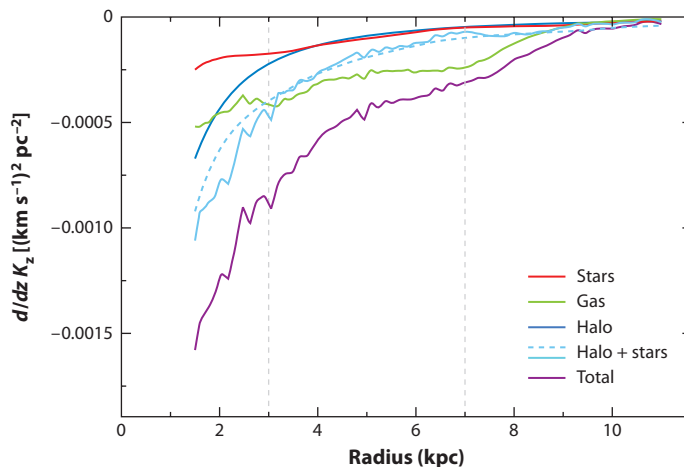


Figure 13

The vertical gradients of the force field for various components in the edge-on galaxy UGC 7321. The line “total” is inferred from the thickness of the HI layer and the HI velocity dispersion; the line “gas” is from the observed HI and corrected for helium. Subtracting these contributions gives the line “halo+stars” (*solid*). The lines “halo + stars” (*dashed*), are the best fits, where that for the stars comes from the observed luminosity distribution with the best fitting mass-to-light ratio. The measured halo flattening was $q = 1.0 \pm 0.1$. The vertical dotted gray lines show the radial regime used for the fit. (From O’Brien, Freeman & van der Kruit 2010c).

dark halo model is spherical. More analysis is required for the rest of the sample to draw firm conclusions.

In the Galaxy, the flaring of the disk can be studied in much more detail. An extensive study has been performed recently by Kalberla et al. (2007) based on the Leiden/Argentina/Bonn all-sky survey of Galactic HI (see also Kalberla & Kerp 2009). In this study, they map the Galactic HI layer and its flaring and warp in much detail and they fit the observations with models containing a dark matter disk as well as a dark matter halo. Their best fitting model has a local disk surface density of $52.5 M_{\odot} \text{ pc}^{-2}$ with a scalelength of 2.5 to 4.5 kpc. This corresponds to a maximum disk-alone rotation velocity of, respectively, 200 to 130 km sec^{-1} . So again, if the Galaxy has a normal scalelength (~ 4 kpc) for its rotation velocity, it is far below maximum disk, but if the scalelength is 2.5 kpc, it is close to maximum disk. A complete analysis of the flaring HI disk in terms of Galactic dark matter distribution yields evidence for a significant dark matter disk with a large scalelength of order 8 kpc and, in addition, a dark matter ring at 13 to 18 kpc. This ring could be the remnant of a merged dwarf galaxy.

The distribution of the density in the inner parts of dark halos has been a subject of much attention, as a consequence of the cold dark matter (CDM) paradigm (Blumenthal et al. 1984, 1986), in which structure grows hierarchically with small objects collapsing first and then merging into massive objects. Cosmological n -body simulations based on Λ CDM (Dubinski & Carlberg 1991; Navarro, Frenk & White 1996, 1997) have long predicted that the inner density profile of the dark matter halo ($\rho \propto r^{\alpha}$) would have an exponential slope α of about -1 (a cusp), whereas observations seemed to suggest a slope near zero (a core). The high spatial resolution of the THINGS data (de Blok et al. 2008) is well suited to investigate this matter. They find that, for massive disk-dominated galaxies, all halo models appear to fit equally well, whereas for low-mass galaxies a core-dominated halo is clearly preferred over a cusp-like halo. This cusp-core controversy (with α assuming somewhat different values) is a long-lasting hot item in the study

of HI-rich, dwarf galaxies and LSB systems, where the contribution of the dark matter to the rotation curve is large even in the inner regions. Recently, de Blok (2010) has summarized the situation in such systems, concluding that the problem is still unsolved, even with the use of current high-resolution rotation curves.

4.3. Outer HI and Warps

The warping of the outer parts of the neutral hydrogen layer of our Galaxy has been known for a long time. It was discovered independently in early surveys of the Galactic HI in the north by Burke (1957) and in the south by Kerr and Hindman (see Kerr 1957). In external spiral galaxies, the first indication came from work by Rogstad, Lockart & Wright (1974), when they obtained aperture synthesis observations of the HI in M83. The distribution and the velocity field of the HI both showed features that could be interpreted as a warping of the gaseous disk in circular motions in inclined rings. This later became known as the tilted-ring description for kinematic warps, and many more galaxies have been shown to have such deviations using this method (e.g., Bosma 1981a,b). The case that this warping occurs in many spiral galaxies was strengthened by the early observations of edge-on systems. Sancisi (1976) was the first to perform such observations and showed that the HI in four out of five observed edge-ons (including NGC 4565 and NGC 5907) displayed strong deviations from a single plane. Sancisi (1983) discussed these warps in somewhat more detail and, in particular, noted that in the radial direction the HI surface densities often display steep drop-offs followed by a shoulder or tail at larger radii.

The most extreme (prodigious) warp in an edge-on system was observed by Bottema, Shostak & van der Kruit (1987) (see also Bottema 1995, 1996) in NGC 4013. García-Ruiz and colleagues (García-Ruiz 2001; García-Ruiz, Sancisi & Kuijken 2002) presented 21-cm observations of a sample of 26 edge-on galaxies in the northern hemisphere. This showed that HI warps are ubiquitous; the researchers state in the abstract to their paper that “all galaxies that have an extended HI disk with respect to the optical are warped.” Studies of possible warps in the stellar disks have also been made (for recent results, see Section 3.7); although there is evidence for such stellar warps in most edge-on galaxies, the amplitude is very small compared to what is observed in the HI.

The origin of warps has been the subject of extensive study and has been reviewed, for example, by García-Ruiz, Sancisi & Kuijken (2002), Shen & Sellwood (2006), Binney (2007), and Sellwood (2011a). Although none of the models is completely satisfactory, most workers seem to agree that it has something to do with a constant accretion of material with an angular momentum vector misaligned to that of the main disk. In models by Jiang & Binney (1999) and Shen & Sellwood (2006), this results in an inclined outer torus in the dark matter halo that distorts the existing disk and causes it to become warped. The possibility of a misalignment in the angular momenta and, therefore, of the principal planes of the stellar disk and the dark halo (Debattista & Sellwood 1999) has recently received some observational support from the observations of Battaglia et al. (2006) of NGC 5055. The HI data suggest that the inner flat disk and the outer warped part of the HI have different kinematic centers and systemic velocities, suggesting a dark matter halo with not only a different orientation, but also an offset with respect to the disk. The detailed study of the HI in NGC 3718 by Sparke et al. (2009) shows an extensive warping, for which the observed twist can be explained as a result of differential precession in a fairly round dark halo with the same orientation as the disk. Briggs (1990) used existing observations and tilted-ring models in moderately inclined galaxies to define a set of “rules of behavior for galactic warps” (see his abstract). One was that “warps change character at a transition radius near R_{Ho} .” The latter radius is the Holmberg radius (see Section 3.8) listed for 300 bright galaxies in Holmberg (1958).

The onset of HI warps seems to occur very close to the radius of the truncation in the stellar disk (van der Kruit 2001). This can be illustrated with two archetypal examples. In an edge-on

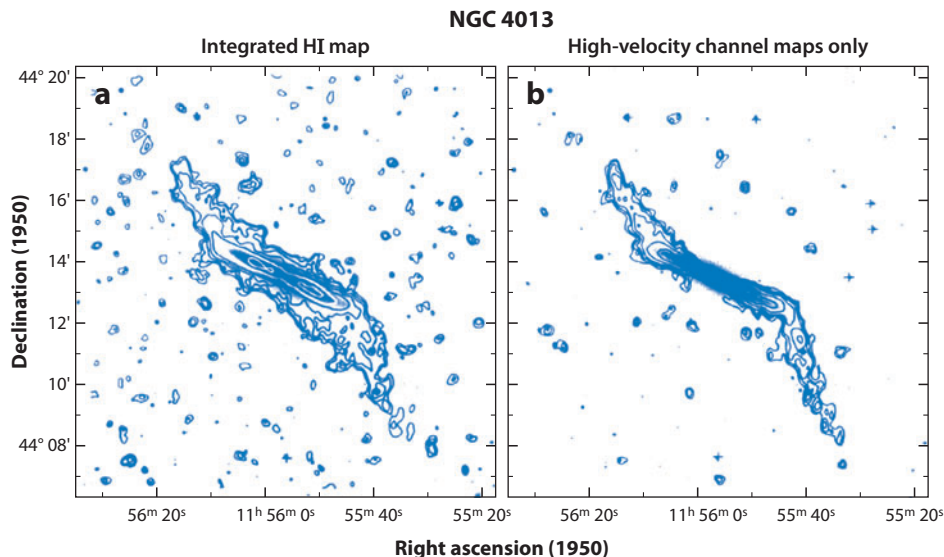


Figure 14

The HI distribution in the edge-on spiral galaxy NGC 4013 (Bottema, Shostak & van der Kruit 1987). (a) The integrated HI map, and (b) only the high-velocity channel maps. The latter selects the HI along a line perpendicular to the line of sight to the galaxy. The warp is less well defined in panel *a*, because the azimuthal angle in the plane of the galaxy, along which the deviation of the warp is largest, is not precisely perpendicular to the line of sight. The warp starts very abruptly at almost exactly the truncation radius of the stellar disk. (From Bottema 1995).

galaxy, the most pronounced warp known is in NGC 4013 (Bottema, Shostak & van der Kruit 1987; Bottema 1995, 1996). The HI warp starts very abruptly at the truncation of the stellar disk (see **Figure 14**) and is accompanied by a significant drop in rotational velocity. The latter suggests a truncation in the disk mass distribution as well as in the light. A face-on spiral with an HI warp is NGC 628 (Shostak & van der Kruit 1984, Kamphuis & Briggs 1996). The velocity fields suggest a warp in the HI, starting at the edge of the optical disk.

In an extended study, van der Kruit (2008) listed the following general characteristics of HI warps. Whenever a galaxy has an HI disk extended with respect to the optical disk, it has an HI warp (García-Ruiz, Sancisi & Kuijken 2002). Many galaxies, but not all, in this sample have relatively sharp truncations in their stellar disks. When an edge-on galaxy has an HI warp, the onset occurs just beyond the truncation radius. Similarly, in less inclined galaxies, the warp is seen at the boundaries of the observable optical disk (Briggs 1990). In many cases the rotation curve shows a feature at about the truncation radius (Casertano 1983, Bottema 1996), which indicates that the truncation occurs also in the mass. The onset of the warp is abrupt and discontinuous and coincides in the large majority of cases with a steep drop in the radial HI surface density distribution, after which this distribution flattens off considerably. The inner disks are extremely flat (both stellar disks as well as in gas and dust), and the onset of the warp is abrupt; beyond that, according to Briggs (1990), the warp defines a “new reference frame” (see his abstract).

These findings suggest that the inner flat disk and the outer warped disk are distinct components with different formation histories, probably involving different epochs. The inner disk forms initially, and the warped outer disk forms as a result of much later infall of gas with a higher angular momentum in a different orientation. This is also consistent with an origin of the disk truncations

that is related to the maximum specific angular momentum available during its formation, because then the truncation is also in the disk mass, giving rise to the abruptness of the onset of the warps.

The misalignment of the material in the inner disk and the outer disk and warp has been modelled by Roškar et al. (2010) as a result of the interaction between infalling cold gas and a misaligned hot gaseous halo. The gas that forms the warp is torqued and aligned with the hot gaseous halo rather than the inner disk. In this model, the outer accreted gas thus responds differently to the halo than the gas that has formed the inner disk. Although this may be consistent with the observed correlation of the onset of the warp and the truncation or break in the stellar disk, the abruptness of the onset of the warp may not follow naturally. Furthermore, this mechanism requires the existence of a hot gaseous halo, and the question is whether these are present in galaxies with smaller rotation amplitudes; the presence of warps in M33-size galaxies would then be another argument against this hypothesis.

To what extent have star formation and chemical enrichment taken place in these gaseous warps? The early work of Ferguson et al. (1998a,b) established the presence of star formation in regions beyond two R_{25} in a few galaxies through the detection of faint HII regions, whereas emission line ratios indicated very low abundances of oxygen and nitrogen in these regions. Since then, much work has been done and more is in progress, in particular in ANGST (Dalcanton et al. 2009). Early results of this project have been published for M81 (Williams et al. 2009b, Gogarten et al. 2009) and NGC 300 (Gogarten et al. 2010), but those do not yet refer to distances beyond the visible spiral structure. However, the disks do contain mostly old stars at these radii, in agreement with the view that the disk inside the truncation region and the radial onset of the HI warp forms at an early epoch in the galaxy's evolution. In NGC 2976 (Williams et al. 2010), populations of old ages are found at all radii, also beyond the break in the luminosity profile, but star formation does not appear now to extend into this outer zone. This galaxy may have been in interaction recently with the M81 group.

Shostak & van der Kruit (1984, see their figure 3) pointed out that in NGC 628 (M74) the extended, warped HI displays spiral structure that shows a smooth continuation of the prominent spiral structure in the main disk, right through the onset of the warp. Particularly interesting for studying star formation and its history in disks beyond the truncation is the comparison of outer HI with UV imaging from GALEX. Bigiel et al. (2010a) compare the HI from the THINGS (HI) survey with the far-UV data from GALEX and conclude that, although star formation does clearly take place in the outer HI, its efficiency is extremely low compared to that within the optical radius (truncation). A detailed comparison of images for M83 (Bigiel et al. 2010b; see also **Figure 15**) shows a clear correlation between star formation and HI surface density. The conclusion that star formation is proceeding in this galaxy in the very outer parts also follows from the work of Davidge (2010), comparing GALEX imaging to deep optical (Gemini) images of the outer regions of M83.

4.4. Dustlanes in Disks

We do not review in detail the distributions and properties of dust in disks of galaxies. However, we noted above that dustlanes are very straight, such as illustrated in **Figure 9**, at least in disks of massive galaxies and indicate that galaxy disks are extraordinarily flat. It has been known for a long time that dustlanes sometimes are less well defined in galaxies of later type and dwarfs. A good example is NGC 4244, which is a late-type, relatively small, pure-disk galaxy (van der Kruit & Searle 1981a), where the dustlane is not sharply outlined against the stellar disk. Dalcanton, Yoachim & Bernstein (2004) studied a sample of edge-on galaxies and found that systems with maximum rotation velocities larger than 120 km s^{-1} have well-defined dustlanes, whereas in those with smaller rotations the scaleheight of the dust is systematically larger and the distribution

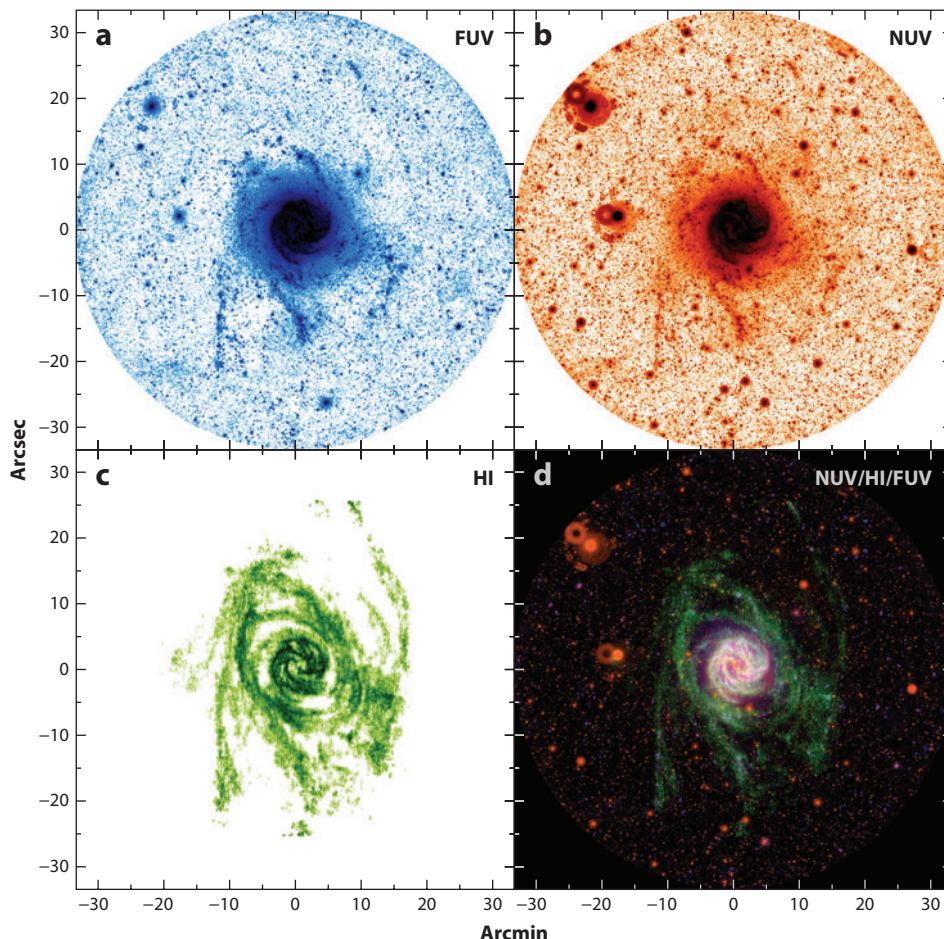


Figure 15

Images of M83, (a) GALEX far-UV, (b) near-UV, (c) HI map from THINGS, and (d) a combination of the three with the HI smoothed (From Bigiel et al. 2010a).

much more diffuse. Indeed, NGC 4244 has a maximum rotation velocity of about 115 km s^{-1} . This finding may have important implications for our understanding of the star-formation history and evolution of disks.

Dalcanton, Yoachim & Bernstein (2004) suggest that the transition at 120 km s^{-1} marks the rotation speed above which the disks become gravitationally unstable, whereby instabilities in the disk lead to fragmentation of the gas component with high density during a collapse that then gives rise to thin dustlanes. In a study of the vertical distributions in a number of low-mass, edge-on galaxies, Seth, Dalcanton & de Jong (2005) find that not only does the dynamical heating of the stellar population appear to occur at a much reduced rate compared to the Galactic disk in the Solar Neighborhood, but in these low-mass systems the vertical distribution of the young stellar population and of the dust layer is thicker than those in the Milky Way. This is consistent with a cold ISM in slowly rotating galaxies that has a larger scaleheight and, therefore, with an absence of well-defined dustlanes in such systems. Seth, Dalcanton & de Jong (2005) fit the distributions with an isothermal sheet ($n = 1$ in Equation 1 with $z_0 = 2b_z$). In NGC 4144 (rotation velocity 67 km s^{-1}), the dust has a scaleheight z_0 of about 0.5 kpc or an exponential scaleheight of half that. For comparison, in the Milky Way the three-dimensional distribution of dust has been modelled

by Drimmel & Spergel (2001): Their flaring dust disk has an exponential scaleheight at the solar radius of about 0.2 kpc.

We may examine more massive edge-on galaxies with rotation velocities well over 200 km s^{-1} to compare with the low-rotation systems. For example, three such galaxies with obvious dustlanes are NGC 4565, 891, and 7814, for which minor axis profiles (in blue light) are available in the papers of van der Kruit & Searle (1981a,b, 1982b). When we determine the height above the symmetry plane at which the effect of the dust extinction is about one magnitude compared to the extrapolated minor axis profile of the stellar light, we get values of, respectively, 0.9, 0.7, and 0.6 kpc. These are undoubtedly overestimates when used as indications for the dust scaleheights; Kylafis & Bahcall (1987), for example, find that the dust scaleheight in NGC 891 is 0.22 kpc, compared to the stellar scaleheight of 0.5 kpc (van der Kruit & Searle 1981b). Wainscoat, Hyland & Freeman (1989) determined in IC 2531 (an NGC 891-like, edge-on galaxy) that the scaleheight of the old disk stars is about 0.5 kpc, whereas that of the dust is a quarter of that. A similar determination of the height at which the minor-axis profile indicates an absorption of one magnitude compared to the extrapolated profile yields about 0.5 kpc. On this basis, the exponential scaleheights of the dust layers in the three systems just mentioned are of the order of 3 or 4 times less than those of the old stellar disks. The important inference is that the diffuse dust layers in slow rotators have, in absolute measures, thicknesses that are not very different from those in massive galaxies with high rotation velocities.

In early-type, edge-on galaxies such as NGC 7814 and NGC 7123, where the spheroids dominate the light (and presumably stellar mass) distributions, the situation appears different. The dust distributions in these systems have scaleheights comparable to those of the stellar disks (Wainscoat, Hyland & Freeman 1989), which are of the order of 0.5 to 1 kpc. This may be the result of much longer dissipation times due to the lower gas content, so that the scaleheights of the stars (from which the dust comes) and the dust are similar.

In the sample of late-type, gas-rich, dwarf, edge-on galaxies studied by O’Brien, Freeman & van der Kruit (2010b), the mean HI velocity dispersion increases as a function of the maximum rotational velocity of the HI disk from about 5 to 8 km s^{-1} for rotation velocities of 70 to 120 km s^{-1} . The scaleheight b of a Gaussian dust layer is related to the ISM velocity dispersion σ by

$$\frac{\sigma^2}{b^2} = -\frac{\partial K_z}{\partial z} = 4\pi G\rho_o, \quad (21)$$

where ρ_o is the mid-plane total density. The density $\rho_o = \Sigma/2b_z$, where Σ is the typical surface density of a disk. Σ and the stellar scaleheight are both approximately proportional to the maximum circular velocity V_c (Kregel, van der Kruit & de Grijs 2002; Kregel, van der Kruit & Freeman 2005; Gurovich et al. 2010), so the typical value of ρ_o is independent of V_c , and we expect the scaleheight of the dust layer to be directly proportional to the ISM velocity dispersion σ . In the O’Brien sample of galaxies, the galaxy with the largest V_c (IC2531) shows a clean, well-defined dustlane, as expected from the Dalcanton et al. observations. However, there is no evidence for a decrease in σ as V_c increases in the O’Brien et al. sample, so those data do, therefore, not support the variable turbulence explanation for the change in dustlane morphology with rotation velocity.

5. CHEMICAL EVOLUTION AND ABUNDANCE GRADIENTS

The stars and gas in galactic disks have a mean metallicity that depends on the luminosity of the galaxy (e.g., Tremonti et al. 2004) and often shows a radial gradient. In a large galaxy like the Milky Way, the typical disk metallicity [Fe/H] is near that of the Sun. For example, in the Solar Neighborhood, the metallicity of the disk stars has a mean of about -0.2 and ranges from about

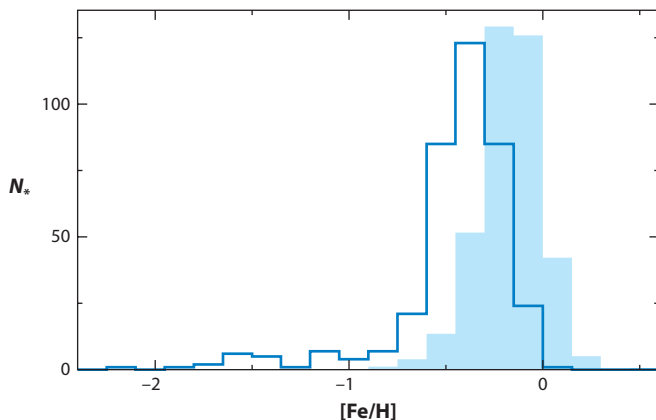


Figure 16

Metallicity distribution function for stars in the bar of the Large Magellanic Cloud, compared to the Solar Neighborhood metallicity distribution function (MDF) from McWilliam (1990) (*light blue shading*). The Solar Neighborhood MDF is about 0.2 dex more metal-rich (From Cole et al. 2005).

+0.3 to -1.0 (e.g., McWilliam 1990). **Figure 16** compares the stellar metallicity distribution functions (MDFs) of the Solar Neighborhood and the bar of the LMC. As expected from the lower luminosity of the LMC, the LMC MDF is displaced toward lower metallicities, but the shapes of the two MDFs are similar.

The MDF is believed to come from the local chemical evolution of the stars and ISM, including the effect of infall of gas from outside the Galaxy. The presence of a fairly tightly defined radial abundance gradient in the stars and in the gas in many disk galaxies suggests that the chemical evolution of the disk is determined mainly by local chemical evolution with limited radial exchange of evolution products. Much of the theory of chemical evolution of disk galaxies is based on this assumption (e.g., Chiappini, Matteucci & Gratton 1997); this view is, however, currently under challenge.

From the basic theory of chemical evolution via the continued formation and evolution of stars and enrichment of the ISM, one might expect that the metallicity of disk stars would gradually increase with time. McWilliam (1997) pointed out in his review that it was not clear observationally at the time that any age-metallicity relation (AMR) exists among the stars of the Solar Neighborhood. This is still the situation today. Edvardsson et al. (1993) found evidence for a weak decrease of $[\text{Fe}/\text{H}]$ with age among the disk stars, but later work (e.g., Nordström et al. 2004) is less conclusive. From the white dwarf luminosity function and the directly measured ages of disk stars (e.g., Knox, Hawkins & Hambly 1999; Edvardsson et al. 1993; Sandage, Lubin & Vandenberg 2003), the age of the Galactic thin disk is about 8–10 Gyr. The open cluster NGC 6791 has an age of about 8–10 Gyr and an abundance $[\text{Fe}/\text{H}] = +0.2$, indicating that enrichment to solar level occurred very quickly in the Galactic disk, on a gigayear timescale. An early AMR figure by Sandage & Eggen (1969), based partly on open cluster ages and metallicities, shows a very rapid early evolution of the galactic abundances up to near-solar abundances and then little further change; this is still a fair representation of the current state of knowledge.

The rapidly rising and then flat AMR in the disk of the Milky Way contrasts with the situation in the LMC. Dolphin (2000) derived the star-formation history and AMR for two fields in the LMC disk. The star-formation rate shows early and late phases of star formation, with a very slow period between about 3 and 7 Gyr ago, and the AMR shows a smooth rise from below -1.5 at 10 Gyr ago to the present metallicity of $[\text{Fe}/\text{H}] = -0.4$. A smoothly rising AMR is seen also in

the outer regions of M33 (Barker et al. 2007b). This difference in the morphology of the AMR between the Milky Way and the smaller galaxies is likely to come from the different star-formation histories of larger and smaller disk systems (the downsizing phenomenon).

5.1. Gas-Phase Abundance Gradients

Many galaxies show a clear radial gradient in their gas-phase abundances. Zaritsky et al. (1994) assembled data on oxygen abundance gradients in 39 disk galaxies covering a range of luminosities. They found the now-familiar correlations between oxygen abundance and luminosity, circular velocity and morphological type. The size of the abundance gradients (in dex/isophotal radius) did not correlate with luminosity or type. The presence of a bar appears to flatten or even erase the abundance gradient (see also Alloin et al. 1981), probably due to the noncircular motions, which the bar induces in the gas of the disk.

Magrini et al. (2007) modelled the chemical evolution of M33, assuming that the galaxy is accreting gas from an external reservoir. A model with an infall rate of about $1 M_{\odot} \text{ year}^{-1}$ reproduces the observational constraints, including the relatively high star-formation rate and the shallow abundance gradient. The model indicates that the metallicity in the disk has increased with time at all radii, and the abundance gradient has continuously flattened over the past 8 Gyr (see also Gogarten et al. 2010 for a comparison with the evolution of the somewhat similar disk galaxy NGC 300).

For the Milky Way, Shaver et al. (1983) combined radio and optical spectroscopy to measure abundances for HII regions between about 3 and 14 kpc from the Galactic center. Fich & Silkey (1991) extended the observations to a radius of about 18 kpc. A well-defined gradient in the oxygen and nitrogen abundances of -0.07 to $-0.08 \text{ dex kpc}^{-1}$ is found. Dennefeld & Kunth (1981) see a comparable gradient in nitrogen in the HII regions of the disk of M31.

5.2. Stellar Abundance Gradients

The abundance gradient for relatively young stars in the disk of the Milky Way is nicely delineated by the Cepheids (Luck, Kovtyukh & Andrievsky 2006). The gradient is about $-0.06 \text{ dex kpc}^{-1}$, in good agreement with the gas-phase gradient derived by Shaver et al. (1983). The two-dimensional distribution of the Cepheid abundances over the Galactic plane shows some localized departures from axisymmetry at the level of about 0.2 dex in abundance. These departures may come from radial gas flows associated with the spiral structure.

For the older stars in the outer disk (open clusters and red giants), the abundance gradient appears to be somewhat steeper, as seen in the study by Carney, Yong & Teixeira de Almeida (2005). The abundances fall to about -0.5 at 11 kpc but then stay approximately constant at this level out to radii beyond 20 kpc (**Figure 17**). The figure also compares the $[\alpha/\text{Fe}]$ ratio for the older objects and the Cepheids. It indicates that the abundance gradient in the outer disk is flatter now than it was a few gigayears ago, and also that the $[\alpha/\text{Fe}]$ ratio is nearer the solar value now than it was at the time of formation of the outer old clusters. These observations suggest that the chemical evolution of the disk gradually flattens the abundance gradient and reduces the $[\alpha/\text{Fe}]$ ratio. In the outer regions, episodic accretion of gas may trigger bursts of star formation that could erase the abundance gradient and produce the α -enriched abundances seen in the older objects. A similar bottoming out of the abundance gradient beyond about 15 kpc is seen by Worthey et al. (2005) in the outer disk of M31. We note that the environment of the outer disk in M31 has had a complex star-formation history, with much evidence for an extended period of accretion of

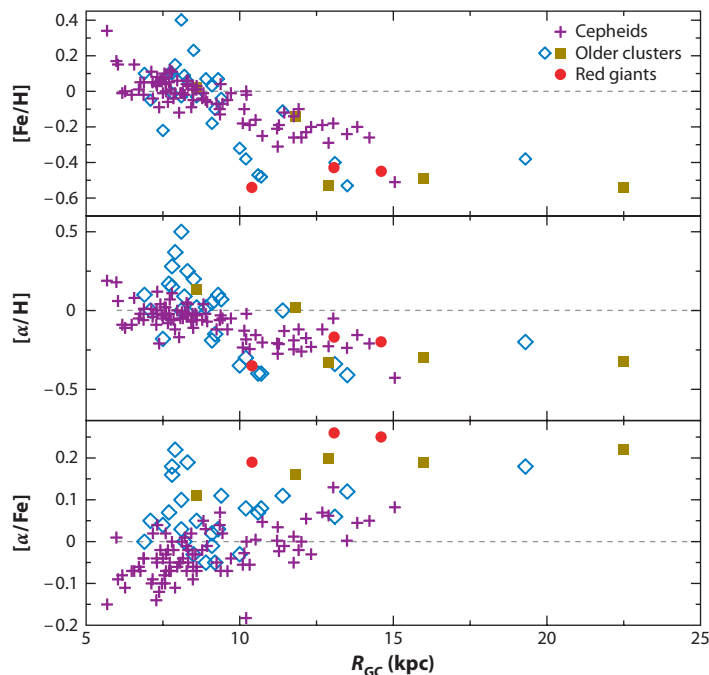


Figure 17

Upper panel: The radial abundance distribution for Cepheids (purple crosses) and older clusters (blue diamonds and dark yellow squares) and red giants (red circles) in the Galactic disk. *Lower panels:* The radial $[\alpha/\text{H}]$ and $[\alpha/\text{Fe}]$ distributions for the same objects (From Carney, Yong & Teixeira de Almeida 2005).

smaller galaxies (e.g., McConnachie et al. 2009), which complicates the interpretation of radial gradients in this system.

Cioni (2009) used the radial change of the ratio of C- and M-type AGB stars in the LMC and M33 to evaluate their stellar abundance gradients. Both show a radial abundance gradient. This is particularly clearly seen in M33: The gradient in the disk persists to a radius of about 8 kpc, which is the radius at which the radial truncation of the disk occurs. At larger radii, the abundance gradient becomes much flatter. Barker et al. (2007a) also found evidence that the radial abundance gradient of M33 flattens in the outer regions.

The abundance gradients of disk galaxies may not only flatten at large radii but can also reverse. The galaxy NGC 300 is similar to M33 in appearance and absolute magnitude, and it also has a negligible bulge component. The two galaxies do, however, differ in the details of the structure of their disks. M33 shows a very well-defined truncation of its disk, at a radius of a few scalelengths (Ferguson et al. 2007), whereas the disk of NGC 300 has an unbroken exponential surface density distribution extending to a radius of at least 10 scalelengths (Bland-Hawthorn, Vlahić & Freeman 2005). The negative abundance gradient in NGC 300 persists to a radius of about 10 kpc and then appears to reverse, with the metal abundance increasing with radius. Vlahić, Bland-Hawthorn & Freeman (2009) present two possible scenarios for the reversal of the abundance gradient. One is associated with accretion and local chemical evolution. The other scenario involves radial mixing driven by resonant scattering of stars via transient spiral disturbances while preserving their near-circular orbits, as discussed by Sellwood & Binney (2002) and Roškar et al. (2008b). In this picture, the stars in the outermost disk did not form in situ but were scattered from the inner galaxy into the outer disk. The scattering occurs from near the corotation radius of the individual spiral disturbance. The radial extent of the scattering depends on the strength of the transient spiral wave, and the radius from which the scattering occurs depends on its pattern speed. If the inner disk of the galaxy has the usual negative abundance gradient, then the abundance distribution in

the outer disk (which is populated by stars scattered from the inner disk) would depend on the distribution of pattern speeds and pattern strengths in the inner disk. A reversal in the current abundance gradient could come from an epoch of spiral disturbances whose strength increases with their pattern speed: more metal-rich stars from smaller radii are then more strongly scattered radially. Such an epoch of spiral disturbances could also explain the difference in structure between the truncated disk of M33 and the exponential disk of NGC 300. In this scenario, the outer disk of NGC 300 is more strongly populated by radial mixing, building up the continued exponential. For an alternative view, see Gogarten et al. (2010).

The chemical evolution of disks is usually calculated assuming that each annulus in the disk evolves independently, with infall of gas from intergalactic space but with no radial exchange of processed gas or stars (e.g., Chiappini, Matteucci & Gratton 1997). In this picture, one might expect a relationship between the age of stars and their metallicity. The apparent lack of a well-defined AMR in the Solar Neighborhood has motivated alternative views of the chemical evolution of disks, involving radial flows of gas and radial mixing of stars. Schönrich & Binney (2009a) have constructed such a theory that seems to fit very well the observed stellar distribution of thin-disk stars in the $[\alpha/\text{Fe}]$ – $[\text{Fe}/\text{H}]$ plane, and also the existing AMR data. We caution, however, that the AMR data in the Solar Neighborhood are still quite uncertain.

6. SCALING LAWS FOR DISK GALAXIES

Disk galaxies demonstrate several scaling laws, i.e., relations of observable parameters to the luminosity or stellar mass of the galaxies. Some scaling laws involve parameters associated with the stellar component of the galaxies: e.g., the stellar mass–metallicity relation and the luminosity–radius relation. Others relate stellar properties to dark matter properties: e.g., the Tully–Fisher relation between the stellar luminosity L (or stellar mass or baryonic mass) and the rotation speed of the galaxy, and the scaling relations between the luminosity of the stellar component and the central density of the dark matter halos. These scaling laws provide insight into the formation and evolution of disk galaxies.

When examining the scaling laws and other relations between observables for disk galaxies, it is useful to ask how many independent parameters there are in the ensemble of information. Principal component analysis (PCA) can provide insight, although it may be difficult to identify which of the parameters are fundamental (Brosche 1973). Recently, Disney et al. (2008) combined data from the HIPASS survey of HI in galaxies (Meyer et al. 2004) with SDSS data and derived six parameters: two optical radii (containing 50% and 90% of the light), luminosity, HI mass, dynamical mass, and $(g-r)$ color. PCA shows that the correlations are dominated by only one significant principal component. This indicates a somewhat unexpected organizational uniformity in galaxy properties.

6.1. The Tully–Fisher Law

This law, in its original form of absolute blue magnitude M_B versus the velocity width of the integrated HI profile, was discovered by Tully & Fisher (1977). For their profile width, they used W_{20} , the line width at 20% of the peak intensity, which has become widely but not universally used in Tully–Fisher relation (TFR) studies. The TFR quickly became an important tool for measuring the absolute magnitudes and distances of galaxies from their HI profile width. The magnitudes need to be corrected for Galactic and internal absorption, and the velocity widths corrected for the inclination of the disk and turbulence in the galaxy’s ISM. The slope of the TFR depends on wavelength (see, for example, Sakai et al. 2000). The slope of the $\log L - \log W_{20}$ relation

goes from about 3.2 at B to about 4.4 at H , and the scatter about the TFR is smaller at longer wavelengths.

The TFR is an important and complex constraint on galaxy formation theory. Each of the variables in the TFR (luminosity and profile width) is itself the product of many complex and interacting processes involved in the formation and evolution of disk galaxies, and these processes contribute to the slope, zero-point, and scatter of the TFR. The luminosity measures the integrated star-formation history and evolution of the baryons. The H I profile width is a measure of the maximum value of $R\partial\Phi/\partial R$ in the plane of the H I disk, where R is the radius and Φ the potential. This potential comes partly from the stellar component and partly from the dark matter halo. It therefore depends on the lengthscale of the stellar component (i.e., on how much the baryons have contracted during the formation of the galaxy) and, hence, on the angular momentum of the stellar component.

The dimensionless spin parameter (Peebles 1971)

$$\lambda = \frac{J|E|^{1/2}}{GM^{5/2}}, \quad (22)$$

(where J is the system's spin angular momentum, E its binding energy, and M its mass) is relevant here. λ is a measure of how far a system is from centrifugal equilibrium. Cosmological simulations predict the distribution of λ for dark halos that form in a CDM universe (e.g., Efstathiou & Jones 1979). The distribution of λ is typically lognormal, with a mean value of about 0.06. In systems with higher values of λ , the baryons settle into disks that are more extended, more slowly rotating, and of lower surface brightness in the mean (see, e.g., Dalcanton et al. 1997) for more details). Furthermore, the parameters involved in the TFR are likely to evolve as the galaxy grows: The stellar mass will increase according to the star-formation history, the baryonic mass will be affected by feedback and accretion, and the rotational velocity is likely to change as the stellar mass increases and the dark matter halo is gradually built up. We can expect all of these changes to continue to the present time.

Although the brighter disk galaxies lie on a well-defined luminosity-velocity relation, the fainter galaxies with circular velocities less than about 100 km s^{-1} are observed to have luminosities that lie below the relation defined by the brighter galaxies. Many of these fainter disk galaxies are gas (H I) rich, so the stellar mass is only a fraction of their baryonic content. If the baryonic (stellar + H I) mass is used instead of the stellar luminosity or mass, the fainter disk systems move up to lie on the same baryonic TFR as the brighter galaxies (Freeman 1999, McGaugh et al. 2000), with a relatively small scatter of 0.33 mag. This suggests that the TFR is really a relationship between the rotational velocity and the total baryonic mass M_{bar} (see also McGaugh 2005). The change in the slope of the $L-W_{20}$ relation with wavelength is partly due to the way in which the L/M_{bar} ratio changes with M_{bar} at different wavelengths, which in turn probably reflects the different star-formation histories of disk galaxies of different masses. In the mean, the less massive galaxies are now more affected by current star formation (downsizing), and we can expect more scatter in their L/M_{bar} ratio.

There is still some disagreement about the slope of the baryonic Tully-Fisher relation (BTFR). Various researchers find slopes between $M_{\text{bar}} \propto V^3$ and $M_{\text{bar}} \propto V^4$, where V is the rotational velocity (e.g., Stark et al. 2009, Trachernach et al. 2009, Gurovich et al. 2010). CDM theory predicts a slope closer to 3, so it is important to settle this question observationally. The studies quoted estimate the stellar masses from M/L ratios based on various models. In a more direct approach, Kregel, van der Kruit & Freeman (2005) use stellar disk masses derived from stellar dynamical analysis; after adding the H I content, they find a slope for the BTFR of 3.33 ± 0.37 over 2 dex, with a scatter of 0.21 dex.

One potentially important difference in approach comes from the way in which different researchers measure the rotational velocity (see Cantinella et al. 2007 for more discussion). Some researchers use the profile width W_{20} as their velocity measure; the relationship between this quantity and the asymptotic (flat) rotational velocity of the galaxy becomes less well defined for lower mass galaxies, in which the HI often does not extend to the flat part of the rotation curve. Other researchers restrict their samples to galaxies in which the rotation curve is observed to reach the flat region and use this flat level of the rotation curve as their velocity measure. Although the flat level of the rotation curve provides a consistent estimate of the rotation, this is itself a selection effect, restricting the sample of galaxies to those in which the HI extends to the flat rotation curve region. The selected galaxies are therefore biased toward systems in which either the HI is intrinsically more extended or the dark matter halos are more centrally concentrated with relatively smaller scalelengths and larger concentrations. As one might expect from the above discussion, analyses based on W_{20} appear to give lower (flatter) slopes for the BTFR than those based on the flat region of the rotation curve. The concept of the radial TFR, in which the luminosity is plotted against the rotational velocity at a range of fiducial radii (Yegorova & Salucci 2007), may be helpful for comparing galaxies with different rotation curve morphologies in a consistent manner. Ideally, to relate the baryonic content of disk galaxies to the properties of the dark halos, we would like to use the circular velocity of the dark halo at the virial radius, but for most galaxies this quantity cannot be measured at present (see Courteau et al. 2007 for a useful discussion).

The interpretation of the BTFR is not straightforward. For normal high surface brightness disk galaxies, the rotation speed depends on the contributions to the gravitational potential from both the stellar distribution and the dark matter, including any effects of the stellar distribution on the dark matter (baryonic contraction). This in turn involves the evolution of the stellar disk itself. In gas-rich and LSB galaxies, the contribution of the luminous matter to the potential field is relatively small but, even in this simpler situation, the BTFR involves the ratio of baryon to dark matter mass, the structure of the dark matter halo, and the radial extent or maximum angular momentum of the HI gas. Zwaan et al. (1995) and Sprayberry et al. (1995) constructed a TFR law for LSB galaxies: These galaxies have surface brightnesses that are typically at least a magnitude fainter than the normal galaxies. They found that the TFR for LSB and normal disk galaxies were very similar in slope and zero point. Although this result may seem surprising, it makes sense if interpreted in the context of the BTFR. The stellar luminosity is used as a proxy for the baryonic mass, with some scatter and bias depending on the gas fraction (and adopted stellar M/L ratio). The velocity for these galaxies reflects the circular velocity of the dark matter potential, because the contribution to the gravitational field from the stellar component is relatively insignificant.

The following clever argument of Courteau & Rix (1999) makes use of the scatter in the Tully-Fisher relation. The amplitude of the rotation curve of the self-gravitating exponential disk is

$$V_{\text{disk}} \propto \sqrt{b \Sigma_0} \propto \sqrt{\frac{M_{\text{disk}}}{b}}. \quad (23)$$

For fixed disk mass M_{disk} we then get by differentiation

$$\frac{\partial \log V_{\text{max}}}{\partial \log b} = -0.5. \quad (24)$$

So at a given absolute magnitude (or mass), a lower scalelength disk should have a higher rotation velocity. If all galaxies were maximum disk, then this anticorrelation should be visible in the scatter of the TFR. It is, however, not observed, and the inference is that on average $V_{\text{disk}} \sim 0.6 V_{\text{total}}$ and galaxies in general do not have maximal disks. We note that this argument ignores the contribution

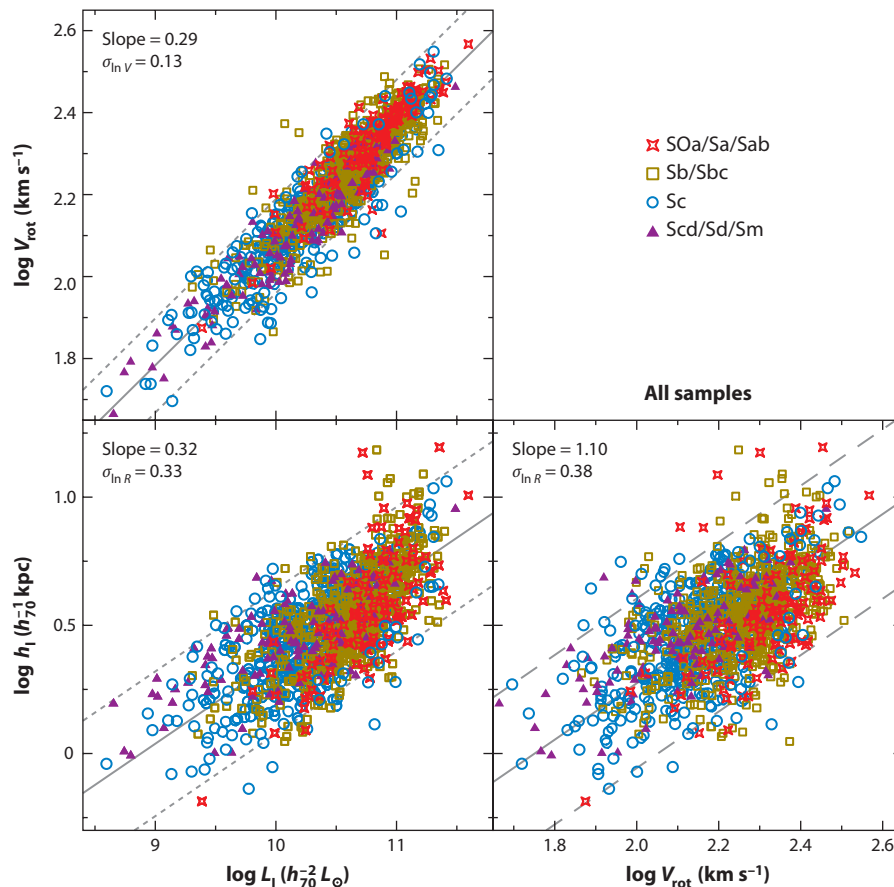


Figure 18

Scaling relations between the rotation velocity V , the scalelength b , and the luminosity L , the latter two in the I -band (From Courteau et al. 2007).

of the gas to the total baryonic mass, which can be significant even for relatively bright galaxies (e.g., Gurovich et al. 2010).

6.2. Scaling Laws Involving the Galaxy Diameter

In their pioneering paper, Tully & Fisher (1977) also considered the relationship between galaxy optical diameter and rotational velocity. Courteau et al. (2007) made an extensive study of the distributions of L and stellar scalelength b (in the I and K bands) and V_{rot} for a sample of 1,300 galaxies. The scalelength reflects the angular momentum distribution of the star-forming baryons but probably includes further complications of the baryonic dissipation and settling to equilibrium.

The scatter in the relations involving b is larger than for the L – V relation (see **Figure 18**), as one might expect from the additional complexity of the underlying physics and also the difficulty of measuring disk scalelengths accurately. The mean relations found by Courteau et al. (2007) are

$$V_{\text{rot}} \propto L^{0.29}, \quad b \propto L^{0.32}, \quad \text{and} \quad b \propto V_{\text{rot}}^{1.10} \quad (25)$$

in the I -band. The relations involving b show some morphological dependence, but no significant morphological dependence is seen in the V_{rot} – L relation.

6.3. The Mass-Metallicity Relation

The mass-metallicity relationship pertains to the baryonic component of the galaxies. The relationship between stellar mass or luminosity and metallicity in galaxies goes back at least to Lequeux et al. (1979). A study of a large sample of SDSS galaxies by Tremonti et al. (2004) gives references and demonstrates a tight correlation between the stellar mass and the gas-phase oxygen abundance extending over 3 orders of magnitude in stellar mass and a factor of 10 in oxygen abundance. Kirby et al. (2008) show that the relationship between luminosity and metallicity continues down to the faintest known dwarf spheroidal galaxies with absolute V -magnitudes fainter than -4 . The deeper potential wells of the more massive galaxies are believed to retain more effectively the metal-enriched ejecta of supernovae (Larson 1974, Dekel & Silk 1986), which can be lost via galactic winds. Tassis et al. (2008) have argued, however, that this kind of supernova feedback may not be essential for generating the mass-metallicity relation; the increasingly inefficient conversion of gas into stars in the lower mass galaxies may be responsible.

6.4. The Surface Density–Mass Relation

This relationship again pertains to the baryonic component of the galaxies; as for the mass-metallicity relationship, it provides some constraints on the theory of the evolution of the baryonic component. In the mean, the surface density of galaxies appears to increase with increasing stellar mass or luminosity, as shown first by Kormendy (1985) and followed up by Dekel & Silk (1986) for a sample of nearby ellipticals and irregular galaxies with stellar masses less than about $10^{10.5} M_{\odot}$. For disk galaxies, Gurovich et al. (2010) found a similar relationship: the baryonic (stellar + H I) surface density is observed to increase approximately linearly with W_{20} . Again, this scaling law can be interpreted in terms of supernova-driven loss of gas or as due to increasingly inefficient star formation for systems of lower masses.

6.5. Scalings Laws for Dark Matter Halos

The properties of the dark matter halos of disk galaxies appear to scale with the luminosity of their stellar component. Kormendy & Freeman (2004) analyzed the rotation curves of spirals and dwarf irregular galaxies to estimate parameters for their dark matter halos. They modelled the dark halo density distributions as isothermal spheres with a central core of density ρ_0 and a core radius r_c . Estimates for the dark halos of dwarf spheroidal galaxies were also included, using the velocity dispersion profiles of these systems. Kormendy & Freeman found that the core density ρ_0 decreases with luminosity, as $\rho_0 \propto L^{-0.28}$. The core densities increase from about $10^{-2.5} M_{\odot} \text{ pc}^{-3}$ for the brighter spirals to a rather high value of about $10^{-0.5} M_{\odot} \text{ pc}^{-3}$ for the fainter dwarf irregular and spheroidal galaxies. The core radius r_c increases with luminosity, as $r_c \propto L^{+0.32}$, so the surface density $\rho_0 r_c$ of the dark matter halos is approximately independent of the luminosity of the stellar component. This remarkable observational result was confirmed by Donato et al. (2009) with more recent data for the dark halos of the dwarf galaxies. The surface density $\rho_0 r_c$ is constant at about $140 M_{\odot} \text{ pc}^{-2}$ over about 15 mag in stellar luminosity.

The dark halo scaling laws reflect the changing density of the Universe as halos of different masses are formed, with the less massive halos forming earlier. The difference in halo densities indicates that the smallest dwarfs formed about 7 units of redshift earlier than the largest spirals. Djorgovsky (1992) showed that protogalactic clumps, which separate from an evolving density field with power spectrum $|\delta_k|^2 \sim k^n$, have a scaling law between density and radius $\rho \sim r^{-3(3+n)/(5+n)}$.

The observed scaling laws for dark matter halos correspond to $n \approx -2$, close to what is expected for Λ CDM on galactic scales.

7. THICK DISKS

Most spirals, including our Galaxy, have a second thicker disk component surrounding the thin disk. Thick disks were discovered in other galaxies via surface photometry (Burstein 1979, Tsikoudi 1980) and then in the Milky Way through star counts (Gilmore & Reid 1983). It appears that thick disks are very common in disk galaxies and that they are mostly very old. The thick disk is therefore an important component in understanding the assembly of disk galaxies.

7.1. Statistics of Incidence

The photographic surface photometry of van der Kruit & Searle (1981a,b, 1982a) showed that thick disks were common in disk galaxies but perhaps not ubiquitous (see also Fry et al. 1999). At the time, evidence indicated that the thick disk was associated with the presence of a central bulge. A more recent extensive study of a large sample of edge-on galaxies by Yoachim & Dalcanton (2006) showed that thick disks are probably present in all or almost all disk galaxies. They found that the ratio of thick-disk stars to thin-disk stars depends on the luminosity or circular velocity of the galaxy: It is about 10% for large spirals like the Milky Way and rises to about 50% for the smallest disk systems.

Our Galaxy has a thick disk. Star counts by Gilmore & Reid (1983) at high Galactic latitude showed two vertically exponential components: the thin disk and the more extended thick disk. Its scaleheight is about 1,000 pc, compared to about 300 pc for the old thin disk, and its surface brightness is about 10% of the surface brightness of the thin disk, but there is still some disagreement about these parameters.

7.2. Structure of Thick Disks

From within our Galaxy, it is difficult to estimate reliably the scaleheight and scalelength of the thick disk. Values for the scaleheight between about 0.5 and 1.2 kpc have been reported. A recent analysis of the SEGUE photometry gives a relatively short exponential scaleheight of 0.75 ± 0.07 kpc and an exponential scalelength of 4.1 ± 0.4 kpc (de Jong et al. 2010). For comparison, the scaleheight of the thin disk is about 250 to 300 pc; the scalelength of the thin disk is poorly determined but is probably between 2 and 4 kpc. Their model gives the stellar density of the thick disk near the sun to be about $0.0050 M_{\odot} \text{ pc}^{-3}$, about 7% of the stellar density of the thin disk near the sun (about $0.07 M_{\odot} \text{ pc}^{-3}$).

Thick disks are not easy to see in galaxy images. **Figure 19** shows that in NGC 4762 [that has a bright thick disk (Tsikoudi 1980)], the outer extent of the faint starlight has an approximate diamond shape, indicating the double exponential light distribution of a thick disk. In **Figure 10**, we see the same thing in the outer outline in the bottom picture for NGC 4565 at the deepest stretch. The luminosity distribution of the edge-on galaxy NGC 891, which is often regarded as an analog for the Milky Way (van der Kruit 1984), shows after subtraction of the disk a light distribution that becomes progressively more flattened at fainter levels (see figure 7 in van der Kruit & Searle 1981b); in van der Kruit (1984), it is shown that this distribution can be interpreted as a superposition of a thin and thick disk plus a small, central bulge. Recent studies show that the scaleheight of its thick disk is 1.44 ± 0.03 kpc, and its radial scalelength is 4.8 ± 0.1 kpc, only slightly longer than that of the thin disk (Ibata, Mouhcine & Rejkuba 2009). The relationship

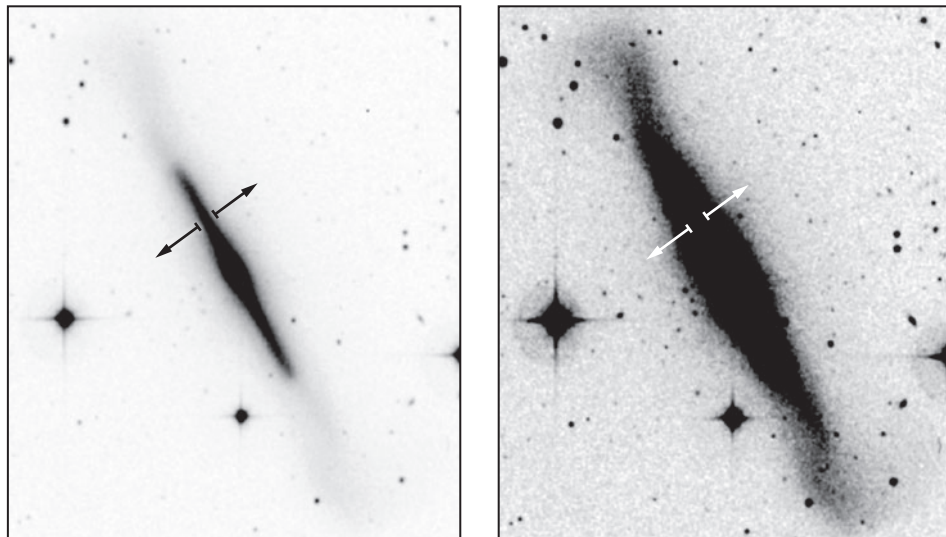


Figure 19

The S0 galaxy NGC 4762, which has a very bright thick disk, as was first described by Tsikoudi (1980). The z extent, indicated by the arrows, is where the thin disk dominates. On the right the outer extent of the thick disk is slanted with respect to the symmetry plane (producing an approximately diamond shape), indicative of a double exponential light distribution. These images were produced with the use of the *Digital Sky Survey*.

between the scalelengths of the thin and thick disk is an important constraint on the various formation mechanisms of thick disks, as discussed below.

7.3. Kinematics and Chemical Properties

Little information is available on the kinematics and chemical properties of thick disks in galaxies other than the Milky Way. The larger scaleheight of the Galactic thick disk means that its velocity dispersion is higher than for the thin disk [about 40 km s^{-1} in the vertical direction near the sun, compared to about 20 km s^{-1} for the thin disk] (e.g., A.C. Quillen, D.R. Garnett, unpublished, arXiv:0004210). The stars of the thick disk are usually identified by their larger motions relative to the Local Standard of Rest, but kinematic selection is inevitably prone to contamination by the more abundant thin-disk stars. Recently, it has become clear that the Galactic thick disk is a discrete component, kinematically and chemically distinct from the thin disk. It now appears that thick disk stars can be more reliably selected by their chemical properties.

Near the Galactic plane, the rotational lag of the thick disk relative to the LSR is only about 30 km s^{-1} (Chiba & Beers 2000, Dambis 2009), but its rotational velocity appears to decrease with height above the plane. The stars of the thick disk are old ($> 10 \text{ Gyr}$) and more metal poor than the thin disk. The metallicity distribution of the thick disk has most of the stars with $[\text{Fe}/\text{H}]$ between about -0.5 and -1.0 , with a tail of metal-poor stars extending to about -2.2 . The thick-disk stars are enhanced in α elements relative to thin-disk stars of the same $[\text{Fe}/\text{H}]$ (e.g., **Figure 20**, taken from Fuhrmann 2008), indicating a more rapid history of chemical evolution. The thick disk does not show a significant vertical abundance gradient (Gilmore, Wyse & Jones 1995). It appears to be chemically and kinematically distinct from the thin disk.

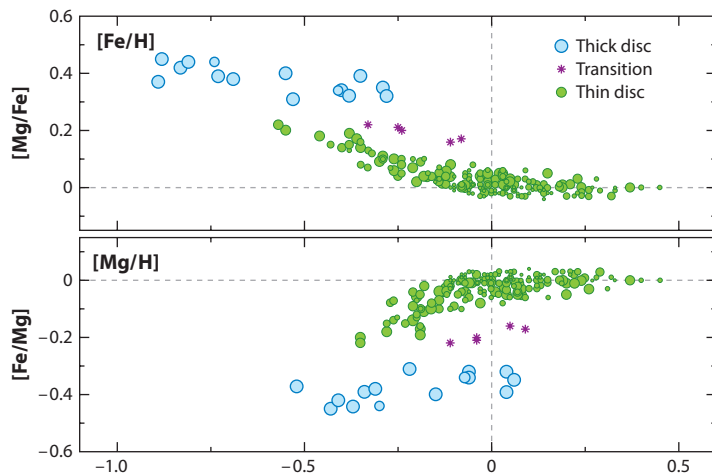


Figure 20

Mg enrichment of the thick disk relative to the thin disk, indicating that the thick disk is a chemically distinct population (From Fehrmann 2008).

A decomposition of the kinematics and distribution of stars near the Galactic poles, by Veltz et al. (2008), nicely illustrates the three main kinematically discrete stellar components of the Galaxy: a thin disk with a scaleheight of 225 pc and a mean vertical velocity dispersion of about 18 km s^{-1} ; a thick disk with a scaleheight of 1,048 pc and mean velocity dispersion of 40 km s^{-1} ; and a halo component with a velocity dispersion of about 65 km s^{-1} .

The old thick disk presents a kinematically recognizable relic of the early Galaxy and is, therefore, a very significant component for studying galaxy formation. Because its stars spend most of their time away from the Galactic plane, the thick disk is unlikely to have suffered much secular heating since the time of its formation. Its dynamical evolution was probably dominated by the changing potential field of the Galaxy associated with the continuing growth of the Galaxy since the time at which the thick disk was formed.

For the thick disks of other galaxies, broadband colors suggest that the thick disks are again old and metal poor relative to their thin disks. Yoachim & Dalcanton (2008) studied the rotation of the thick disks of a small sample of extragalactic thick disks. In one galaxy (FGC 227),¹² they found that the thick disk appeared to be counter-rotating relative to its thin disk. If confirmed, this difficult observation would have important implications for the origin of thick disks.

7.4. Relation of Thick Disk to Other Galactic Components

At this time, there is no convincing evidence that the thick disk is in any way related to the halo or the bulge of its parent galaxy. The almost ubiquitous nature of thick disks, independent of the bulge to disk ratio, argues against any causal relation with the bulge. In the Milky Way, some chemical similarities of bulge and thick-disk stars are observed. For example, the $[\alpha/Fe]$ ratio of the thin-disk stars near the Sun is somewhat like the enhanced $[\alpha/Fe]$ ratios seen in bulge stars (Meléndez et al. 2008), but this is probably more a reflection of the rapid star-formation history of both components rather than any deeper relationship. The metal-poor tail of the metallicity distribution of the thick disk reaches down to metallicities usually associated with halo stars ($[Fe/H] < -1$), but the kinematics are different [the metal-poor thick-disk stars are rotating more rapidly than the halo stars (e.g., Carollo et al. 2010) and do not hint at any cosmogonic relationship of

¹²FGC is the Flat Galaxy Catalogue of Karachentsev, Karachentseva & Parnovskij (1993).

thick disk and halo]. Gilmore (1995) found that in the Galaxy, the cumulative angular momentum distribution function for stars in the thick disk is rather similar to that of the thin disk, but distinctly different from that of the stellar halo and the bulge.

Thin disks and thick disks do appear to be causally linked: The survey of Yoachim & Dalcanton (2006) shows that all or almost all galaxies selected as having a thin disk also have a thick disk. Thick-disk formation seems to be a normal event in the early formation of thin disks, but the details of how disks form are not yet understood.

7.5. Thick Disk Formation Scenarios

Thick disks appear to be old and very common, puffed up relative to their parent thin disks, and (at least in the case of the Milky Way) to have suffered rapid chemical evolution. Scenarios for their formation include:

- Thick disks come from energetic early star burst events, maybe associated with gas-rich mergers (Samland & Gerhard 2003, Brook et al. 2004).
- Thick disks are the debris of accreted galaxies that were dragged down by dynamical friction into the plane of the parent galaxy and then disrupted (Walker, Mihos & Hernquist 1996; Abadi et al. 2003). To provide the observed metallicity of the Galactic thick disk ($[\text{Fe}/\text{H}] \sim -0.7$), the accreted galaxies that built up the Galactic thick disk would have been more massive than the Small Magellanic Cloud and would have had to be chemically evolved at the time of their accretion. The possible discovery of a counter-rotating thick disk (Yoachim & Dalcanton 2008) (FGC 227; see above) would favor this mechanism.
- The thick disk's energy comes from the disruption of massive clusters or star-forming aggregates (Kroupa 2002b), possibly like the massive clumps seen in the high redshift clump cluster galaxies. Other researchers have discussed the formation of thick disks through the merging of clumps and heating by clumps in clump cluster galaxies (e.g., Bournaud, Elmegreen & Martig 2009).
- The thick disk may be associated with the effects of radial mixing of stars and gas in the evolving Galaxy (Schönrich & Binney 2009a,b).
- The thick disk represents the remnant early thin disk, heated by accretion events. In this picture, the thin disk begins to form at a redshift of 2 or 3 and is partly disrupted and puffed up during the active merger epoch. Subsequently, the rest of the gas gradually settles to form the present thin disk (e.g., Quinn & Goodman 1986, Freeman 1987).

Sales et al. (2009) have shown that the predicted distribution of orbital eccentricities for nearby thick-disk stars is different for several of these formation scenarios. As large samples of accurate orbital eccentricities become available for thick disk stars, they can be used to exclude some of the proposed formation mechanisms.

8. FORMATION OF DISKS

In this section, we turn to formation models of galaxy disks, describing first formation scenarios and corresponding paradigms and then reviewing briefly observations of disks at high redshift and other matters related to the formation process.

8.1. Disk Formation Scenarios

Stellar disks are close to centrifugal equilibrium, suggesting dissipation of baryons to a near-equilibrium structure before the gas became dense enough to initiate the onset of the main epoch

of star formation. This picture goes back at least to Eggen, Lynden-Bell & Sandage (1962) and Sandage, Freeman & Stokes (1970) in the pre-dark matter era and was followed by many innovative landmark papers in the late 1970s and early 1980s on the cooling of gas and dissipational formation of disks in the potential of the preformed dark matter halo. Rees & Ostriker (1977) discussed the cooling of gas and the thermalizing of infalling gas. White & Rees (1978) described the two-stage theory of galaxy formation, in which the dark matter clustered under the influence of gravity and the gas cooled into the dark matter halos. Fall & Efstathiou (1980) considered the dissipational collapse of a disk within a dark halo, conserving its detailed $M(b)$ distribution as suggested by Mestel (1963). Assuming that the specific angular momenta of the dark matter and gas were similar, they showed that the gas would collapse by at least a factor of 10. Gunn (1982) showed that in this hypothesis approximately exponential stellar disks arise naturally, and van der Kruit (1987) showed that these would then have radial truncations at about 4.5 scalelengths. Blumenthal et al. (1984) discussed the various possible kinds of dark matter (cold, warm, hot) and their implications for the formation of galaxies by cooling. Later versions of this basic picture were discussed by Dalcanton et al. (1997) and Mo, Mao & White (1998). The so-called rotation curve conspiracy—that the properties of disk and halo are precisely those necessary to produce essentially flat, featureless rotation curves and to provide the Tully-Fisher law—was heuristically explained in the context discussed here by Gunn (1987) and Ryden & Gunn (1987).

In summary, this paradigm involves the dark matter halo forming gravitationally and relaxing to virial equilibrium; then infalling gas is shock-heated to the halo virial temperature and then cools radiatively from inside out, gradually building up the disk and forming stars quiescently.

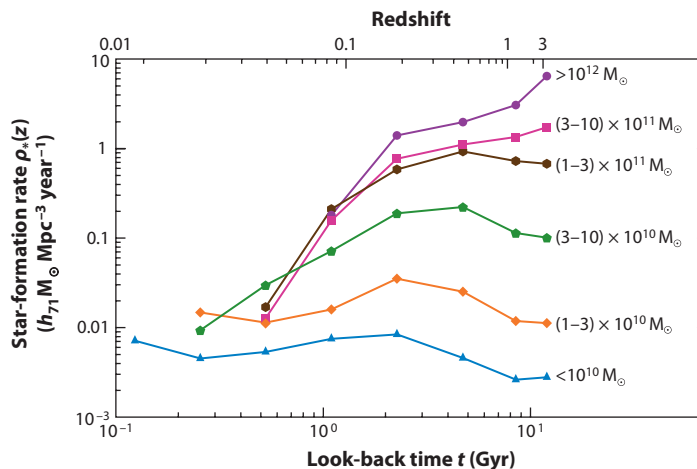
The subsequent star-formation history of disks is very different from galaxy to galaxy. In the S0 galaxies, the star formation has already come to a halt through gas exhaustion or gas stripping. In the Galactic thin disk, star formation began about 10 Gyr ago (Edvardsson et al. 1993; Knox, Hawkins & Hambly 1999), and a wide range of stellar age is seen, indicating that disk formation was an extended process starting about 10 Gyr ago and continuing to the present time. The star-formation history of the disk is not very well constrained, but is consistent with a roughly constant star-formation rate (e.g., Rocha-Pinto et al. 2000) with fluctuations of about a factor of 2 on gigayear timescales. In the lower luminosity systems, the main epoch of star formation did not begin right away, and much of the current star formation in the Universe is now taking place in these smaller disk galaxies. This is the phenomenon of downsizing: star formation in the early Universe occurred mainly in the larger systems and has gradually proceeded to progressively smaller galaxies (see **Figure 21**).

This is nicely shown by Noeske et al. (2007a,b). They analyzed the star-formation rate as a function of stellar mass M_* and redshift. In galaxies that are forming stars, the star-formation rate depends on the stellar mass of the galaxies. The observed range of star-formation rate remains approximately constant with redshift, but the sequence moves to higher star-formation rate with increasing redshift. The dominant mode of evolution since $z = 2$ is a gradual decline of the average star-formation rate. At a given mass, the star-formation rate at $z = 2$ was larger by factors of ~ 4 and ~ 30 than that in star-forming galaxies at $z = 1$ and 0, respectively (Daddi et al. 2007). The star formation drives the growth of disks. Trujillo et al. (2006) studied the evolution of the luminosity-size and stellar mass-size relation in galaxies since $z = 3$ and found that, at a given luminosity, galaxies were three times smaller at $z = 2.5$ than now; at a given M_* , they are two times smaller. In the Local Group, Williams et al. (2009a) directly measured the evolution of the scale length of M33, which has increased from 1 kpc 10 Gyr ago to 1.8 kpc at more recent times.

The present high, specific star-formation rate of many less massive galaxies reflects the late onset of their dominant star-formation episode, after which the star-formation rate gradually

Figure 21

The history of star formation as a function of stellar mass of the galaxy. The curves have been offset by 0.5 in the log, except for the most massive one, where it has been an additional 1.0. The phenomenon of star formation occurring in the early Universe mainly in large systems while later shifting to smaller systems is known as downsizing (From Heavens et al. 2004).



declines. The less massive galaxies appear to have a longer e-folding time and a later onset of their star-formation history.

The color distributions of galaxies reflect this mass dependence of their star-formation history. At low redshifts, the color distribution is bimodal, showing the blue cloud of star-forming galaxies at lower stellar masses and the overlapping red sequence of more luminous systems in which star formation has now stopped or is at a very low rate (Blanton et al. 2003, Kauffmann et al. 2003a). The restframe color distribution is now known to be bimodal at all redshifts $z < 2.5$ (e.g., Brammer et al. 2009). The red sequence persists to beyond $z = 2$, indicating that many galaxies had completed their star-forming lives by this time. Galaxies in the green valley between the red sequence and the blue cloud may be in transition between the two sequences, as blue cloud galaxies whose star formation is running down, but also as red sequence systems in which the star formation has been revitalized (e.g., Beaulieu et al. 2010). However, it seems more likely now that most of these green valley galaxies are reddened star-forming systems.

The bimodality manifests itself in several ways. Blue galaxies, as defined by their color and their star-formation rates, dominate the stellar mass function below a transition mass of about $3 \times 10^{10} M_{\odot}$. It persists to redshifts of at least 2.5. The bulge-to-disk ratio shows a related transition from disk-dominated blue galaxies below the transition mass to spheroid-dominated red sequence galaxies above the transition mass (e.g., Kauffmann et al. 2003b). The surface brightness μ -stellar mass M_* relation changes from $\mu \propto M_*^{0.6}$ at lower masses to $\mu \sim \text{constant}$ at higher masses. The mean mass-metallicity relation also shows a break at the transition mass (e.g., Tremonti et al. 2004). Dalcanton, Yoachim & Bernstein (2004) observed a break in the morphology of dustlanes of edge-on disk galaxies at a similar transition mass, changing from diffuse for lower mass disks to sharply defined for higher mass disks. This could be related to infalling cold gas streams enhancing star formation and turbulence in the less massive galaxies (see Sections 4.4 and 8.3).

The role of mergers in the evolution of disk galaxies remains uncertain. The thin disks of disk galaxies are relatively fragile and are easily puffed up by even minor mergers (Quinn & Goodman 1986, Toth & Ostriker 1992). CDM simulations show a high level of merger activity on all scales. These mergers tend to excite star formation, puff up the disks, and build up spheroidal components in the simulations. This makes it difficult for CDM simulations to generate large spirals like the Milky Way, with relatively small spheroidal components. Although there has been discussion by simulators about the unusually quiescent merger history of the Milky Way, such systems are not unusual. Kormendy et al. (2010) have shown that at least 11 of 19 nearby disk galaxies with circular

velocities $>150 \text{ km s}^{-1}$ show no evidence for a classical bulge. They argue that pure-disk galaxies are far from rare.

Lotz et al. (2008) studied the evolution of the merger rate since redshift $z = 1.2$. They find that the fraction of galaxies involved in mergers is about 10%, and conclude that the decrease in star-formation rate density since $z = 1$ is a result of the declining star-formation rate in disk galaxies rather than a decrease in major mergers. However, Hammer et al. (2005, 2009) argue, from the episodic star-formation history of most intermediate-mass spirals and from the incidence of peculiar morphologies and anomalous kinematics in a sample of galaxies at median redshift $z = 0.65$, that they have experienced their last major merger event within the past 6–8 Gyr and that reprocessing of spirals by gas-rich mergers may be an important aspect of the formation of present-day disks. From their GOODS galaxy sample, Bundy et al. (2009) show that mergers contribute little to galaxy growth since $z = 1.2$ for galaxies with $M_* < 3 \times 10^{10} M_\odot$. For the more massive galaxies, which are mostly spheroidal systems, mergers are more important; they estimate that about 30% have undergone (mostly dry or gas-free) mergers.

The Milky Way is an important part of assessing the significance of mergers in building up large spiral galaxies. The unique possibility to make very detailed chemical studies of stars in the Milky Way provides an independent opportunity to evaluate the merger history of our large disk galaxy via chemical tagging techniques (Freeman & Bland-Hawthorn 2002).

8.2. Disks at High Redshift

One of the most fundamental observations that the HST made possible is the imaging of galaxies when they were very young. Studies of the Hubble Deep Fields (Williams et al. 1996, 2000; Beckwith et al. 2006) showed observationally that few galaxies, which resemble present-day spirals or ellipticals are present at redshifts >4 . Simulations indicate that disks should be present at redshifts around 2 (e.g., Sommer-Larsen et al. 2003): Is this consistent with observations? If disks are present at these redshifts, what are they like? How do their baryonic mass distributions compare with those of disk galaxies at low redshifts?

Labbé et al. (2003) observed the Hubble Deep Field-South in the near-IR (from the ground) and found six galaxies at redshifts $z = 1.4$ to 3.0 that have disklike morphologies. The galaxies are regular and large in the near-IR (corresponding to rest-frame optical), with face-on effective radii of 5.0–7.5 kpc, which is comparable to the Milky Way. The surface brightness profiles are consistent with an exponential law over 2 to 3 effective radii. The HST morphologies (rest-frame UV) are irregular and show large complex aggregates of star-forming regions (~ 15 kpc across), symmetrically distributed around the centers.

Genzel et al. (2006) described the rapid formation of a luminous star-forming disk galaxy at a redshift of $z = 2.38$. Their integral field unit observations indicate that a large protodisk is channelling gas toward a growing central bulge. The high surface density of gas and the high rate of star formation show a system in rapid assembly, with no obvious evidence for a major merger. Integral-field spectroscopy by Förster Schreiber et al. (2009) of several UV-selected galaxies with stellar masses $\sim 3 \times 10^{10} M_\odot$, star-formation rates of $\sim 70 M_\odot \text{ year}^{-1}$, and redshifts between 1.3 and 2.6 provides rotation curves and indicators of dynamical evolution. The morphology is typically clumpy. About one-third of the galaxies are turbulent and rotation-dominated, another third are compact and dominated by velocity dispersion, whereas the rest are interacting or merging systems. The rotation-dominated fraction is higher for higher masses.

Elmegreen et al. (2009a,b) investigated the relationship to modern spirals of clumpy high-redshift galaxies in the GOODS, GEMS, and Hubble UDF surveys. The clump properties indicate

the gradual dispersal of clumps to form disks and bulges, with little indication of merger activity. The morphological similarity of these systems to modern dwarf irregulars suggests that the clumpy morphology comes from gravitational instability in the turbulent gas. They note that about 50% of these clump cluster galaxies have massive red clumps that could be interpreted as young bulges. We have already discussed the clump cluster galaxies in the context of the formation of the thick disk component (Section 6.5).

Kriek et al. (2009) studied 19 massive galaxies at $z \sim 2.3$: 9 of them are compact quiescent systems and 10 are emission-line systems (6 star-forming galaxies and 4 AGNs). The star-forming galaxies again have clumpy morphologies. In the rest-frame $(U-B) - M_*$ plane, the galaxies appear bimodal: The large star-forming galaxies lie in a blue cloud, and the compact quiescent galaxies in a red sequence. A bimodal distribution similar to that at lower redshifts is already in place at redshifts >2 .

In summary, it appears that the formation of disk galaxies is already well advanced at redshifts >2 , but the systems have mostly not yet settled to a quiescent disk in rotational equilibrium. The clumpy structure of the massive star-forming systems is likely to be an important factor in the subsequent evolution of these systems and in the formation of their thick disks and bulges. The role of mergers in building up these disk galaxies may not be as important as it appears to be from CDM simulations.

8.3. Baryon Acquisition by Disk Galaxies

In the scenarios for disk formation that emerged soon after the discovery of dark matter in disk galaxies, the gas was shock-thermalized to the virial temperature and then gradually cooled to form the disk. Simulations (e.g., Sommer-Larsen et al. 1999) suggest that this hot halo is further populated by gas blown out from the disk via feedback into the hot halo. This feedback provides a way to reduce the problem of angular momentum loss that led to unrealistically low angular momenta for disks seen in earlier simulations. These simulations are successful in reproducing the peak in the star-formation rate seen within individual galaxies at $z \sim 2$.

More recent simulations point to the likelihood of cold gas accretion into disk galaxies. Smoothed particle hydrodynamics simulations by Kereš et al. (2005) showed that typically about half of the gas shock-heats to the virial temperature of the potential well ($\sim 10^6$ K in a Milky-Way-like galaxy), whereas the other half radiates its gravitational energy at $T < 10^5$ K. A cold mode of infall is seen for stellar masses $< 2 \times 10^{10} M_\odot$. This cold gas often falls in via the cosmic filaments, allowing galaxies to draw their gas from a large volume. Kereš et al. (2009) found that most of the baryonic mass is acquired through the filamentary cold accretion of gas that was never shock-heated to its virial temperature. This cold accretion is the main driver of the cosmic star-formation history.

Hot halos are seen only for dark halo masses $> 2 - 3 \times 10^{11} M_\odot$. Dekel & Birnboim (2006) ascribed the bimodality of galaxy properties to the nature of the gas acquisition. Galaxies with stellar masses $< 3 \times 10^{10} M_\odot$ are mostly ungrouped star-forming disk systems, whereas the more massive galaxies are mostly grouped old red spheroids. They argue that the bimodality is driven by the thermal properties of the inflowing gas. In halos with masses $< 10^{12} M_\odot$, the disks are built by cold streams, giving efficient early star formation regulated by supernova feedback. In the more massive halos, the infalling gas is shock-heated and is further vulnerable to AGN feedback, shutting off the gas supply and leading to red and dead spheroids at redshift $z \sim 1$. Simulations by Dekel, Sari & Ceverino (2009) showed that the evolution of massive disk systems is governed by interplay between smooth and clumpy cold streams, disk instability, and bulge formation. The streams maintain an unstable gas-rich disk, generating giant clumps that can migrate into the bulge

in a few dynamical times. The streams prolong this clumpy phase for several Gyr. The clumps form stars in dense subclumps and each clump converts to stars in ~ 0.5 Gyr. The star forming disk is extended because the incoming streams keep the outer disk dense and unstable, and also because of angular momentum transport by secular processes within the disk (e.g., Kormendy & Kennicutt 2004). Observationally, the large chemical tagging surveys which will soon begin (HERMES, APOGEE) will be able to evaluate the role of giant clumps in the formation of the thin and thick disks of the Milky Way (e.g., Bland-Hawthorn et al. 2010). The debris of the dispersed giant clumps should be very apparent from the chemical tagging analysis.

The Milky Way is surrounded by a system of infalling high-velocity HI clouds (HVCs) whose nature is not yet fully understood. The associated infall rate is estimated at about $0.2 M_{\odot} \text{ year}^{-1}$ (e.g., Peek, Putman & Sommer-Larsen 2008), an order of magnitude smaller than the current star-formation rate of the Milky Way. Maller & Bullock (2004) proposed that the cooling of the Galactic hot corona is thermally unstable and generates pressure-confined HVCs with masses $\sim 5 \times 10^6 M_{\odot}$, which contribute to fueling the continued star formation of the disk. Binney, Nipoti & Fraternali (2009) argued however that thermal instability of the hot halo is unlikely to be the source of the Galactic HVC system.

Some disk galaxies (e.g., NGC 891: Oosterloo, Fraternali & Sancisi 2007) show thick HI layers surrounding their galactic disks, which is lagging in rotation relative to the gas in the disk. This gas is accompanied by ionized gas (observed in H α) that shares the lag in rotation velocity (Heald et al. 2007, Kamphuis et al. 2007a) and by dust (Kamphuis et al. 2007b). In more face-on systems, this HI appears associated with regions of star formation (e.g., Kamphuis, Sancisi & van der Hulst 1991), indicating that at least a part of it may have originated in the disk. Fraternali & Binney (2008) and Marinacci et al. (2010) suggest that these layers are associated with gas that has been swept up from the hot corona by galactic fountain clouds ejected from the disk by star formation. In this way, the star formation in the disk is self-fueling, through the gas brought down from the hot corona.

Deep HI images of other disk systems show a very extended rotating HI distribution. M83 (see Section 4.3 and **Figure 15**, and <http://www.atnf.csiro.au/people/bkoribal/m83/m83.html>) is an example, with HI extending far beyond the optical extent of the system. Its outermost HI shows spectacular HI arms and filaments, some of which are forming stars at a low level (Bigiel et al. 2010a). It seems unlikely that this structure should be interpreted as spiral structure in an extended HI disk, because the density of the HI is so low. It may represent a slow filamentary infall of HI into the disk. The observed star formation in this outer HI disk indicates that the outer disk is still in the process of construction. NGC 6946 is another more orderly example of such a very extended HI disk (Boomsma et al. 2008).

9. S0 GALAXIES

Hubble (1936) introduced S0 galaxies as the transition type between elliptical galaxies and spirals. Spitzer & Baade (1951) suggested they were spirals stripped of their dust, gas, and arms as a result of collisions in clusters of galaxies. Sandage, Freeman & Stokes (1970) argued that the morphological type of a galaxy is defined at the time of the formation of the old disk stars, and S0 galaxies are those in which, at the time of the completion of the formation of the disk, there was little gas left for star formation. Subsequently, the observation of a high proportion of S0 galaxies in clusters (Oemler 1974), the evolution of blue galaxies populations in clusters with redshift (Butcher & Oemler 1978), and the increasing ratio of S0s compared to spiral in regions of higher galaxy density (Dressler 1980) led to the general acceptance that S0 galaxies in clusters are stripped spirals. Larson, Tinsley & Caldwell (1980) reconsidered the issue. They remarked

that the apparent rate of consumption of gas by star formation leads to the paradoxical situation that spirals exhaust their gas supplies on a timescale considerably less than the Hubble time (see their abstract). The solution they suggested to this was that spirals constantly replenish their gas content from a reservoir in a gaseous envelope remaining from their formation and, therefore, can sustain star formation over a much longer timescale, whereas S0 galaxies would have lost these envelopes early on and, therefore, do run out of gas on a relatively short timescale.

One way to further address the issue of whether S0s are stripped spirals is to investigate the structure and, in particular, the kinematics of disks in S0s in order to investigate whether or not there are differences in the stellar dynamics. We do not fully review the work on S0 galaxies, but concentrate on this aspect and refer to comprehensive reviews of S0 galaxies, for example, those presented by Quilis, Moore & Bower (2000) and Fritze-von Alvensleben (2004); we also point out that the importance of ram-pressure stripping in environments like Virgo has convincingly been demonstrated by Chung et al. (2009).

Although S0s have a relatively bright surface brightness, measurements of their kinematics remained difficult, and this prevented for a long time a detailed understanding of their dynamics. One of the earliest identified and most easily accessible S0s is NGC 3115. Oort (1940), already as early as during the 1930s (!) considered its dynamics; his motivation was to study issues of stability, as he was interested in the origin and maintenance of spiral structure (the first part of the paper concerns the origin of the deviation of the vertex as caused by spiral arms). Although his photometry shows evidence for a disk component (concentration of light near the major axis), he does not treat it as a separate component. The velocity data (only a few points of the rotation curve by Humason as reported in the annual report of the Mount Wilson Observatory) were insufficient for a significant treatment. Oort concludes that, if these data are correct, the distribution of mass does not correspond to that of the light and quotes mass-to-light ratios of order 250. Minkowski (1960) reported, in a review at a meeting on “*Les Recherches Galactiques et Extragalactiques et la Photographie Électronique*” in Paris in 1959, a new rotation curve that showed an initial rise, then a secondary minimum followed by another strong rise. In the discussion after Minkowski’s paper, Oort reported that he was able to reproduce this behavior on the assumption of a proportionality of mass to light and a large velocity dispersion, which was reported also by Minkowski.¹³

Oort urged Maarten Schmidt to remeasure the rotation of NGC 3115 and together they took spectra in 1968 on the 200-inch Hale Telescope. It took until 1974 before Williams (1975) reduced the data. Oort never used this for a detailed dynamical study, his interests having turned to problems of galactic nuclei and cosmology (Oort 1977, 1981, 1983). In the meantime, measurements of the light distribution improved (Miller & Prendergast 1968; Strom et al. 1977, 1978), but although color information seemed to support the existence of color variations and the rotation curve allowed an estimate of the mass of the disk as a fraction of the total ($\lesssim 0.4$), no comprehensive dynamical model was possible without better spectroscopy. The detailed surface photometry study of Tsikoudi (1979) constituted the first attempt to separate photometric components. The most accurate measurements of the stellar kinematics, confirming the flat shape of the stellar rotation and providing also evidence for a supermassive black hole in the center, have been presented by Kormendy & Richstone (1992).

The kinematic data necessary for a detailed dynamical modelling started to become available only in the 1980s, first in the central regions (Rubin, Peterson & Ford 1980) and then over a more

¹³Oort was, however, not satisfied with his solution and never published it. He did illustrate it during his lectures on Stellar Dynamics in Leiden, as the notes of one of us—P.C.K. is a student of Oort—show and mentioned there that he felt that the rotation curve might very well be wrong and needed confirmation.

extended region (Illingworth & Schechter 1982). In the latter study, the kinematics of the disk were estimated from a decomposition of the contributions to the observed velocities and velocity dispersions. The main result of the study was the important deduction, which later was proved to be more general, that in bulges of disk galaxies rotation plays a bigger role in supporting its shape and density distribution than in ellipticals.

Kormendy (1984a,b) was the first to measure the velocity dispersion in the disk of an S0 galaxy. His main aim was to estimate the Toomre (1964) Q -parameter for local stability. Both in NGC 1553 and in the barred S0 NGC 936, he was able to estimate Q and found it to be well above unity (more like 2 or 3). He therefore concluded that S0 galaxies may differ from spirals in that their stellar disks are too hot (in addition to suffering from lack of gas, which would lower the overall Q) to form small-scale structure.

For NGC 3115, the observations of photometry and kinematics have become more sophisticated in recent years (e.g., Capaccioli, Vietri & Held 1988; Silva et al. 1989; Capaccioli et al. 1993; Michard 2007), but the issue has become much more complicated. A simple answer to the question of whether an S0 originated as a spiral that was swept of its gas or a system that formed its disk with little gas that was not replenished has not emerged. *Gemini* multiobject long-slit spectroscopy by Norris, Sharples & Kuntscher (2006) shows that there is a difference between the $[\alpha/\text{Fe}]$ in the bulge (~ 0.3) and the disk (close to solar), whereas the average age of stars in the disk (5–8 Gyr) is significantly less than in the bulge (10–12 Gyr). The fact that the disk is bluer than the bulge would then primarily be an age difference. Star formation in the disk of this archetypal S0 has proceeded at least for some time after the formation of the bulge.

We note that the advent of new techniques has greatly improved the observational possibilities. SAURON can measure kinematic data using integral field spectroscopy, such as in the study of the S0 galaxy NGC 7332 by Falcón-Barroso et al. (2004). In this system, the stellar populations in the disk (but also in the bulge) are again relatively young, so that star formation must have proceeded in the disk until fairly recently. In addition there is evidence for a strong influence by a bar.

Another recent development is the use of PNe to measure the kinematics. This has the advantage that velocities and dispersions can be measured in faint outer parts of galaxies (e.g., Coccato et al. 2009). Comparing photometry, absorption-line, and PNe kinematics shows that there is good agreement between the PNe number density distribution and the stellar surface brightness and also a good agreement between PNe and absorption line kinematics. An application of this technique to an S0 galaxy is the study of NGC 1023 by Noordermeer et al. (2008), where the PNe were measured with a very good distribution over the face of the system. With these data, it is possible to test whether an S0 could result from a minor merger such that its kinematics become dominated by random motions. The inner parts are fitted quite well with a disk that is rotationally supported, but the outer parts would suggest a minor merger event. Information like this on more systems is required to answer the basic questions.

Finally, an interesting approach is that of Aragón-Salamanca, Bedregal & Merrifield (2006) and Barr et al. (2007), who use globular clusters to measuring the fading of S0 galaxies. They do this by comparing the specific frequency of globular clusters (their number per unit luminosity, S_N) between S0s and normal spirals. This innovative and powerful method has led to the picture in which the disk has faded by a factor of three or so. S0s with younger ages have values for S_N that are more like those of spirals. This is consistent with the view that S0s are formed as a result of removal of gas from normal spirals.

Although the kinematics of S0s would suggest that their disks have been present on a long timescale, the evidence for relatively recent star formation indicates that their history is more complicated than previously thought.

DISCLOSURE STATEMENT

The authors are not aware of any affiliations, memberships, funding, or financial holdings that might be perceived as affecting the objectivity of this review.

ACKNOWLEDGMENTS

A major part of this review was written during work visits by P.C.K. to Mount Stromlo Observatory. P.C.K. thanks the Research School for Astronomy and Astrophysics of the Australian National University and its directors for hospitality and facilities over the years in support of such visits. He is grateful to the Governing Board of the University of Groningen for the appointment as distinguished Jacobus C. Kapteyn Professor of Astronomy, and the Faculty of Mathematics and Natural Sciences for an accompanying annual research grant that supported, among other things, his travels to scientific meetings and work visits. Additional financial support was provided from an annual research grant as a member of the Area Board for Exact Sciences of the Netherlands Organisation for Scientific Research (NWO). We are grateful for the detailed and very useful remarks and suggestions by the scientific editor, John Kormendy. K.C.F. is very grateful to many colleagues for discussions of galactic disks, and particularly to Gérard de Vaucouleurs and Allan Sandage. P.C.K. acknowledges many stimulating collaborations, of which he wishes to acknowledge here especially that with Leonard Searle.

LITERATURE CITED

- Abadi MG, Navarro JF, Steinmetz M, Eke VR. 2003. *Ap. J.* 597:21
- Abe F, Bond IA, Carter BS, Dodd RJ, Fujimoto M, et al. 1999. *Astron. J.* 118:261
- Allen RJ, Goss WM, van Woerden H. 1973. *Astron. Astrophys.* 29:447
- Allen RJ, Shu FH. 1979. *Ap. J.* 227:67
- Alloin D, Edmunds MG, Lindblad PO, Pagel BEJ. 1981. *Astron. Astrophys.* 101:377
- Ann HB. 2007. *J. Korean Astron. Soc.* 40:9
- Ann HB, Park J-C. 2006. *New Astron.* 11:293
- Aragón-Salamanca A, Bedregal AG, Merrifield MR. 2006. *MNRAS* 458:101
- Argyle E. 1965. *Astron. J.* 141:750
- Arp HC. 1965. *Ap. J.* 142:402
- Athanassoula E, Sellwood JA. 1986. *MNRAS* 221:213
- Baade W. 1944. *Ap. J.* 100:137
- Babcock HW. 1939. *Lick Obs. Bull.* 19:41
- Bahcall JN. 1986. *Annu. Rev. Astron. Astrophys.* 24:577
- Baldwin JE, Field C, Warner PJ, Wright MCH. 1971. *MNRAS* 154:445
- Banerjee A, Matthews LD, Jog CJ. 2010. *New Astron.* 15:89
- Barbanis B, Woltjer L. 1967. *Ap. J.* 150:461
- Barker MK, Sarajedini A, Geisler D, Harding P, Schommer R. 2007a. *Astron. J.* 133:1125
- Barker MK, Sarajedini A, Geisler D, Harding P, Schommer R. 2007b. *Astron. J.* 133:1138
- Barnes JE. 1988. *MNRAS* 331:699
- Barr JM, Bedregal AG, Aragón-Salamanca A, Merrifield MR, Bamford SP. 2007. *Astron. Astrophys.* 470:173
- Bastian N, Covey KR, Meyer MR. 2010. *Annu. Rev. Astron. Astrophys.* 48:339
- Battaglia G, Fraternali F, Oosterloo T, Sancisi R. 2006. *Astron. Astrophys.* 447:49
- Battener E, Florido E, Jiménez-Vicente J. 2002. *Astron. Astrophys.* 338:313
- Beaulieu SF, Freeman KC, Hidalgo SL, Norman CA, Quinn PJ, et al. 2010. *Astron. J.* 139:984
- Beck R. 2008. In *Formation and Evolution of Galaxy Disks, ASP Conf. Ser.* 396, p. 35
- Beckwith SVW, Stiavelli M, Koekemoer AM, Caldwell JAR, Ferguson HC, et al. 2006. *Astron. J.* 132:1729
- Begeman K. 1987. *HI rotation curves of spiral galaxies*. PhD thesis. Univ. Groningen

- Bell EF, de Jong RS. 2000. *MNRAS* 312:497
- Bell EF, de Jong RS. 2001. *MNRAS* 550:212
- Bellini A, Bedin LR, Piotto G, Milone AP, Marino AF, et al. 2010. *Astron. J.* 140:631
- Bershadsky MA, Verheijen MAW, Swaters RA, Andersen DR, Westfall KB, Martinsson T. 2010a. *Ap. J.* 716:198
- Bershadsky MA, Verheijen MAW, Westfall KB, Andersen DR, Swaters RA, Martinsson T. 2010b. *Ap. J.* 716:234
- Bigiel F, Leroy A, Seibert M, Walter F, Blitz L, et al. 2010a. *Ap. J.* 720:31
- Bigiel F, Leroy A, Walter F, Blitz L, Brinks E, et al. 2010b. *Astron. J.* 140:1194
- Binney JJ. 2007. See de Jong 2007, p. 67
- Binney JJ, Nipoti C, Fraternali F. 2009. *MNRAS* 397:1804
- Bland-Hawthorn J, Karlsson T, Sharma S, Krumholz M, Silk J. 2010. *Ap. J.* 721:582
- Bland-Hawthorn J, Vlajić M, Freeman KC, Draine BT. 2005. *Ap. J.* 629:249
- Blanton MR, Hogg DW, Bahcall NA, Baldry IK, Brinkmann J, et al. 2003. *Ap. J.* 594:186
- Block DL, Freeman KC, Puerari I, eds. 2010. *Galaxies and Their Masks*. New York: Springer
- Blumenthal GR, Faber SM, Flores R, Primack JR. 1986. *Ap. J.* 301:27
- Blumenthal GR, Faber SM, Primack JR, Rees MJ. 1984. *Nature* 311:517
- Böker T. 2008. *Ap. J.* 672:L111
- Böker T, Laine S, van der Marel RP, Sarzi M, Rix H-W, et al. 2002. *Astron. J.* 123:1389
- Böker T, Sarzi M, McLaughlin DE, van der Marel RP, Rix H-W, et al. 2004. *Astron. J.* 127:105
- Boomsma R, Oosterloo TA, Fraternali F, van der Hulst JM, Sancisi R. 2008. *Astron. Astrophys.* 490:555
- Bosma A. 1981a. *Astron. J.* 86:1791
- Bosma A. 1981b. *Astron. J.* 86:1825
- Bosma A, Freeman KC. 1993. *Astron. J.* 106:1394
- Bottema R. 1993. *Astron. Astrophys.* 275:16
- Bottema R. 1995. *Astron. Astrophys.* 295:605
- Bottema R. 1996. *Astron. Astrophys.* 306:345
- Bottema R. 1997. *Astron. Astrophys.* 328:517
- Bottema R. 2003. *MNRAS* 344:358
- Bottema R, Shostak GS, van der Kruit PC. 1987. *Nature* 328:401
- Bournaud F, Elmegreen BG, Martig M. 2009. *Ap. J.* 707:L1
- Brammer GB, Whitaker KE, van Dokkum PG, Marchesini D, Labbé I, et al. 2009. *Ap. J.* 706:L173
- Briggs FH. 1990. *Ap. J.* 352:15
- Broeils AH. 1992. *Dark and visual matter in spiral galaxies*. PhD thesis. Univ. Groningen
- Broeils AH, Rhee M-H. 1997. *Astron. Astrophys.* 324:877
- Brook CB, Kawata D, Gibson BK, Freeman KC. 2004. *Ap. J.* 612:894
- Brosche P. 1973. *Astron. Astrophys.* 23:259
- Bruzual G, Charlot S. 2003. *MNRAS* 344:1000
- Bundy K, Fukugita M, Ellis RS, Targett TA, Belli S, Kodama T. 2009. *Ap. J.* 697:1369
- Burbidge EM, Burbidge GR, Shelton JW. 1967. *Ap. J.* 150:783
- Burke BF. 1957. *Astron. J.* 62:90
- Burstein D. 1979. *Ap. J.* 234:829
- Butcher HR, Oemler A. 1978. *Ap. J.* 219:18
- Byun Y-I. 1998. *Chin. J. Phys.* 36:677
- Byun Y-I, Freeman KC. 1995. *Ap. J.* 448:563
- Camm GL. 1950. *MNRAS* 110:305
- Cantinella B, Haynes MP, Giovanelli R. 2007. *Astron. J.* 134:334
- Capaccioli M, Cappellaro E, Held EV, Vietri M. 1993. *Astron. Astrophys.* 274:69
- Capaccioli M, Vietri M, Held EV. 1988. *MNRAS* 234:335
- Carignan C, Freeman KC. 1985. *Ap. J.* 294:494
- Carlberg RG, Sellwood JA. 1985. *Ap. J.* 292:79
- Carney BW, Yong D, Teixeira de Almeida ML. 2005. *Astron. J.* 130:1111
- Carollo D, Beers TC, Chiba M, Norris JE, Freeman KC, et al. 2010. *Ap. J.* 712:692
- Casertano S. 1983. *MNRAS* 203:735
- Chabrier G. 2003. *Publ. Astron. Soc. Pac.* 115:763

- Chiappini C, Matteucci F, Gratton R. 1997. *Ap. J.* 477:765
- Chiba M, Beers TC. 2000. *Astron. J.* 119:2843
- Chung A, van Gorkom JH, Kenney JDP, Crowl H, Vollmer B. 2009. *Astron. J.* 138:1741
- Cioni ML. 2009. *Astron. Astrophys.* 506:1137
- Coccato L, Gerhard O, Arnaboldi M, Das P, Douglas NG, et al. 2009. *MNRAS* 394:1249
- Cole AA, Tolstoy E, Gallagher JS, Smecker-Hane TA. 2005. *Astron. J.* 129:1465
- Condon JJ. 1992. *Annu. Rev. Astron. Astrophys.* 30:575
- Courteau S. 1996. *Ap. J. Suppl.* 103:363
- Courteau S, de Jong RS. 2009. *Unveiling the Mass*. <http://www.astro.queensu.ca/GalaxyMasses09/programme.php>
- Courteau S, Dutton A, van den Bosch FC, MacArthur LA, Dekel A, et al. 2007. *Ap. J.* 671:203
- Courteau S, Rix H-W. 1999. *Ap. J.* 513:561
- Cuddeford P, Amendt P. 1992. *MNRAS* 256:166
- da Costa GS, Jerjen H. 2002. In *The Dynamics, Structure & History of Galaxies*, *ASP Conf. Ser.* 273, p. 85
- Daddi E, Dickinson M, Morrison G, Chary R, Cimatti A, et al. 2007. *Ap. J.* 670:156
- Dalcanton JJ, Spergel DN, Summers FJ. 1997. *Ap. J.* 482:659
- Dalcanton JJ, Williams BF, Seth AC, Dolphin A, Holtzman J, et al. 2009. *Ap. J. Suppl.* 183:67
- Dalcanton JJ, Yoachim P, Bernstein RA. 2004. *Ap. J.* 608:189
- Dambis AK. 2009. *MNRAS* 396:553
- Davidge TJ. 2010. *Ap. J.* 718:1428
- Debattista VP, Mayer L, Carollo CM, Moore B, Wadsley J, Quinn T. 2006. *Ap. J.* 645:209
- Debattista VP, Sellwood JA. 1999. *Ap. J.* 513:L107
- Debattista VP, Sellwood J. 2000. *Ap. J.* 543:704
- de Blok WJG. 2010. *Adv. Astron.* 2010:789293
- de Blok WJG, McGaugh SS. 1997. *MNRAS* 290:533
- de Blok WJG, van der Hulst JM. 1998a. *Astron. Astrophys.* 335:421
- de Blok WJG, van der Hulst JM. 1998b. *Astron. Astrophys.* 336:49
- de Blok WJG, Walter F, Brinks E, Trachternach C, Oh S-H, Kennicutt RC. 2008. *Astron. J.* 136:2648
- de Grijs R. 1997. *Edge-on disk galaxies: a structure analysis in the optical and infrared*. PhD thesis. Univ. Groningen. <http://dissertations.ub.rug.nl/FILES/faculties/science/1997/r.de.grijs/c5.pdf>
- de Grijs R. 1998. *MNRAS* 299:595
- de Grijs R, Peletier RF. 1997. *Astron. Astrophys.* 320:L21
- de Grijs R, Peletier RF, van der Kruit PC. 1997. *Astron. Astrophys.* 327:966
- Dehnen W, Binney JJ. 1998. *MNRAS* 298:387
- de Jong JTA, Yanny B, Rix H-W, Dolphin AE, Martin NF, et al. 2010. *Ap. J.* 714:663
- de Jong RS. 1996a. *Astron. Astrophys. Suppl.* 118:557
- de Jong RS. 1996b. *Astron. Astrophys.* 313:45
- de Jong RS. 1996c. *Astron. Astrophys.* 313:377
- de Jong RS, ed. 2007. *Astrophys. Space Sci. Proc.: Island Universes: Structure and Evolution of Disk Galaxies*. Dordrecht: Springer
- de Jong RS, Bell EF. 2009. In *Unveiling the Mass*. http://www.astro.queensu.ca/GalaxyMasses09/data/deJong_GMasses09.pdf
- de Jong RS, Seth AC, Bell EF, Brown TM, Bullock JS, et al. 2007a. *LAU Symp.* 241:503
- de Jong RS, Seth AC, Radburn-Smith DJ, Bell EF, Brown TM, et al. 2007b. *Ap. J.* 667:L49
- de Jong RS, van der Kruit PC. 1994. *Astron. Astrophys. Suppl.* 106:451
- Dekel A, Birnboim Y. 2006. *MNRAS* 368:2
- Dekel A, Sari R, Ceverino D. 2009. *Ap. J.* 703:785
- Dekel A, Silk J. 1986. *Ap. J.* 303:39
- Dennefeld M, Kunth D. 1981. *Astron. J.* 86:989
- de Vaucouleurs G. 1958. *Ap. J.* 128:465
- de Vaucouleurs G. 1959a. *Ap. J.* 130:718
- de Vaucouleurs G. 1959b. *Handb. Fys.* 53:511

- Dickinson M, Giavalisco M, the GOODS Team. 2003. In *ESO Astrophys. Symp.: The Mass of Galaxies at Low and High Redshift*, p. 324
- Disney MJ. 1976. *Nature* 263:573
- Disney MJ, Philipps S. 1983. *MNRAS* 205:1253
- Disney MJ, Romano JD, Garcia-Appadoo DA, West AAQ, Dalcanton JJ, Cortese L. 2008. *Nature* 455:1082
- Djorgovsky G. 1992. In *Cosmology and Large-Scale Structure in the Universe, ASP Conf. Ser.* 24, p. 19
- Dolphin AE. 2000. *MNRAS* 313:281
- Donato F, Gentile G, Salucci P, Frigerio Martins C, Wilkinson MI, et al. 2009. *MNRAS* 397:1169
- Dressler A. 1980. *Ap. J.* 236:351
- Drimmel R, Spergel DN. 2001. *Ap. J.* 556:181
- Dubinski J, Carlberg RG. 1991. *Ap. J.* 378:496
- Edvardsson B, Andersen J, Gustafsson B, Lambert DL, Nissen PE, Tomkin J. 1993. *Astron. Astrophys.* 275:101
- Edvardsson B, Gustafsson B, Nissen PE, Andersen J, Lambert DL, Tomkin J. 1994. In *Panchromatic View of Galaxies: Their Evolutionary Puzzle*, ed. G Hensler, Ch Theis, J Gallagher, p. 401. Gif Sur Yvette, Fr.: Ed. Front.
- Efstathiou G, Jones BJT. 1979. *MNRAS* 186:133
- Efstathiou G, Lake G, Negroponte J. 1982. *MNRAS* 199:1069
- Eggen OJ, Lynden-Bell D, Sandage AR. 1962. *Ap. J.* 136:478
- Elmegreen BG, Elmegreen DM, Fernandez MX, Lemonias JJ. 2009a. *Ap. J.* 692:12
- Elmegreen BG, Elmegreen DM, Leitner SN. 2003. *Ap. J.* 590:271
- Elmegreen DM, Elmegreen BG, Marcus MT, Shahinyan K, Yau A, Petersen M. 2009b. *Ap. J.* 701:306
- Emerson DT. 1976. *MNRAS* 176:321
- Erwin P, Pohlen M, Beckman JE, Gutierrez L, Aladro R. 2007. In *Pathways Through an Eclectic Universe, ASP Conf. Ser.* 390:251
- Faber SM, Gallagher JS. 1979. *Annu. Rev. Astron. Astrophys.* 17:136
- Falcón-Barroso J, Peletier RF, Emsellem E, Kuntschner H, Fathi K, et al. 2004. *MNRAS* 350:35
- Fall SM, Efstathiou G. 1980. *MNRAS* 193:189
- Famaey B, van Caelenberg K, Dejonghe H. 2002. *MNRAS* 335:201
- Fathi K. 2010. *Ap. J.* 722:L120
- Fathi K, Allen M, Boch T, Hatziminaoglou E, Peletier RF. 2010. *MNRAS* 406:1595
- Ferguson AMN. 2007. In *From Stars to Galaxies: Building the Pieces up to Build up the Universe, ASP Conf. Ser.* 374, p. 239
- Ferguson AMN, Gallagher JS, Wyse RFG. 1998a. *Astron. J.* 116:673
- Ferguson AMN, Irwin M, Chapman S, Ibata R, Lewis G, Tanvir N. 2007. See de Jong 2007, p. 239
- Ferguson AMN, Wyse RFG, Gallagher JS, Hunter DA. 1998b. *Ap. J.* 506:L19
- Ferrarini L, Ford H. 2005. *Space Sci. Rev.* 116:523
- Fich M, Silkey M. 1991. *Ap. J.* 366:107
- Florido E, Battaner E, Guizarro A, Garzón F, Castillo-Morales A. 2006. *Astron. Astrophys.* 455:467
- Florido E, Prieto M, Battaner E, Mediavilla E, Sanchez-Saavedra ML. 1991. *Astron. Astrophys.* 242:301
- Förster Schreiber NM, Genzel R, Bouché N, Cresci G, Davies R, et al. 2009. *Ap. J.* 706:1364
- Fraternali F, Binney JJ. 2008. *MNRAS* 386:935
- Freeman KC. 1970. *Ap. J.* 160:811
- Freeman KC. 1975. In *Galaxies and the Universe, Stars and Stellar Systems*, ed. A Sandage, M Sandage, J Kristian, 9:409. Chicago: Univ. Chicago Press
- Freeman KC. 1987. *Annu. Rev. Astron. Astrophys.* 25:603
- Freeman KC. 1991. In *Dynamics of Disc Galaxies*, ed. B Sundelius, p. 15. Göteborg: Univ. Göteborg
- Freeman KC. 1993. In *The Globular Cluster-Galaxy Connection, ASP Conf. Ser.* 48, p. 608
- Freeman KC. 1999. In *The Low Surface Brightness Universe, ASP Conf. Ser.* 170, p. 3
- Freeman KC. 2007. See de Jong 2007, p. 3
- Freeman KC, Bland-Hawthorn J. 2002. *Annu. Rev. Astron. Astrophys.* 40:487
- Freudenreich HT. 1998. *Ap. J.* 492:495
- Fritze-von Alvensleben U. 2004. *Astrophys. Space Sci. Libr.* 319:81

- Fry AM, Morrison HL, Harding P, Boroson TA. 1999. *Astron. J.* 118:1209
- Funes JG, Corsini EM, eds. 2008. In *Formation and Evolution of Galaxy Disks*, *ASP Conf. Ser.* 396
- Furhmann K. 2008. *MNRAS* 384:173
- Gadotti DA. 2009. *MNRAS* 393:1531
- García-Ruiz I. 2001. *Warps in disk galaxies*. PhD thesis Univ. Groningen. <http://dissertations.ub.rug.nl/faculties/science/2001/i.garcia-ruiz/>
- García-Ruiz I, Sancisi R, Kuijken KH. 2002. *Astron. Astrophys.* 394:769
- Garnett DR, Shields GA. 1987. *Ap. J.* 317:82
- Gebhardt K, Lauer TR, Kormendy J, Pinkney J, Bower GA, et al. 2001. *Astron. J.* 122:2469
- Genzel R, Tacconi LJ, Eisenhauer F, Förster Schreiber NM, Cimatti A, et al. 2006. *Nature* 442:786
- Gerssen J, Kuijken KH, Merrifield MR. 1997. *MNRAS* 288:618
- Gerssen J, Kuijken KH, Merrifield MR. 2000. *MNRAS* 317:545
- Gilmore G. 1995. *IAU Symp.* 164:99
- Gilmore G, King IR, van der Kruit PC. 1990. *The Milky Way as a Galaxy*, ed. R Buser, I King. Mill Valley, CA: Univ. Sci. Books
- Gilmore G, Reid IN. 1983. *MNRAS* 202:1025
- Gilmore G, Wyse RFG, Jones JB. 1995. *Astron. J.* 109:1095
- Gilmore G, Wyse RFG, Kuijken KH. 1989. *Annu. Rev. Astron. Astrophys.* 27:555
- Gogarten SM, Dalcanton JJ, Williams BF, Roškar R, Holtzman J, et al. 2010. *Ap. J.* 712:858
- Gogarten SM, Dalcanton JJ, Williams BF, Seth AC, Dolphin A, et al. 2009. *Ap. J.* 691:115
- Gomez AE, Delhaye J, Grenier S, Jaschek C, Arenou F, Jaschek M. 1990. *Astron. Astrophys.* 236:95
- Graham AW, de Blok WJG. 2001. *Ap. J.* 556:177
- Gunn JE. 1982. In *Astrophysical Cosmology*, ed. HA Brück, GV Coyne, MS Longair, p. 233. Vatican: Pont. Acad. Sci.
- Gunn JE. 1987. *IAU Symp.* 117:537
- Gunn JE, Gott JR. 1972. *Ap. J.* 176:1
- Gurovich S, Freeman KC, Jerjen H, Staveley-Smith L, Puerari I. 2010. *Astron. J.* 140:663
- Hammer F, Flores H, Elbaz D, Zheng XZ, Liang YC, Cesarsky C. 2005. *Astron. Astrophys.* 430:115
- Hammer F, Flores H, Puech M, Yang YB, Athanassoula E, et al. 2009. *Astron. Astrophys.* 507:1313
- Hammer F, Puech M, Chemin L, Flores H, Lehnert MD. 2007. *Ap. J.* 662:322
- Hänninen J, Flynn C. 2000. *MNRAS* 337:731
- Hänninen J, Flynn C. 2002. *Astron. Astrophys.* 421:1001
- Hawaiian Starlight. 1999. *Exploring the Universe from Mauna Kea*. <http://www.cfht.hawaii.edu/HawaiianStarlight/Posters/NGC891-CFHT-Cuillandre-Coelum-1999.jpg>
- Hayes MP, van Zee L, Hogg DE, Roberts MS, Maddalena RJ. 1998. *Astron. J.* 115:62
- Heald GH, Rand RJ, Benjamin RA, Bershadsky MA. 2007. *Ap. J.* 663:933
- Heavens A, Panter B, Jimenez R, Dunlop J. 2004. *Nature* 428:625
- Helmi A. 2004. *MNRAS* 351:643
- Helmi A. 2008. *Astron. Astrophys. Rev.* 15:145
- Herrmann KA, Ciardullo R. 2009a. *Ap. J.* 703:894
- Herrmann KA, Ciardullo R. 2009b. *Ap. J.* 705:1686
- Herrmann KA, Ciardullo R, Feldmeier JJ, Vinciguerra M. 2008. *Ap. J.* 683:630
- Herschel W. 1785. *Philos. Trans.* 75:213
- Hohl F. 1971. *Ap. J.* 168:343
- Holmberg EB. 1937. *Ann. Obs. Lund*, No. 6
- Holmberg EB. 1958. *Medd. Lunds Astron. Obs.* II, No. 136
- Hubble EP. 1936. *The Realm of the Nebulae*. New Haven, CT: Yale Univ. Press
- Humason ML, Mayall NU, Sandage AR. 1956. *Astron. J.* 61:97
- Ibata R, Mouhcine M, Rejkuba M. 2009. *MNRAS* 395:126
- Ida S, Kokuba E, Makino J. 1993. *MNRAS* 263:875
- Illingworth G, Schechter PL. 1982. *Ap. J.* 256:481
- Jenkins A. 1992. *MNRAS* 257:620
- Jenkins A, Binney JJ. 1990. *MNRAS* 245:305

- Jiang I-G, Binney JJ. 1999. *MNRAS* 303:L7
- Kalberla PMW, Dedes L, Kerp J, Huad U. 2007. *Astron. Astrophys.* 469:11
- Kalberla PMW, Kerp J. 2009. *Annu. Rev. Astron. Astrophys.* 47:27
- Kalnajs AJ. 1987. *IAU Symp.* 117:289
- Kamphuis JJ, Briggs FH. 1996. *Astron. Astrophys.* 253:335
- Kamphuis JJ, Sancisi R, van der Hulst JM. 1991. *Astron. Astrophys.* 244:L29
- Kamphuis JJ, Sijbring D, van Albada TS. 1996. *Astron. Astrophys.* 116:15
- Kamphuis P, Holwerda BW, Allen RJ, Peletier RF, van der Kruit PC. 2007a. *Astron. Astrophys.* 471:L1
- Kamphuis P, Peletier RF, Dettmar R-J, van der Hulst JM, van der Kruit PC, Allen RJ. 2007b. *Astron. Astrophys.* 468:951
- Kapteyn JC. 1909a. *Ap. J.* 29:46
- Kapteyn JC. 1909b. *Ap. J.* 30:284. Erratum. 1909. *Ap. J.* 30:398
- Kapteyn JC. 1914. *Ap. J.* 40:187
- Kapteyn JC. 1922. *Ap. J.* 55:302
- Kapteyn JC, van Rhijn PJ. 1920. *Ap. J.* 52:23
- Karachentsev ID, Karachentseva VE, Parnovskij SL. 1993. *Astron. Nachr.* 314:97
- Kauffmann G, Heckman TM, White SDM, Charlot S, Tremonti C, et al. 2003a. *MNRAS* 341:33
- Kauffmann G, Heckman TM, White SDM, Charlot S, Tremonti C, et al. 2003b. *MNRAS* 341:54
- Kautsch SJ. 2009. *Publ. Astron. Soc. Pac.* 121:1297
- Kennicutt RC. 1983. *Ap. J.* 272:54
- Kennicutt RC. 1989. *Ap. J.* 344:685
- Kennicutt RC. 1998. *Annu. Rev. Astron. Astrophys.* 36:189
- Kennicutt RC, Armus L, Bendo G, Calzetti D, Dale DA, et al. 2003. *Publ. Astron. Soc. Pac.* 115:928
- Kent S. 1987. *Ap. J.* 93:816
- Kereš D, Katz N, Fardal M, Davé R, Weinberg DH. 2009. *MNRAS* 385:160
- Kereš D, Katz N, Weinberg DH, Davé R. 2005. *MNRAS* 363:2
- Kerr FJ. 1957. *Astron. J.* 62:93
- King IR. 1971. *Publ. Astron. Soc. Pac.* 83:377
- Kirby E, Simon JD, Geha M, Guhathakurta P, Frebel A. 2008. *Ap. J.* 685:L43
- Knapen JH, van der Kruit PC. 1991. *Astron. Astrophys.* 248:57
- Knox RA, Hawkins MRS, Hambly NC. 1999. *MNRAS* 306:736
- Kormendy J. 1977. *Ap. J.* 217:406
- Kormendy J. 1984a. *Ap. J.* 286:116
- Kormendy J. 1984b. *Ap. J.* 286:132
- Kormendy J. 1985. *Ap. J.* 295:73
- Kormendy J. 2007. *IAU Symp.* 245:107
- Kormendy J, Drory N, Bender R, Cornell ME. 2010. *Ap. J.* 723:54
- Kormendy J, Freeman KC. 2004. In *IAU Symp.* 220: *Dark Matter in Galaxies*, p. 377
- Kormendy J, Kennicutt RC. 2004. *Annu. Rev. Astron. Astrophys.* 42:603
- Kormendy J, McClure RD. 1993. *Astron. J.* 105:1793
- Kormendy J, Norman CA. 1979. *Ap. J.* 233:539
- Kormendy J, Richstone D. 1992. *Ap. J.* 393:559
- Kormendy J, Richstone D. 1995. *Annu. Rev. Astron. Astrophys.* 33:581
- Kregel M, Sancisi R. 2001. *Astron. Astrophys.* 376:59
- Kregel M, van der Kruit PC. 2004a. *MNRAS* 352:787
- Kregel M, van der Kruit PC. 2004b. *MNRAS* 355:143
- Kregel M, van der Kruit PC. 2005. *MNRAS* 358:481
- Kregel M, van der Kruit PC, de Blok WJG. 2004. *MNRAS* 352:768
- Kregel M, van der Kruit PC, de Grijs R. 2002. *MNRAS* 334:646
- Kregel M, van der Kruit PC, Freeman KC. 2004. *MNRAS* 351:1247
- Kregel M, van der Kruit PC, Freeman KC. 2005. *MNRAS* 358:503
- Kriek M, van Dokkum PG, Franx M, Illingworth GD, Magee DK. 2009. *Ap. J.* 705:L71
- Kroupa P. 2001. *MNRAS* 322:231

- Kroupa P. 2002a. *Science* 295:82
- Kroupa P. 2002b. *MNRAS* 330:707
- Kylafis N, Bahcall JN. 1987. *Ap. J.* 317:637
- Labbé I, Rudnick G, Franx M, Daddi E, van Dokkum PG, et al. 2003. *Ap. J.* 591:95
- Lacey CG. 1984. *MNRAS* 208:687
- Larson RB. 1974. *MNRAS* 169:229
- Larson RB. 1976. *MNRAS* 176:31
- Larson RB, Tinsley BM. 1978. *Ap. J.* 219:46
- Larson RB, Tinsley BM, Caldwell CN. 1980. *Ap. J.* 237:692
- Lequeux J, Peimbert M, Rayo JF, Serrano A, Torres-Peimbert S, et al. 1979. *Astron. Astrophys.* 80:155
- Lewis JR, Freeman KC. 1989. *Astron. J.* 97:139
- Lotz J, Davis M, Faber SM, Guhathakurta P, Gwyn S, et al. 2008. *Ap. J.* 672:177
- Luck RE, Kovtyukh VV, Andrievsky SM. 2006. *Astron. J.* 132:902
- Magrini L, Corbelli E, Galli D. 2007. *Astron. Astrophys.* 470:843
- Maller AH, Bullock JS. 2004. *MNRAS* 355:694
- Marinacci F, Binney JJ, Fraternali F, Nipoti C, Ciotti L, et al. 2010. *MNRAS* 404:1464
- Martin DC, Fanson J, Schiminovich D, Morrissey P, Friedman PG, et al. 2008. *Ap. J.* 619:L1
- Martínez-Delgado D, Gabany RJ, Peñarrubia RJ, Rix H-W, Majewski SR, et al. 2009. *Highlights of Spanish Astronomy, Astrophys. Space Sci. Proc.*, p. 163
- Martínez-Delgado D, Peñarrubia RJ, Ganaby RJ, Trujillo I, Majewski SR, Pohlen M. 2008. *Ap. J.* 689:184
- Mathewson DS, Ford VL, Buchhorn M. 1992. *Ap. J. Suppl.* 81:413
- Matthews LD. 2000. *Astron. J.* 120:1764
- Matthews LD, Gallagher JS, van Driel W. 1999. *Astron. J.* 118:2751
- Matthews LD, Uson JM. 2008a. *Astron. J.* 135:291
- Matthews LD, Uson JM. 2008b. *Ap. J.* 688:237
- Matthews LD, van Driel W, Gallagher JS. 1998. *Astron. J.* 116:1169
- Matthews LD, Wood K. 2003. *Ap. J.* 593:721
- McConnachie AW, Irwin MJ, Ibata RA, Dubinski J, Widrow LM, et al. 2009. *Nature* 461:66
- McGaugh SS. 2005. *Ap. J.* 632:859
- McGaugh SS. 2009. In *Unveiling the Mass*. http://www.astro.queensu.ca/GalaxyMasses09/data/McGaugh_GMasses09.pdf
- McGaugh SS, Schombert JM, Bothun GD, de Blok WJG. 2000. *Ap. J.* 533:L99
- McWilliam A. 1990. *Ap. J. Suppl.* 74:1075
- McWilliam A. 1997. *Annu. Rev. Astron. Astrophys.* 35:503
- Meléndez J, Asplund M, Alves-Brito A, Cunha K, Barbuy B, et al. 2008. *Astron. Astrophys.* 484:L21
- Mestel L. 1963. *MNRAS* 126:553
- Meusinger H, Reimann H-G, Stecklum B. 1991. *Astron. Astrophys.* 245:57
- Meyer MJ, Zwaan MA, Webster RL, Staveley-Smith L, Ryan-Weber E, et al. 2004. *MNRAS* 350:1195
- Michard R. 2007. *Astron. Astrophys.* 464:507
- Mignard F. 2000. *Astron. Astrophys.* 354:522
- Mihos JC, McGaugh SS, de Blok WJG. 1997. *Ap. J.* 477:79
- Miller RH, Prendergast KH. 1968. *Ap. J.* 153:35
- Miller RH, Prendergast KH, Quirk WJ. 1970. *Ap. J.* 161:903
- Minchev I, Quillen AC. 2006. *MNRAS* 368:623
- Minkowski R. 1960. *Ann. Astrophys.* 23:385
- Mo H, Mao S, White SDM. 1998. *MNRAS* 295:319
- Morrison HL, Boroson TA, Harding P. 1994. *Astron. J.* 108:1191
- Mould JR. 1984. *Publ. Astron. Soc. Pac.* 96:773
- Navarro JF, Frenk CS, White SDM. 1996. *Ap. J.* 462:563
- Navarro JF, Frenk CS, White SDM. 1997. *Ap. J.* 490:493
- Noeske KG, Faber SM, Weiner BJ, Koo DC, Primack JR, et al. 2007a. *Ap. J.* 660:L47
- Noeske KG, Weiner BJ, Faber SM, Papovich C, Koo DC, et al. 2007b. *Ap. J.* 660:L43
- Noordermeer E, Merrifield MR, Coccato L, Arnaboldi M, Capaccioli M, et al. 2008. *MNRAS* 384:943

- Noordermeer E, Sparke LS, Levine SE. 2001. *MNRAS* 328:1064
- Noordermeer E, van der Hulst JM, Sancisi R, Swaters RA, van Albada TS. 2005. *Astron. Astrophys.* 442:137
- Noordermeer E, van der Hulst JM, Sancisi R, Swaters RA, van Albada TS. 2007. *MNRAS* 376:1513
- Nordström B, Mayor M, Andersen J, Holmberg J, Pont F, et al. 2004. *Astron. Astrophys.* 418:989
- Norris MA, Sharples RM, Kuntscher H. 2006. *MNRAS* 367:815
- O’Brien JC, Freeman KC, van der Kruit PC. 2010a. *Astron. Astrophys.* 515:A61
- O’Brien JC, Freeman KC, van der Kruit PC. 2010b. *Astron. Astrophys.* 515:A62
- O’Brien JC, Freeman KC, van der Kruit PC. 2010c. *Astron. Astrophys.* 515:A63
- O’Brien JC, Freeman KC, van der Kruit PC, Bosma A. 2010. *Astron. Astrophys.* 515:A60
- O’Connell DJK, ed. 1958. *Stellar Populations*. Vatican City: Vatican Obs.
- Oemler A. 1974. *Ap. J.* 194:1
- Olling RP. 1995. *Astron. J.* 110:591
- Olling RP. 1996a. *Astron. J.* 112:481
- Olling RP. 1996b. *Astron. J.* 112:457
- Oort JH. 1932. *Bull. Astron. Inst. Neth.* 6:249
- Oort JH. 1940. *Ap. J.* 91:273
- Oort JH. 1965. In *Stars and Stellar Systems*, Vol. 5, ed. A Blaauw, M Schmidt, ch, 21, p. 455. Chicago: Univ. Chicago Press
- Oort JH. 1977. *Annu. Rev. Astron. Astrophys.* 15:259
- Oort JH. 1981. *Annu. Rev. Astron. Astrophys.* 19:1
- Oort JH. 1983. *Annu. Rev. Astron. Astrophys.* 21:373
- Oosterloo T, Fraternali F, Sancisi R. 2007. *Astron. J.* 134:1019
- Ostriker JP, Peebles PJE. 1973. *Ap. J.* 186:467
- Pacholka W. 2009. APOD (27-Jan-2009). antwrp.gsfc.nasa.gov/apod/ap090127.html
- Pastorini G, Marconi A, Capetti A, Axon DJ, Alonso-Herrero A, et al. 2007. *Astron. Astrophys.* 469:405
- Patterson FS. 1940. *Harvard Bull.* 914:9
- Pease FG. 1914. *Proc. Natl. Acad. Sci. USA* 2:517
- Peebles PJE. 1971. *Astron. Astrophys.* 11:377
- Peek JEG, Putman ME, Sommer-Larsen J. 2008. *Ap. J.* 674:227
- Peletier RF, de Grijs R. 1998. *MNRAS* 300:L3
- Pérez I, Fux R, Freeman KC. 2004. *Astron. Astrophys.* 424:799
- Pohlen M, Balcels M, Lütticke R, Dettmar R-J. 2003. *Astron. Astrophys.* 409:485
- Pohlen M, Dettmar R-J, Lütticke R, Aronica G. 2002. *Astron. Astrophys.* 392:807
- Pohlen M, Trujillo I. 2006. *Astron. Astrophys.* 454:759
- Pohlen M, Zaroubi S, Peletier RF, Dettmar R-J. 2007. *MNRAS* 378:594
- Quilis V, Moore B, Bower R. 2000. *Science* 288:1617
- Quinn P, Goodman J. 1986. *Ap. J.* 309:472
- Rees M, Ostriker J. 1977. *MNRAS* 179:541
- Reid M, Menten KM, Zheng XW, Brunthaler A, Moscadelli L, et al. 2009. *Ap. J.* 700:137
- Reshetnikov V, Battaner E, Combes F, Jiménez-Vicente J. 2002. *Astron. Astrophys.* 382:513
- Reylé C, Marshall DJ, Robin AC, Schulteis M. 2009. *Astron. Astrophys.* 495:819
- Reynolds RH. 1913. *MNRAS* 74:132
- Rix H-W, Zaritsky D. 1995. *Ap. J.* 447:82
- Roberts MS. 2008. In *Frontiers of Astrophysics, ASP Conf. Ser.* 395, p. 283
- Roberts MS, Hayes MP. 1994. *Annu. Rev. Astron. Astrophys.* 32:115
- Roberts MS, Whitehurst RN. 1975. *Ap. J.* 201:327
- Robin AC, Crézé M, Mohan V. 1992. *Ap. J.* 400:L25
- Rocha-Pinto HJ, Scalo J, Maciel WJ, Flynn C. 2000. *Ap. J.* 531:L115
- Rogstad DH, Lockart IA, Wright MCH. 1974. *Ap. J.* 193:309
- Rogstad DH, Shostak SS. 1971. *Astron. Astrophys.* 176:315
- Rosales-Ortega FF, Kennicutt RC, Sánchez SF, Díaz AI, Pasquali A, et al. 2010. *MNRAS* 405:735
- Roškar R, Debattista VP, Brooks AM, Quinn TR, Brook CB, et al. 2010. *MNRAS* 408:783
- Roškar R, Debattista VP, Quinn TR, Stinton GS, Wadsley J. 2008a. *Ap. J.* 684:L79

- Roškar R, Debattista VP, Stinton GS, Quinn TR, Kaufmann T, Wadsley J. 2008b. *Ap. J.* 675:L65
- Rossa J, van der Marel RP, Böker T, Gerssen J, Ho LC, et al. 2006. *Astron. J.* 132:1074
- Rubin VC, Burstein D, Ford WK, Thonnard N. 1985. *Ap. J.* 289:81
- Rubin VC, Peterson CJ, Ford WK. 1980. *Ap. J.* 239:50
- Ruphy S, Robin AC, Epchtein N, Copet E, Bertin E, et al. 1996. *Astron. Astrophys.* 313:L21
- Ryden BS, Gunn JE. 1987. *Ap. J.* 318:15
- Sackett PD. 1997. *Ap. J.* 483:103
- Sackett PD. 1999. In *Galaxy Dynamics, ASP Conf. Ser.* 182, p. 393
- Sackett PD, Rix H-W, Jarvis BJ, Freeman KC. 1994. *Ap. J.* 436:629
- Saha K, de Jong RS, Holwerda BW. 2009. *MNRAS* 396:409
- Sakai S, Mould JR, Hughes SMG, Huchra JP, Macri LM, et al. 2000. *Ap. J.* 529:698
- Sales LV, Helmi A, Abadi MG, Brook CB, Gómez FA, et al. 2009. *MNRAS* 400:L61
- Salpeter EE. 1959. *Ap. J.* 129:608
- Samland M, Gerhard O. 2003. *Astron. Astrophys.* 399:961
- Sanchez-Saavedra ML, Battaner E, Florido E. 1990. *Ap. Space Sci.* 171:239
- Sancisi R. 1976. *Astron. Astrophys.* 53:159
- Sancisi R. 1983. In *Internal Kinematics and Dynamics of Galaxies, IAU Symp.* 100, p. 55
- Sancisi R, Allen RJ. 1979. *Astron. Astrophys.* 64:73
- Sandage AR. 1961. *The Hubble Atlas of Galaxies*. Washington: Carnegie Inst.
- Sandage AR. 1986. *Annu. Rev. Astron. Astrophys.* 24:421
- Sandage AR. 2005. *Annu. Rev. Astron. Astrophys.* 43:581
- Sandage AR, Eggen OJ. 1969. *Ap. J.* 158:669
- Sandage AR, Freeman KC, Stokes NR. 1970. *Ap. J.* 160:831
- Sandage AR, Lubin LM, VandenBerg DA. 2003. *Publ. Astron. Soc. Pac.* 115:1187
- Sanders RH, McGaugh SS. 2002. *Annu. Rev. Astron. Astrophys.* 40:263
- Satyapal S, Böker T, Mcalpine W, Gliozzi M, Abel NP, et al. 2009. *Ap. J.* 704:439
- Schaye J. 2004. *Ap. J.* 609:667
- Schmidt M. 1959. *Ap. J.* 129:243
- Schmidt M. 1963. *Ap. J.* 137:758
- Schombert JM, Bothun GD. 1987. *Astron. J.* 93:60
- Schönrich R, Binney JJ. 2009a. *MNRAS* 396:203
- Schönrich R, Binney JJ. 2009b. *MNRAS* 399:1145
- Schwarzkopf U, Dettmar R-J. 2001. *Astron. Astrophys.* 373:402
- Schweizer F. 1986. *Science* 231:227
- Searle L. 1973. *Ap. J.* 168:327
- Searle L, Sargent WLW. 1972. *Ap. J.* 173:25
- Searle L, Sargent WLW, Bagnuolo WG. 1973. *Ap. J.* 179:427
- Searle L, Zinn R. 1978. *Ap. J.* 225:357
- Sellwood JA. 2008. In *Formation and Evolution of Galaxy Disks, ASP Conf. Ser.* 396, p. 241
- Sellwood JA. 2011a. In *Planets, Stars and Stellar Systems* 5. In press (arXiv:1006.4855)
- Sellwood JA. 2011b. In *Evolution of Planetary and Stellar Systems*. In press (arXiv:1001.5430)
- Sellwood JA, Binney J. 2002. *MNRAS* 336:785
- Sellwood JA, Carlberg RG. 1984. *Ap. J.* 282:61
- Sérsic JL. 1963. *Bol. Asoc. Argent. Astron.* 6:41
- Seth AC, Dalcanton JJ, de Jong RS. 2005. *Astron. J.* 130:1575
- Shaver PA, McGee RX, Newton LM, Danks AC, Pottasch SR. 1983. *MNRAS* 204:53
- Shen J, Sellwood JA. 2006. *MNRAS* 370:2
- Sheth K, Elmegreen DM, Elmegreen BG, Capak P, Abraham RG, et al. 2008. *Ap. J.* 675:1141
- Sheth K, Regan M, Hinz JL, Gil de Paz A, Menéndez-Delmestre K, et al. 2010. *Publ. Astron. Soc. Pac.* 122:1397
- Shostak GS, van der Kruit PC. 1984. *Astron. Astrophys.* 132:20
- Sicking FJ. 1997. *The thickness of the HI layer in spiral galaxies*. PhD thesis. Univ. Groningen.
<http://dissertations.ub.rug.nl/faculties/science/1997/f.j.sicking/>
- Silva DR, Boroson TA, Thompson IB, Jedrzejewski RI. 1989. *Astron. J.* 98:131

- Skrutskie MF, Cutri RM, Stiening R, Weinberg MD, Schneider S, et al. 2006. *Astron. J.* 131:1163
- Sofue Y. 1986. *Ap. J.* 458:120
- Sofue Y, Rubin VC. 2001. *Annu. Rev. Astron. Astrophys.* 39:137
- Soifer BT, Helou G, Werner M. 2008. *Annu. Rev. Astron. Astrophys.* 46:201
- Sommer-Larsen J, Gelato S, Vedel H. 1999. *Ap. J.* 519:501
- Sommer-Larsen J, Götz M, Portinari L. 2003. *Ap. J.* 596:47
- Soubiran C, Bienaymé O, Mishenina TV, Kovtyukh VV. 2008. *Astron. Astrophys.* 480:91
- Sparke LS, van Moorsel G, Schwarz UJ, Vogelaar M. 2009. *Astron. J.* 137:3976
- Spitzer L, Baade W. 1951. *Ap. J.* 113:413
- Spitzer L, Schwarzschild M. 1951. *Ap. J.* 114:385
- Sprayberry D, Bernstein GM, Impey CD, Bothun GD. 1995. *Ap. J.* 438:72
- Stark DV, McGaugh SS, Swaters RA. 2009. *Astron. J.* 138:392
- Strom KM, Strom SE, Jensen EB, Moller J, Thompson LA, Thuan TX. 1977. *Ap. J.* 212:335
- Strom KM, Strom SE, Wells DC, Romanishin W. 1978. *Ap. J.* 220:62
- Swaters RA. 1999. *Dark matter in late-type dwarf galaxies*. PhD thesis. Univ. Groningen. <http://dissertations.ub.rug.nl/faculties/science/1999/r.a.swaters/>
- Swaters RA, Balcells M. 2002. *Astron. Astrophys.* 390:863
- Swaters RA, Schoenmaker RHM, Sancisi R, van Albada TS. 1999. *MNRAS* 304:330
- Swaters RA, van Albada TS, van der Hulst JM, Sancisi R. 2002. *Astron. Astrophys.* 390:829
- Takamiya T, Sofue Y. 2002. *Ap. J.* 576:L15
- Tamburro D, Rix H-W, Leroy AK, Mac Low M-M, Walter F, et al. 2009. *Astron. J.* 137:4424
- Tassis K, Kravtsov AV, Gnedin NY. 2008. *Ap. J.* 682:888
- Tinsley BM. 1980. *Fundam. Cosmic Phys.* 5:287
- Tinsley BM, Larson RB, eds. 1977. *Evolution of Galaxies and Stellar Populations*. New Haven, CT: Yale Univ. Press
- Toomre A. 1964. *Ap. J.* 13:1217
- Toomre A. 1977. *Annu. Rev. Astron. Astrophys.* 15:437
- Toomre A. 1981. In *The Structure and Evolution of Normal Galaxies*, ed. SM Fall, D Lynden-Bell, p. 111. Cambridge, UK: Cambridge Univ. Press
- Toomre A, Toomre J. 1972. *Ap. J.* 178:623
- Toth G, Ostriker JP. 1992. *Ap. J.* 389:5
- Trachernach C, de Blok WJG, McGaugh SS, van der Hulst JM, Dettmar RJ. 2009. *Astron. Astrophys.* 505:577
- Tremonti CA, Heckman TM, Kauffmann G, Brinchmann J, Charlot S, et al. 2004. *Ap. J.* 613:898
- Trujillo I, Förster Schreiber NM, Rudnick G, Barden M, Franx M, et al. 2006. *Ap. J.* 650:18
- Trujillo I, Martínez-Valpuesta I, Martínez-Delgado D, Peñarrubia J, Gabany RJ, Pohlen M. 2009. *Ap. J.* 704:618
- Tsikoudi V. 1979. *Ap. J.* 234:842
- Tsikoudi V. 1980. *Ap. J. Suppl.* 43:356
- Tully B, Fisher R. 1977. *Astron. Astrophys.* 54:661
- Uson JM, Matthews LD. 2003. *Astron. J.* 125:2455
- van Albada TS, Bahcall JN, Begeman K, Sancisi R. 1985. *Ap. J.* 295:305
- van Albada TS, Sancisi R. 1986. *Philos. Trans. Ser. A* 320:447
- van de Hulst HC, Raimond E, van Woerden H. 1957. *Bull. Astron. Inst. Neth.* 14:1
- van der Hulst JM. 2002. In *Seeing through the Dust: The Detection of HI and the Exploration of the ISM in Galaxies*, *ASP Conf. Ser.* 276, p. 84
- van der Hulst JM, van Albada TS, Sancisi R. 2001. In *Gas and Galaxy Evolution*, *ASP Conf. Ser.* 240, p. 451
- van der Kruit PC. 1976. *Astron. Astrophys.* 49:161
- van der Kruit PC. 1979. *Astron. Astrophys. Suppl.* 38:15
- van der Kruit PC. 1981. *Astron. Astrophys.* 99:298
- van der Kruit PC. 1984. *Astron. Astrophys.* 140:470
- van der Kruit PC. 1986. *Astron. Astrophys.* 157:230
- van der Kruit PC. 1987. *Astron. Astrophys.* 173:59
- van der Kruit PC. 1988. *Astron. Astrophys.* 192:117

- van der Kruit PC. 2001. In *Galaxy Disks and Disk Galaxies*, ASP Conf. Ser. 230, p. 119
- van der Kruit PC. 2002. In *The Dynamics, Structure & History of Galaxies*, ASP Conf. Ser. 273, p. 7
- van der Kruit PC. 2007. *Astron. Astrophys.* 466:883
- van der Kruit PC. 2008. In *Formation and Evolution of Galaxy Disks*, ASP Conf. Ser. 396, p. 173
- van der Kruit PC. 2009. In *Unveiling the Mass*. http://www.astro.queensu.ca/GalaxyMasses09/data/vanderKruit_GMasses09.pdf
- van der Kruit PC, Allen RJ. 1976. *Annu. Rev. Astron. Astrophys.* 14:417
- van der Kruit PC, Allen RJ. 1978. *Annu. Rev. Astron. Astrophys.* 16:103
- van der Kruit PC, de Grijs R. 1999. *Astron. Astrophys.* 352:129
- van der Kruit PC, Freeman KC. 1984. *Ap. J.* 278:81
- van der Kruit PC, Freeman KC. 1986. *Ap. J.* 303:556
- van der Kruit PC, Gilmore G, eds. 1995. *Stellar Populations: IAU Symp.* 164. Dordrecht: Kluwer
- van der Kruit PC, Jiménez-Vicente J, Kregel M, Freeman KC. 2001. *Astron. Astrophys.* 379:374
- van der Kruit PC, Searle L. 1981a. *Astron. Astrophys.* 95:105
- van der Kruit PC, Searle L. 1981b. *Astron. Astrophys.* 95:116
- van der Kruit PC, Searle L. 1982a. *Astron. Astrophys.* 110:61
- van der Kruit PC, Searle L. 1982b. *Astron. Astrophys.* 110:79
- van der Kruit PC, Shostak GS. 1982. *Astron. Astrophys.* 105:351
- van der Kruit PC, Shostak GS. 1984. *Astron. Astrophys.* 134:258
- van der Kruit PC, van Berkel K. 2000. *Astrophys. Space Sci. Libr.*, vol. 246. Dordrecht: Kluwer
- van Woerden H. 1967. In *IAU Symp.* 31: *Radio Astronomy and the Galactic System*, p. 3
- Velázquez H, White SDM. 1999. *MNRAS* 304:25
- Veltz L, Bienaymé O, Freeman KC, Binney JJ, Bland-Hawthorn J, et al. 2008. *Astron. Astrophys.* 480:753
- Verheijen MAW. 2001. *Astron. J.* 563:694
- Verheijen MAW, Bershady MA, Swaters RA, Andersen DR, Westfall KB. 2007. See de Jong 2007, p. 95
- Verheijen MAW, Sancisi R. 2001. *Astron. Astrophys.* 370:765
- Villumsen JB. 1985. *Ap. J.* 290:75
- Vlajić M, Bland-Hawthorn J, Freeman KC. 2009. *Ap. J.* 697:361
- Wainscoat RJ, Hyland AR, Freeman KC. 1989. *Ap. J.* 337:163
- Wainscoat RJ, Hyland AR, Freeman KC. 1990. *Ap. J.* 348:85
- Walcher CJ, Böker T, Charlot S, Ho LC, Rix H-W, et al. 2006. *Ap. J.* 649:692
- Walcher CJ, van der Marel RP, McLaughlin D, Rix H-W, Böker T, et al. 2005. *Ap. J.* 618:237
- Walker IR, Mihos JC, Hernquist L. 1996. *Ap. J.* 460:121
- Walter F, Brinks E, de Blok WJG, Bigiel F, Kennicutt RC, et al. 2008. *Astron. J.* 136:2563
- Weiner BJ, Sellwood JA, Williams TB. 2001. *Ap. J.* 546:931
- Westfall KB, Bershady MA, Verheijen MAW, Andersen DR, Swaters RA. 2008. In *Formation and Evolution of Galaxy Disks*, ASP Conf. Ser. 396, p. 41
- Wevers BMHR. 1984. *A study of spiral galaxies*. PhD thesis. Univ. Groningen
- Wevers BMHR, van der Kruit PC, Allen RJ. 1986. *Astron. Astrophys. Suppl.* 66:505
- White S, Rees M. 1978. *MNRAS* 183:341
- Wielen R. 1977. *Astron. Astrophys.* 60:262
- Williams BF, Dalcanton JJ, Dolphin AE, Holtzman J, Sarajedini A. 2009a. *Ap. J.* 695:L15
- Williams BF, Dalcanton JJ, Seth AC, Weisz D, Dolphin A, et al. 2009b. *Ap. J.* 137:419
- Williams BF, Dalcanton JJ, Stilp A, Gilbert KM, Roškar R, et al. 2010. *Ap. J.* 709:135
- Williams RE, Baum S, Bergeron LE, Bernstein N, Blacker BS, et al. 2000. *Astron. J.* 120:2735
- Williams RE, Blacker B, Dickinson M, van Dyke Dixon W, Ferguson HC, et al. 1996. *Ap. J.* 112:1335
- Williams TB. 1975. *Ap. J.* 199:586
- Woolley R, Martin WL, Penston MJ, Sinclair JE, Aslon S. 1977. *MNRAS* 179:81
- Worthey G, España AL, MacArthur LA, Courteau S. 2005. *Ap. J.* 631:820
- Wyder TK, Martin DC, Barlow TA, Foster K, Friedman PG, et al. 2009. *Ap. J.* 696:1834
- Yegorova I, Salucci P. 2007. *MNRAS* 377:507
- Yin J, Hou JL, Prantzos N, Boissier S, Chang RX, et al. 2009. *Astron. Astrophys.* 505:497
- Yoachim P, Dalcanton JJ. 2006. *Astron. J.* 131:226
- Yoachim P, Dalcanton JJ. 2008. *Ap. J.* 682:1004

- Yoachim P, Roškar R, Debattista VP. 2010. *Ap. J.* 716:L4
- York DG, Adelman J, Anderson JE, Anderson SF, Annis J, et al. 2000. *Astron. J.* 120:1579
- Zaritsky D, Kennicutt RC, Huchra JP. 1994. *Ap. J.* 420:87
- Zaritsky D, Rix H-W. 1997. *Ap. J.* 477:118
- Zwaan MA, van der Hulst JM, de Blok WJG, McGaugh SS. 1995. *MNRAS* 273:L35



Contents

An Interesting Voyage <i>Vera C. Rubin</i>	1
Laboratory Astrochemistry: Gas-Phase Processes <i>Ian W.M. Smith</i>	29
Protoplanetary Disks and Their Evolution <i>Jonathan P. Williams and Lucas A. Cieza</i>	67
The Astrophysics of Ultrahigh-Energy Cosmic Rays <i>Kumiko Kotera and Angela V. Olinto</i>	119
Dark Matter Searches with Astroparticle Data <i>Troy A. Porter, Robert P. Johnson, and Peter W. Graham</i>	155
Dynamics of Protoplanetary Disks <i>Philip J. Armitage</i>	195
The Interstellar Medium Surrounding the Sun <i>Priscilla C. Frisch, Seth Redfield, and Jonathan D. Slavin</i>	237
Comets as Building Blocks <i>Michael F. A'Hearn</i>	281
Galaxy Disks <i>P.C. van der Kruit and K.C. Freeman</i>	301
The First Galaxies <i>Volker Bromm and Naoki Yoshida</i>	373
Cosmological Parameters from Observations of Galaxy Clusters <i>Steven W. Allen, August E. Evrard, and Adam B. Mantz</i>	409
The Chemical Composition of Comets—Emerging Taxonomies and Natal Heritage <i>Michael J. Mumma and Steven B. Charnley</i>	471
Physical Properties of Galaxies from $z = 2-4$ <i>Alice E. Shapley</i>	525